Dissertation

submitted to the

Combined Faculties for the Natural Sciences and for Mathematics

of the Ruperto-Carola University of Heidelberg, Germany

for the degree of

Doctor of Natural Sciences

presented by

Nereo Kalebić

born in: Split, Croatia

Oral-examination: .....

Identification of a novel microtubule acetyltransferase ATAT1

Referees: Dr. Cornelius Gross

Prof. Dr. Stephan Frings

Joint Ph.D. programme of the

European Molecular Biology Laboratory

and

Ruperto-Carola University of Heidelberg

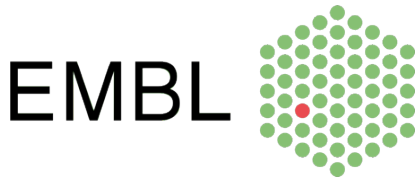

Supervisor:

Dr. Paul A. Heppenstall, EMBL Monterotondo

TAC commitee:

Dr. Cornelius Gross, EMBL Monterotondo

Dr. Francesca Peri, EMBL Heidelberg

Prof. Dr. Stephan Frings, Heidelberg University

Acknowledgements

First and foremost I would like to thank Dr. Paul A. Heppenstall for giving me the opportunity to work on this thesis in his group. I am grateful to the superb guidance, constant support and encouragement he provided throughout my research in his laboratory. His influence was crucial for my development of scientific thinking and strategic project designing.

My sincerest thanks go to Prof. Dr. Marty Chalfie for his support during my research in his group. I would like to acknowledge all the collaborators from EMBL Monterotondo, EMBL Heidelberg, EMBL facilities, Columbia University, Albert Einstein Institute and San Raffaele Scientific Institute for their contribution to this project. It is my great pleasure to thank Dr. Irini Topalidou for everything she taught me about *C.elegans*, but also science in general.

My endless gratitude goes to Concepcion Martinez and Dr. Daniel Bilbao whose help went much beyond the technical and scientific aspects of my Ph.D.

Finally, I would like to express my greatest gratitude to my parents, Sanja Čurković Kalebić and Davor Kalebić, and my girlfriend, Jelena Vragolov, for constant confidence and support in all my aspirations before and during my Ph.D.

Abstract

Mechanotransduction is the process by which a cell converts mechanical energy into electrical or chemical signals. Genetic screens in *C.elegans* emerged as the major source of information about molecules involved in mechanotransduction. Genes identified in these screens have been named *mec* genes for their mechanosensory phenotype. Functions of most of the *mec* genes have been described in both *C.elegans* and mammals, but function of one of the genes, *mec-17*, remained unknown. We identified ATAT1, a mammalian homologue of *mec-17*, and found that it is a microtubule acetyltransferase. Acetylation of α-tubulin is a well conserved posttranslational modification that marks long-lived microtubules but has poorly understood functional significance. Although tubulin deacetylates are well known, ATAT1/*mec-17* is the first major microtubule acetyltransferase identified. We found that ATAT1 is especially expressed in mammalian central nervous system and that intracellularly it co-localizes with microtubules and microtubule associated proteins. We demonstrate that polymerized and stable microtubules rather than soluble tubulin are the predominant substrate of ATAT1 and that it acetylates α-tubulin at lysine 40. Strikingly, ATAT1 also acetylates itself and this underlies a self-regulatory mechanism that is required for effective modification of tubulin. In mammalian cells, ATAT1 is recruited to microtubules by end-binding protein EB-3 where it accelerates plus-end dynamics and promotes microtubule destabilization. Intriguingly, this effect persists in an ATAT1 mutant with no acetyltransferase activity, suggesting that interaction of ATAT1 with microtubules, rather than acetylation *per se*, is the critical factor regulating microtubule stability. We also found that in *C.elegans mec-17* animals show impaired neuronal morphology and disrupted microtubule ultrastructure, in addition to touch-insensitivity. Interestingly, most of these phenotypes, including the touch-insensitivity, are equivalently rescued by both the catalytically inactive *mec-17* mutants and the wild type *mec-17*. Our *in vitro* and *in vivo* evidence suggest that *mec-17*/ATAT1 is the main microtubule acetyltransferase whose role on microtubules goes beyond its enzymatic activity.

Abstract (deutsch) - Kurzbeschreibung

Mechanotransduktion ist ein Prozess bei welchem die Zelle mechanische Energie in elektrische oder chemische Signale umwandelt. Genetisches Screening in *C. elegans* erwies sich als hauptsächliche Quelle für Informationen über Moleküle, die bei Mechanotransduktion eine Rolle spielen. Durch das Screening identifizierte Gene wurden mec genannt, da diese einen mechanosensorischen Phänotyp bewirken. Die Funktion fast aller mec Gene wurde sowohl in *C. elegans* als auch in Säugetieren beschrieben, allerdings ist die Funktion eines Genes, *mec-17*, bislang unbekannt. Wir identifizierten ATAT1, ein Säugetierhomolog von *mec-17* und konnten nachweisen, dass es sich um eine Mikrotubulus Acetyltransferase handelt. Acetylierung des α-Tubulin ist eine hochkonservierte posttranslationale Modifikation, welche langlebige Mikrotubuli markiert, aber bislang kaum geklärte funktionale Bedeutung besitzt. Obwohl bereits Tubulin Deacetylasen bekannt sind, ist ATAT1/*mec-17* die erste Mikrotubulus Acetyltransferase, die identifiziert werden konnte. Wir konnten zeigen, dass ATAT1 insbesondere im Zentralnervensystem von Säugetieren exprimiert wird und dass es intrazellulär mit Mikrotubuli und Mikrotubuli-assoziierten Proteinen colokalisiert. Unsere Ergebnisse beweisen, dass die Hauptsubstrate von ATAT1 nicht lösliches Tubulin, sondern polymerisierte und stabile Mikrotubuli sind. Des Weiteren acetyliert ATAT1 α-Tubulin an Lysin 40. Interessanterweise, acetyliert sich ATAT1 auch selbst, was einem selbstregulatorischen Mechanismus unterliegt, welcher für die effektive Modifikation von Tubulin notwendig ist. In Säugetierzellen wird ATAT1 mittels „end-binding" Proteinen (EB-3) zu den Mikrotubuli rekrutiert, wo es die Dynamiken am Plus-Ende beschleunigt und die Destabilisierung der Mikrotubuli fördert.

Bemerkenswerterweise bleibt dieser Effekt in ATAT1 Mutationen bestehen die keine Acetylierungsaktivität mehr aufweisen. Dies legt nahe, dass die Interaktion von ATAT1 mit Mikrotubuli ein wichtiger Faktor für die Stabilitätsregulierung der Mikrotubuli ist und nicht nur in der Acetylierung *per se* eine Rolle spielt. Des Weiteren konnte ich nachweisen, dass *C.*

elegans' mit Mutationen in *mec-17* neben der Berührungsinsensitivität auch eine beeinträchtigte neuronale Morphologie und eine zerstörte Mikrotubuli-Ultrastruktur aufweisen. Wichtig ist, dass die meisten Phänotypen, einschließlich der Berührungsinsensitivität, durch Gabe von katalytisch inaktiven *mec-17* Mutanten und Wildtyp *mec-17* wiederhergestellt werden können. Unsere *in vitro* und *in vivo* Beweise legen nahe, dass es sich bei *mec-17*/ATAT1 um eine wichtige Acetyltransferase von Mikrotubuli handelt, deren Funktion über die enzymatische Aktivität hinaus geht.

TABLE OF CONTENTS

1 Introduction

1.1 Mechanotransduction

1.1.1 Mechanotransduction in C.elegans

Sensing and responding to a mechanical force is a fundamental characteristic present in virtually all organisms. It is believed that it might even be the most ancient of all senses (Kung, 2005). All cells interact physically with their surroundings and respond to external mechanical forces. Physical contact between cells in animal organism is crucial for proper development and in a case of lack of regulation of the cell contact, diseases such as cancer can arise (Chalfie, 2009). Touch sensation, proprioception, senses of hearing and balance, regulation of systemic fluid homeostasis and blood pressure and many more vital processes are dependant on responsivness to mechanical stimulation (Syntichaki and Tavernarakis, 2004).

Although the importance of mechanotransduction is considerable, the molecules that underlay this process are not well known. One of the main problems is that the expression levels of crucial mechanotransductory components are so low that any biochemical approach to identify them would be futile. That is why the greatest amount of information has been gathered from animal models defective to touch sensitivity. This way the identified genes could be cloned and their products studied. The first eukaryotic organism whose mechanotransduction was studied in this way is *C.elegans* (Chalfie and Sulston, 1981; Sulston et al., 1975), followed much later by *Drosophila* (Eberl et al., 1997; Kernan et al., 1994) and zebrafish (Sidi et al., 2003).

Caenorhabditis elegans is a nematode worm introduced as a model organism by Sydney Brenner (Brenner, 1974). Initially, it proved to be particularly suitable for research in neuroscience, but later it became used also in some other fields such as developmental biology, study of aging etc. Today a lot is known about it; its complete development from the zygote to adult is known (Sulston and Horvitz, 1977; Sulston et al., 1983), its genome became the first metazoan genome sequenced (Consortium, 1998) and all 302 neurons have been identified and their connections described by electron microscopy. Around 10% of neurons in *C.elegans* are mechanoreceptors. They respond to different modalities of stimuli and also display different behavioral responses. These include gentle touch, harsh touch, nose touch, food-mediated slowing, osmotic avoidance and male mating behaviors (O'Hagan and Chalfie, 2006).

Sensitivity to gentle touch is tested by stroking the worm with an eyebrow hair attached to a toothpick. If the animal is touched on the anterior half it moves backwards, while stimulating the tail causes the animal to accelerate forward. Using the eyebrow the force applied to an animal activates only neurons involved in the gentle touch response, while a stronger stimulus (delivered by prodding the animal with a platinum wire) constitutes harsh touch that is mediated by different type of neurons (Chalfie and Sulston, 1981).

A response to gentle touch is mediated by a class of touch receptor neurons that share the same ultrastructure and express many of the same genes (Figure 1) (Chalfie and Sulston, 1981; Chalfie and Thomson, 1979, 1982). These cells include two ALM (anterior lateral microtubule cell) neurons, 2 PLM (posterior lateral microtubule cell) neurons and the AVM and PVM (anterior and posterior ventral microtubule cells) neurons. ALM and AVM neurons sense the touch in the anterior half of the animal, while PLM neurons are responsible for the stimuli delivered in the posterior half of the animal (Figure 1). When first discovered these six touch receptor neurons were referred to as microtubule cells since their most striking

structural characteristic is the presence of distinctive 15-protofilament microtubules not found elsewhere in *C.elegans* body (Chalfie and Thomson, 1979, 1982).

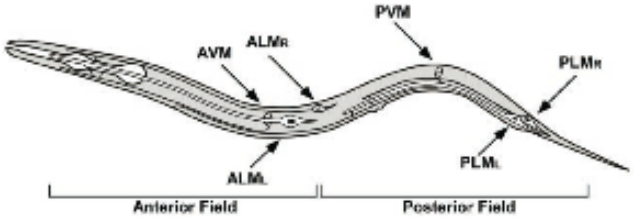

Figure 1. Diagram of touch receptor neurons in *C.elegans*.
Adapted from (Chalfie and Sulston, 1981)

1.1.2 Mec genes

The loss of the response to gentle touch causes the Mec or mechanosensory abnormal phenotype. Screens for mec mutants that are insensitive to gentle touch have identified genes involved in the development and function of touch receptor neurons (Chalfie and Au, 1989; Chalfie and Sulston, 1981).

Several transcription factors are needed for the proper development of touch receptor neurons. *lin-32* and *vab-15* encode transcription factors involved in the generation of touch receptor neurons precursors (Du and Chalfie, 2001; Zhao and Emmons, 1995). UNC-86, a POU-type homeodomain transcription factor maintains correct lineage development and generation of touch receptor neurons (Finney and Ruvkun, 1990; Finney et al., 1988). It also activates the expression of *mec-3,* a master regulator of touch receptor neurons (Chalfie and Sulston, 1981; Zhang et al., 2002). MEC-3 activates expression of most other *mec* genes that makes it essential for proper touch receptor neurons function. Finally, *mec-8* encodes a protein needed for correct mRNA processing of several *mec* genes (Calixto et al., 2010).

The mechanotransduction channel complex in *C.elegans* contains 5 proteins (Figure 2). The core of the complex is made from MEC-4 and MEC-10 proteins that belong to the

degenerin/epithelial sodium channel (DEG/ENaC) superfamily of ion channels that conduct sodium (Chalfie and Wolinsky, 1990; Driscoll and Chalfie, 1991; Huang and Chalfie, 1994). Both of them are necessary for touch sensitivity and their gain-of-function mutations lead to touch receptor neuron degeneration, where their name comes from. While MEC-4 and MEC-10 form pore subunits of the mechanoreceptor channel, products of 3 other genes encode the rest of the complex; *mec-6*, *mec-2* and *unc-24*. MEC-6 is a transmembrane protein similar to mammalian paraoxonases and it is believed to be required for proper channel localization, formation and function (Chelur et al., 2002). MEC-2 is a stomatin-like protein expressed only in touch receptor neurons and necessary for touch sensation, presumably by organizing the lipid environment around the mechanoreceptor complex (Huang et al., 1995; Zhang et al., 2004a). UNC-24 is a protein of a similar function, but expressed in other cells as well, and its effects on mechanosensation are more subtle (Barnes et al., 1996).

The idea that extracellular matrix (ECM) is also involved in mechanosensation comes from the first screens by Martin Chalfie. Later, it was shown that two proteins (MEC-1 and MEC-9) containing multiple EGF and Kunitz domains (Figure 2), as well as a specific type of collagen (MEC-5) are all essential for touch sensitivity (Du et al., 1996; Emtage et al., 2004).

Finally, mechanosensory molecules are found also in the cytoskeleton. Although all *C.elegans* cells have 11-protofilament microtubules, touch receptor neurons are specific for their 15-protofilament microtubules (Chalfie and Thomson, 1982). Because of these unusually large microtubules touch receptor neurons were initially called "microtubule cells". They are made of specific α- and β-tubulin subunits that are encoded by *mec-12* and *mec-7* genes, respectively (Fukushige et al., 1999; Savage et al., 1989). Mutants of each of these genes show touch insensitivity, but the morphology of the neuronal processes is still intact, because 11-protofilament microtubules, normally present in touch recetor neurons as well, replace large 15-protofilament ones (Chalfie and Sulston, 1981; Chalfie and Thomson, 1979). Present evidence suggest that 15-protofilament microtubules have several roles in touch receptor

neurons so their specific roles in mechanosensation might also be multiple (Bounoutas and Chalfie, 2007). Mutations of these two genes affect transport of the members of the mechanotransduction complex to the membrane (Huang et al., 1995), but also microtubules might have a more direct role in the mechanosensation by slowing the adaptation rate of the transduction channel, which in turn leads to production of larger current (Bounoutas and Chalfie, 2007; Bounoutas et al., 2009a). Interestingly, *mec-7* and *mec-12* mutants do not abolish mechanoreceptor current but do reduce it substantially (Bounoutas et al., 2009a) suggesting that the microtubules are not essential for the gating of the channel.

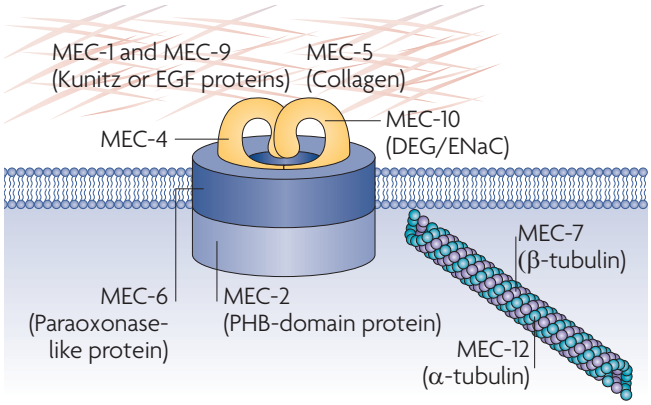

Figure 2. Proteins constituting mechanotransduction complex in *C.elegans.*
Image from (Chalfie, 2009)

Other *mec* genes have been identified by mutagenesis and their functions have recently been revealed: *mec-15* encodes an F-box protein, *mec-14* encodes an oxido-reductase-like protein, both expressed in TRNs and involved in mechanosensation (Bounoutas et al., 2009b). MEC-14 shows similarities with Drosophila *shaker* K^+ channel suggesting it regulates the channel complex. MEC-18 encodes a protein similar to firefly luciferase and CoA ligase whose function in TRNs still remains unknown (Topalidou and Chalfie, unpublished data). Finally, the last remaining *mec* gene is *mec-17* which formed the basis of my research.

1.1.3 Model of mechanotransduction in C.elegans

There is a lot of debate in the field about the gating mechanism in mechanosensation. The main difference is whether the force is conveyed through the lipid bilayer or by associated structures (Chalfie, 2009). The simplest model, coming from studies on mechanosensitive channel on bacteria (Kung, 2005), suggests that the conformation of the channels is influenced by the forces in the lipid bilayer so the channel would open as a consequence of stretching of the membrane. The same principle could also regulate potassium channels in animals and some mechanosensative channels in plants (Chalfie, 2009).

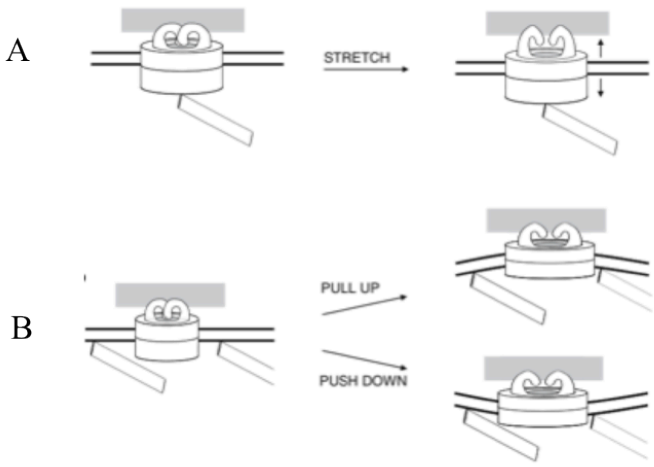

Figure 3. Models of mecanotransduction in the touch receptor neurons in C.elegans. (A) Dual tether model, where the separation of the two tethers (ECM and microtubules) forces the channels to open (B) Single tether model where the placement of the lipid bilayer produces forces that change the conformational state of the channel. Taken from (Bounoutas and Chalfie, 2007)

Dual-tether model predicts that intracellular and extracellular structures tether the transduction channel which in turn enables gating (Figure 3). This model has been proposed for vertebrate hair cell transduction where the channel is tethered to the extracellular tip links and actin cytoskeleton (Gillespie and Walker, 2001). Previously, this model was used to describe *C. elegans* mechanotransduction, (Gu et al., 1996) but has recently been questioned.

The idea that both membrane forces and tethering contribute to channel gating led to the single tether model (Figure 3) where manipulation of a single tether repositions the channel and puts it under different forces in the membrane that in the end gate the channel itself (Kung, 2005). Recently, this model has been proposed for *C.elegans* touch recepter neurons as well (Bounoutas and Chalfie, 2007; Chalfie, 2009).

1.1.4 Mechanotransduction in mammals

There are various specialized mechanosensitive neurons that innervate mammalian skin. Cell bodies of neurons that innervate the head are located in trigenimal ganglia, near the base of the skull. Neurons that innervate the body have their their cell bodies in dorsal root ganglia (DRG), nestled between each vertebra. Each of these cells has a process whose peripheral branch innervates the skin and transduces mechanical stimuli into action potentials. The processes end near the skin as a free nerve ending or in one of the complex organs (Merkel cells, Pacini, Meissner and Ruffini corpuscles) whose structures shape the response to force. Touch receptors can be grouped by their electrophysiological properties into Aβ, Aδ and C-fibers. Gentle touch is mainly mediated by thickly myelinated Aβ afferents with low mechanical thresholds (Lumpkin et al., 2010). In humans and several other mammals C-fibers sensitive to gentle touch have also been found and it is believed that they are involved in social interactions (Loken et al., 2009) or hypersensitivity after injury (Seal et al., 2009).

Mammalian mechanosensory molecules are much less known than their *C.elegans* counterparts. After the discovery of *mec* genes in *C.elegans* respective mammalian homologues have been tested and, interestingly, most of them have been found to be involved in mechanotransduction as well. For example SLP3, a homologue of MEC-2, has been found to be essential for mechanotransduction in a subset of cutaneous touch receptors (Wetzel et al., 2007). On the other hand, mammalian DEG/ENaC isoforms, ASICs (acid-sensing ion

channels) probably only modulate sensory signalling rather than having a direct role in mechanotransduction (Lumpkin and Bautista, 2005). The search for main mammalian mechanotransductory channel still continues, although there were several candidates identified so far. TRP channels, for example, have been shown to be involved in mechanosensation in *Drosophila* and *C.elegans,* but there are no mammalian TRP channels with strong mechanosensory effect found so far. Genetic screens in *Drosophila* identified TRPN1, a channel rich in N-terminal ankryin repeats, as a candidate transduction channel (Walker et al., 2000), but its homologue is not present in the mammalian genome. The only mammalian TRP channel with extended ankryin domain, TRPA1, has been studied, but Trpa1$^{-/-}$ mice have been reported to show small (Kwan et al., 2006) or no (Bautista et al., 2006) phenotype in touch sensitivity. Also TRPV channels have been found to be essential for sensory signalling in both *C.elegans* (Kahn-Kirby and Bergmann, 2006) and *Drosophila* (Kim et al., 2003) but in mammals Trpv4$^{-/-}$ mice show only modest effects on mechanosensory tresholds (Suzuki et al., 2003). Recently a strech-sensitive ion channel TRPC1 has been proposed to take part in the detection of innocous mechanical force. TRPC1$^{-/-}$ mice show 50% reduction in mechanically-evoked action potentials in Aβ and Aδ-D-hair fibers (Garrison et al., 2011). Touch evoked currents in cultured DRG neurons have been known for a long time, but only recently a novel ion channel class, the piezo family, has been identified (Coste et al., 2010). It remains to be seen how Piezo 1 and Piezo 2 relate to mechanotransduction *in vivo*.

In contrast to *C.elegans* touch receptors, little is known about the role of cytoskeleton in mammalian touch receptors. To date no specialized cytoskeleton isoforms have been found in these cells and it is not clear whether both actin and microtubules are involved in mechanotransduction. The idea that actin might take roles of 15-protofilament microtubules from *C.elegans* comes from one study where it was shown that cytochalasin B, an actin depolymerizer, attenuates mehanosensitive currents (Drew et al., 2002).

1.2 Lysine acetylation

1.2.1 Acetylation in the cytoplasm

Lysine acetylation was first discovered in the 60's as a histone-specific posttranslational modification (Allfrey et al., 1964). For 20 years acetylation outside of the nucleus was unknown until finally α-tubulin was described as the first acetylated cytoplasmic protein (L'Hernault and Rosenbaum, 1985; Piperno et al., 1987). Since the beginning it was known that acetylation affects gene expression, but it was only after the discovery of the first histone acetyltransferase, GCN5 (Brownell et al., 1996) and the first histone deacetylase, HDAC1 (Taunton et al., 1996) that it was possible to modulate this activity. The discovery of the first enzymes led to the identification of novel targets in the nucleus. Many transcription factors including p53, GATA1, E2F1 and EKLF have found to be acetylated (Boyes et al., 1998; Gu and Roeder, 1997; Imhof et al., 1997; Zhang and Bieker, 1998) and acetylation was found to stimulate binding of these proteins to DNA.

By the year 2000 there were only a couple of dozen proteins found to be acetylated. The reason is purely technical; since the reagents available for studying protein acetylation were not applicable for any global approach all studies on protein acetylation were focused on a protein-by-protein basis, which proved to be rather inefficient (Norris et al., 2009). In 2006 Kim and colleagues (Kim et al., 2006) published the first global proteomic study on acetylated proteins using antibodies that recognize acetylated lysine (anti-AcK) to enrich for acetylated peptides which then were analyzed by mass spectrometry. This study found around 400 acetylation sites in almost 200 proteins and massively increased our knowledge about the size of acetylome. Many of these proteins were mitochondrial or cytoplasmic and also, many were members of various metabolic pathways.

The most comprehensive study to date, done by Choudhary and colleagues, used the same approach as Kim et al, but introduced an LTQ Orbitrap mass spectrometer with much higher resolution and sensitivity (Choudhary et al., 2009). Also, by applying SILAC technology (stable-isotope labeling by amino acid in cell culture) they determined the quantitative change in specific acetylation events (Mann, 2006). The study identified 3600 lysine acetylation sites on 1750 proteins involved in various cellular processes. Choudhary et al. managed to identify several acetylation-modulated functional networks including RNA splicing, DNA damage repair, nuclear transport, cell cycle, ribosome, chaperons and actin cytoskeleton remodeling (Choudhary et al., 2009).

Two recent reports enriched our knowledge about the role of acetylation in cellular metabolism. A further 703, previously not reported proteins, from the human liver were found to be acetylated (Zhao et al., 2010). This study brings the total size of acetylome to more than 2500 proteins rendering it even larger than the phosphoproteome (2200 proteins, (Olsen et al., 2006)). The same study showed that virtually all enzymes in glycolysis, gluconeogenesis, citric acid cycle, urea cycle, fatty acid metabolism and glycogen metabolism are acetylated in the human liver. It was formerly believed that these processes were regulated only by phosphorylation but these new evidence suggest that acetylation is an equally important mechanism involved in regulation of metabolism and response to nutrient availability. These authors also proposed that acetylation might play a key role in the coordination of different metabolic pathways in response to extracellular conditions (Zhao et al., 2010). Simultaneously, another study (Wang et al., 2010) suggested that in *Salmonella* central metabolism enzymes are acetylated as well and that protein acetylation might be a well conserved mechanism for the regulation of metabolism.

Enzymes that catalyze lysine acetylation are called histone acetyltransferases (HATs) or lysine acetyltransferases (KATs). They transfer the acetyl group from acetyl-CoA to the ε-amino group of the lysine on the target protein. KATs can be divided into 3 major families:

GNAT (Gcn5-related N-acetyltransferases) family, p300/CBP family and MYST family (Allis et al., 2007). In total there are around 22 KATs described today. All of them are found in the nucleus and most of them, like PCAF, HAT1, GCN5, CBP or P300, have also been found in the cytoplasm.

Histone or lysine deacetylases (HDACs or KDACs) are the enzymes that catalyze the deacetylation reaction. They can be divided into 3 classes of which classes I, IIa, IIb and IV are zinc dependant while members of the class III use NAD+ as a cofactor for the deacetylation reaction (Sadoul et al., 2011). Members of the classes I and IV are mainly nuclear proteins while members of the classes IIa and IIb are present in both the nucleus and the cytoplasm with HDAC6, a member of the class IIb, being the only HDAC not present in the nucleus. Among various targets in the cytoplasm, HDAC6 is also a major tubulin deacetylase. Class III is composed of 7 proteins called sirtuins, out of which two are specific for mitochondria, two for nuclei and sirt2 is the only cytoplasm-specific sirtuin that again deacetylates tubulin.

Aceylation in the cytoplasm is functionally extremely important and it is involved in many different cellular processes (Choudhary et al., 2009). Acetylation events are found in the mitochondria, ER, golgi, on the membrane and on the cytoskeleton (Figure 4A). Acetylation is also used for the regulation of the cellular localization of the proteins. For example, most of the proteins that shuttle between the nucleus and the cytoplasm are acetylated (Figure 4B), mainly by p300/CBP, but also by other KATs (Sadoul et al., 2011). Upon acetylation some proteins localize in the cytoplasm, while others favour the nucleus. The nuclear import factors themselves, importin α and importin β, have been found to be acetylated (Choudhary et al., 2009) and importin α acetylation was shown to stimulate formation of the dimer with importin β (Bannister et al., 2000). Mitochondria are the organelles with the highest number of acetylated proteins that are involved in various metabolic processes (Kim et al., 2006;

Wang et al., 2010; Zhao et al., 2010). Recently, it was shown that acetylation can been found in the ER and in the Golgi apparatus (Costantini et al., 2007; Jonas et al., 2008).

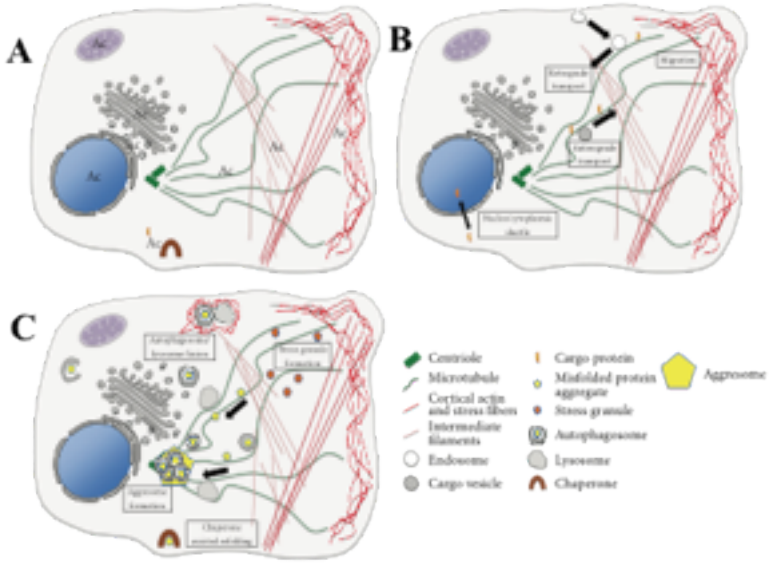

Figure 4. Acetylation events in the cytoplasm. (A) Localization of the acetylation events in the cell. (B) Presence of acetyaltion in many cellular processes including migration, cytoskeleton remodelling and transport. (C) Regulation of stress response and cytoplasmic clean-up systems by acetylation. Adapted from (Sadoul et al., 2011)

Apart of its crucial role in transcriptional regulation, acetylation is implicated in translational regulation and regulation of protein half-life. Although a vast number of ribosomal proteins and translation initiation factors have been found to be acetylated in proteomics studies (Choudhary et al., 2009; Kim et al., 2006), it is still not clear how acetylation influences this process and which enzymes are involved. On the other hand, the role of acetylation in the protein turnover has been well studied and the implicated enzymes described (Sadoul et al., 2008). Acetylation has an important effect on chaperons as well (Figure 4C). Chaperons are proteins important for nucleosome formation, protein folding and assembly of proteins into multisubunit complexes. They are also implicated in the management of missfolded proteins arising from the environmental stress factors like heat-shock or pathological conditions (Sadoul et al., 2011). In all these cellular mechanisms HDAC6 has an important role. The

most famous target of HDAC6 is Hsp90 (heat-shock protein 90), a chaperone essential for the regulation of many signaling proteins (Kovacs et al., 2005; Pearl and Prodromou, 2006). HDAC6 is also essential for the formation of stress granules, made of halted transcripts after the block of mRNA translation, and aggresomes, accumulations of missfolded, ubiquitinated proteins (Kawaguchi et al., 2003; Kwon et al., 2007).

Finally, the cytoskeleton appears to be one of the major sites of acetylation in the cytoplasm. All three cytoskeletal components (actin filaments, microtubules and intermediate filaments) are found to harbour acetylation (Figure 4B).

All actin isoforms (α-, β- and γ-actin) have been found to be acetylated in proteomics studies (Choudhary et al., 2009). β- and γ-actin form stress fibers that are important for cell shape and movement. Acetylation that occurs on K61 of γ-actin results in stabilization of stress fibers (Kim et al., 2006). α-actin, on the other hand, constitutes the microfilaments in muscle cells where MLP (muscle LIM protein), a mechanical sensor which co-localizes with microfilaments, is acetylated by PCAF. Acetylation of MLP is found to enhance the calcium sensitivity of the filaments (Gupta et al., 2008). Other actin-binding proteins are modified by acetylation as well. The Arp2/3 complex, involved in actin nucleation, consists of seven subunits, out of which six are acetylated (Choudhary et al., 2009). Cortactin recruits Arp2/3 complex to the polymerized actin (F-actin, filamentous). Cortactin, too, can be acetylated by p300 and PCAF, which reduces its actin binding capacity. Deacetylation of cortactin, mediated via HDAC6 and Sirt1, induces cell migration (Zhang et al., 2007).

Vimentin and cytokeratin 8, both constituents of intermediate filaments, can be acetylated (Choudhary et al., 2009), but interestingly, acetylation destabilizes their respective polymers (Drake et al., 2009), which is opposite of the reports about actin and microtubules were acetylation is associated with stable polymers.

1.2.2 Microtubule acetylation

Microtubules are a component of the cytoskeleton essential for a plethora of crucial cellular processes such as cell division, motility and shape as well as intracellular transport and organelle positioning. Apart from a large number of different functions in all cells, microtubules also create specialized structures such as cilia and flagella in only some cells. In neurons, microtubules are key components for the establishment of the neuronal polarization, an essential feature of these cells that enables them to perform a variety of unique functions (Conde and Caceres, 2009). In spite of such diverse roles, all microtubules are composed of heterodimers of highly conserved and similar subunits of α- and β-tubulin. Head-to-tail association of these heterodimers leads to the formation of protofilaments that on their turn associate laterally into microtubules (Figure 5). Microtubules are nucleated at the microtubule organizing center (MTOC), but their structure remains highly dynamic throughout lifetime. Microtubules constantly go through phases of growth (polymerization) and shrinkage (depolymerization) with a transition phase termed pause (Mitchison and Kirschner, 1984). Microtubule dynamics are regulated by intrinsic GTPase activity of tubulins and by interactions with microtubule motor proteins and other microtubule-associated proteins (MAPs). Some MAPs such as neuronal MAP1, MAP2 and tau protein stabilize microtubules, whereas some others like microtubule severing enzymes (spastin and katanin) destabilize them (Roll-Mecak and McNally, 2010). Microtubule plus end-tracking proteins (+TIPs) are also involved in controlling microtubule dynamics and interactions with other proteins (Akhmanova and Steinmetz, 2008; Jaworski et al., 2008). Apart from interaction with different MAPs, microtubules regulate their functions also by incorporation of different tubulin isotypes and by post-translational modifications (PTMs). Although it is believed that in mammalian genomes there are almost ten genes for α- and β-tubulin, apart from one report

(Joshi and Cleveland, 1989), at the moment there are no indications that different isotypes might be cell- or function-specific.

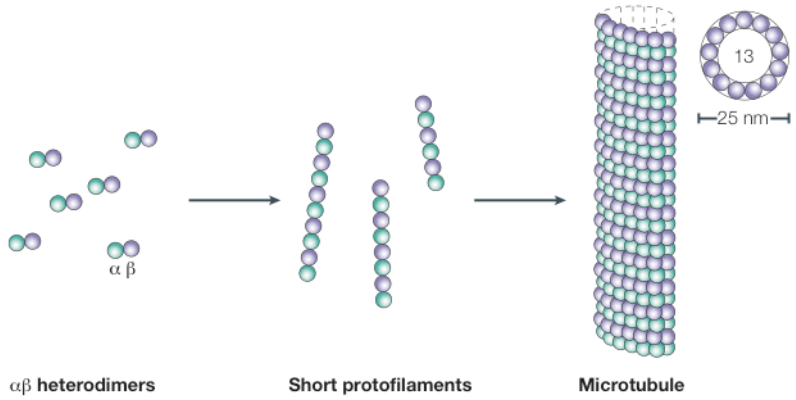

Figure 5. Structure of microtubules. α- and β-tubulin subunits associate into heterodimers that form protofilaments. Association of protofilaments leads to the formation of microtubule that is in mammalian cells usually composed of 13 protofilaments. The outer diameter of a 13-protofilament microtubule is around 25nm. Taken from (Westermann and Weber, 2003)

Microtubules receive diverse PTMs out of which nine have been described so far: detyrosination, Δ2-tubulin generation, acetylation, polyglutamylation, polyglycylation, palmitoylation, sumoylation, phosphorylation and ubiquitylation (Janke and Chloe Bulinski, 2011; Wloga and Gaertig, 2010). In the tyrosination-detyrosination cycle, initial detyrosination at the C-terminus of α-tubulin is mediated by cytosolic carboxypeptidase, while the reverse process is catalyzed by tubulin Tyr ligase (TTL). Detyrosination (Figure 6) has since the beginning been associated with stable microtubules and it is found only on long-lived microtubules, but detyrosination itself does not stabilize them (Webster et al., 1987). Further removal of the next C-terminal Glu residue leads to the irreversible generation of Δ2-tubulin (Figure 6) that presumably permanently stabilizes microtubules (Janke and Chloe Bulinski, 2011). Polygluyamylation and polyglycylation (Figure 6) are extensions of glutamine or glycine side chains on C-terminus of both α- and β-tubulin. They are mediated by TTL-like enzymes and it is believed they control microtubule stability via interaction with

severing enzymes. Long chains of poly-Glu and poly-Gly might serve as docking sites for different MAPs that protect microtubules from severing (Janke and Kneussel, 2010).

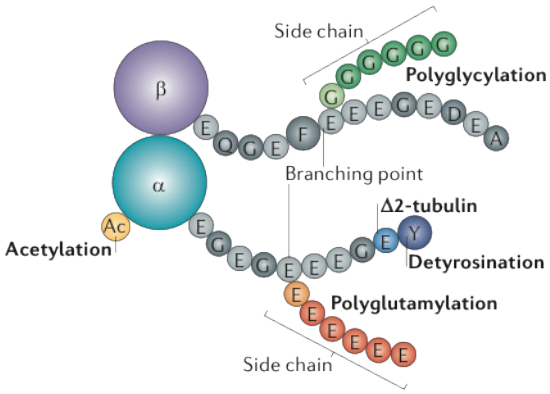

Figure 6. Schematic representation of major tubulin PTMs. Acetylation is the only modification at the luminal side. From (Janke and Chloe Bulinski, 2011)

Microtubule acetylation was first discovered in *Chlamydomonas reinhardtii* by labeling with ^{3}H acetate (L'Hernault and Rosenbaum, 1985). Interestingly, it was immediately suggested that acetylated tubulin might play a role in microtubule assembly since it was found only in the falgella of *Chlamydomonas*, but not in the cytoplasm (L'Hernault and Rosenbaum, 1985). Soon, acetylated microtubules were detected with specific antibodies first in chicken embryo, and then also in mammalian cells (Piperno and Fuller, 1985). Clone 6-11B-1 (Piperno and Fuller, 1985; Piperno et al., 1987) is still the only available antibody against the acetylated tubulin. It was soon shown that it exclusively recognizes lysine 40 on α-tubulin (LeDizet and Piperno, 1987). For the recognition 3 additional amino acids adjacent to K40 are also needed (LeDizet and Piperno, 1991). These amino acids are well conserved in almost all organisms so the antibody was used in every model organisms available, but also this means that antibody will not recognize any other acetylated lysine on tubulin. Because of this for the next 20 years it was believed that tubulin can be acetylated only at lysine 40. In the proteomics study from 2009 several new acetylation sites were found on both α- and β-tubulin

(Choudhary et al., 2009), but so far none has been verified biologically. Recently, the first verified site on β-tubulin (K252) has been reported (Chu et al., 2011).

Since its initial discovery, acetylation has been associated with stable microtubules. It was noticed that under depolymerizing conditions acetylated microtubules were more resistant than non-acetylated ones (Schiff et al., 1979; Schiff and Horwitz, 1980). Microtubules in cells also became acetylated after the application of taxol, a microtubule polymerizer and stabilizer, suggesting that acetylation was a consequence of microtubule stabilization (Black and Keyser, 1987; Cambray-Deakin and Burgoyne, 1987; Webster DR, 1989). Further studies showed that acetylation can occur also on highly dynamic microtubules (Belmadani et al., 2004) and in the early mitotic spindle (Schatten et al., 1988) suggesting that acetylation, although mostly present on stable microtubules, occurs also on dynamic ones.

The enzymes involved in tubulin acetylation were identified long after the discovery of the modification itself. Around 10 years ago, HDAC6 (Hubbert et al., 2002; Matsuyama et al., 2002b) and SIRT2 (North et al., 2003) were shown to be responsible for microtubule deacetylation. Interestingly, both of the enzymes have additional substrates other than α-tubulin, with HDAC6 having more than 10 identified targets in the cytoplasm. However, enzymes that acetylate microtubules were much harder to identify. Although several protein extracts with tubulin acetyl-transferase activity had been isolated from *Chlamydomonas* (Maruta et al., 1986), at the beginning of my project, only one enzyme, namely ARD1-NAT1 (arrest-defective 1-amino terminal, α-amino, acetyltransferase 1) had been suggested to mildly affect tubulin acetylation (Ohkawa et al., 2008). In 2009 another acetyltransferase complex (ELP, elongator protein complex) was shown to affect the acetylation of α-tubulin (Creppe et al., 2009). ELP participates in transcriptional elongation, where the subunit ELP3 acetylates histone H3. Interestingly, in neurons with perturbed neuronal migration and branching upon ELP3 knock down, a reduction in microtubule acetylation was been observed as well (Creppe et al., 2009). This function of ELP3 was also confirmed in *in vitro*

experiments (Creppe et al., 2009). Furthermore, a recent screening in *C.elegans* confirmed the hypothesis that ELP3 is a tubulin acetyltransferase (Solinger et al., 2010). However, both reports suggest ELP3 to be a tubulin acetyltransferase in the developing neurons, without a clear role of ELP3 later in mature cells. Very recently, the acetyltransferase SAN has been shown to acetylate soluble β-tubulin at K252 (Chu et al., 2011). Finally, last year two independent groups showed that the major tubulin acetyltransferase in *Tetrachymena* and *C.elegans* is MEC-17, one of the mechanosensory important molecules in *C.elegans* (Akella et al., 2010; Shida et al., 2010). My thesis has focused on the identification of this enzyme.

1.2.3 Role of microtubule acetylation in cells and disease

An interesting feature of tubulin acetylation that distinguishes it from all other tubulin PTMs, is that the only verified site of acetylation, K40, is situated on the luminal side of a microtubule (Figure 6). It is not clear how acetylation-modulation enzymes reach this site since presumably it would take a long time for diffusion of the enzyme from the microtubule ends. Additionally, it is difficult to imagine the functional significance of acetylation on a site that is in the lumen, since it would be unlikely to serve as a docking site for other proteins.

In *Tetrahymena thermophila* mutants lacking K40 on microtubules, growth characteristics and cilia-dependent movement are the same as in wild type organisms, suggesting that K40 acetylation is not essential for survival (Gaertig et al., 1995). In *C.elegans* MEC-12 is the only isotype of α-tubulin that contains K40. *mec-12* mutant animals display touch insensitivity, that is rescued by over expression of *mec-12* gene, but, interestingly, it is also rescued by the over expression of an non-acetylatable *mec-12* K40Q mutant (Fukushige et al., 1999). This suggests that acetylation on α-tubulin is not needed for mechanosensation in *C.elegans*. Similarly, studies on mice suggest that increased tubulin acetylation, generated in HDAC6

knock-out mice, does not affect the viability or development of these animals (Zhang et al., 2008a).

HDAC6-mediated deacetylation was shown to affect microtubule stability. Initially, HDAC6 inhibitors were demonstrated not to affect microtubule stability measured by staining with detyrosinated tubulin antibody (Palazzo et al., 2003), but over expression of HDAC6 in mammalian cells led to increased susceptibility of microtubules to drug-induced depolymerization (Matsuyama et al., 2002b) and in HDAC6 inhibited cells most parameters of microtubule dynamics were decreased (Tran et al., 2007a). More recent studies, however, show that HDAC6 protein rather than acetylation *per se*, regulates microtubule dynamics (Zilberman et al., 2009a). Another recent report claims that acetylation affects microtubule stability via severing enzymes (Sudo and Baas, 2010). The authors argue that since the severing enzymes reach through the microtubule lattice to pull out subunits, acetylation on the luminal side might provide an ideal location (Sudo and Baas, 2010). Alternatively, the conformational changes on the microtubule lattice, as a consenquence of K40 acetylation, might create a docking site for severing enzymes on the outer surface of microtubules. Taken together these data still do not show consistently whether acetylation affects microtubule stability.

Neurons with their unique properties harbour the largest number of different tubulin PTMs, including acetylation (Conde and Caceres, 2009). Increased acetylation accompanies neuronal differentiation and in mature cells it is particularly enriched in axons, where it probably helps in polarizing the neuron (Black and Keyser, 1987; Cambray-Deakin and Burgoyne, 1987). Defects in neuronal development in ELP silenced mice suggest that ELP3-mediated acetylation might be responsible for neuronal development (Creppe et al., 2009), but it is still unclear what the role of acetylation is in mature neurons and axonal transport. Microtubule transport is mediated by motor proteins kinesins and dyneins. Present data suggest that K40 acetylation increases binding of kinesin KIF5 to microtubules (Dompierre et al., 2007; Reed

et al., 2006). After this initial observation, another study suggested that the neurodegenerative Huntington disease might originate from a defect in tubulin acetylation (Dompierre et al., 2007). Acetylation should facilitate transport of BDNF (brain-derived neurotrophic factor) in neurons expressing mutant Huntington disease protein (Dompierre et al., 2007). Other neurodegenerative diseases have also been associated with acetylation. In Parkinson's disease hyperacetylation, caused by inhibition of the SIRT2, resulted in decreased α-synuclein-mediated neurotoxicity (Du et al., 2010; Outeiro et al., 2007; Suzuki and Koike, 2007). Also HDAC6 has recently been involved in abnormal transport observed in neurodegenerative diseases (Chen et al., 2010). The major problem of all these studies is the use of HDAC6/SIRT2 inhibitors in their experiments since both HDAC6 and SIRT2 have several other targets other than tubulin it is difficult to discriminate which of these effects indeed depend on tubulin acetylation and which on other processes.

Although tubulin acetylation is highly enriched in cilia and flagellum two different lines of evidence suggest that acetylation is not essential for the development or function of cilia. Expression of a non-acetylatable form of α-tubulin did not cause any morphological changes on cilia (Gaertig et al., 1995). Additionally, mice lacking HDAC6 had no impairment in male fertility (Zhang et al., 2008a).

Microtubules are essential for the formation of the mitotic spindle and progression of cell cycle. Very soon after its discovery, acetylation was detected in the spindle and in the midbody leading to the association of HDAC6 with cancer. HDAC6 expression has been correlated with better survival in breast cancer (Zhang et al., 2004b) and HDAC6-dependant tubulin deacetylation was shown to increase cell motility contributing to the malignant character of cancer (Hubbert et al., 2002; Zhang et al., 2004b), although it is not clear if this motility is a consequence of tubulin acetylation or acetylation of some other protein.

1.2.4 mec-17

Very little was known about MEC-17 when research presented in this thesis started. *mec-17* was initially discovered together with other *mec* genes in screenings performed by Martin Chalfie (Chalfie and Au, 1989). From the beginning *mec-17* showed some specific characteristics. Although all other genes were present in multiple alleles, screening resulted in only one *mec-17* allele (*u265*) that was obtained in two separate mutagenesis experiments. Moreover, *mec-17* animals showed another specific characteristic - they were touch sensitive as newly hatched, but then they became insensitive as they matured. This suggests that *mec-17* is involved in maintenance of touch-sensitivity (Chalfie and Au, 1989). Later it was reported (Chelur and Chalfie, 1996) that concomitant with the loss of touch sensitivity, expression of *mec-7* and *mec-3* are reduced in *mec-17* animals. Because of this it was believed that MEC-17 is a transcription factor involved in maintenance of touch-receptor neuron differentiation. All further attempts to generate additional alleles were futile. Finally, in 2002 the original *u265* mutant was sequenced and two point mutations on the N-terminal part of the protein were found (Zhang et al., 2002). In the same study *mec-17* was shown to be a touch-neuron specific gene with a very high expression level (the highest of all the *mec-3*-dependent genes in the array). Homologues in *Drosophila*, mouse and human were also found but *mec-17*'s function still remained a mystery.

In bioinformatic databases the putative domain from MEC-17-family proteins was annotated as DUF738 (domain of unknown function 738). A bioinformatics study using a variety of fold recognition and distant homology detection methods suggested that DUF738 belongs to the superfamily of Gcn5-related N-acetyltransferases (GNAT) and that MEC-17 might operate as a histone acetyltransferase (Steczkiewicz et al., 2006).

By the end of my Ph.D. research two independent groups reported that MEC-17 functions as a tubulin acetyltransferase in invertebrates and vertebrates (Akella et al., 2010; Shida et al.,

2010). Both groups used a variety of *in vitro* and *in vivo* approaches to support this statement. Neither of the two groups, however, tried to explain the mechanism by which MEC-17 causes touch insensitivity. It also remained unknown how acetylation affects microtubule stability.

1.2.5 Aim of the project

The overall aim of my project was to identify and characterize a novel gene, mammalian homologue of the *C.elegans* gene *mec-17*. Initially we identified this gene through an analysis of mammalian orthologues of *C.elegans* mec genes.

Once we gained the basic knowledge on the *mec-17* biology, we continued with a more mechanistic approach to understand how it functions in cells and *in vitro*. Finally, to fully assess the function and importance of a novel gene, *in vivo* studies were needed. We reasoned that using *C.elegans* would give us greatest amount of information since the system is well established. For that purpose we performed, in collaboration with Prof. Dr. Martin Chalfie at Columbia University in New York, an in-depth analysis of *mec-17* mutant worms. We also established an *in vivo* approach in mouse to define the role of this gene in the mammalian system.

2 Results

2.1 ATAT1 is a tubulin acetyltransferase

2.1.1 Screening of mouse homologues of *C.elegans* transcription factors involved in somatosensation

As discussed above, several mamalian orthologues of *C.elegans mec* genes have been shown to be involved in mammalian mechanotransduction. However, many *mec* genes still remain uncharacterized in mammals. Among the genes that are involved in touch sensation in *C.elegans,* there are several transcription factors required for the development of touch receptor neurons or expression of other *mec* genes. We identified four genes of interest whose mammalian homologues have not been studied in somatosensation: *mec-3, unc-86, mec-17* and *ceh-14*. MEC-3 is a LIM homeodomain transcription factor required for differentiation and maturation of touch receptor neurons (Chalfie and Sulston, 1981; Zhang et al., 2002). It is considered to be the master regulator of other *mec* genes. Its expression depends upon UNC-86 and maintenance of expression was thought to depend on MEC-17 and MEC-3 itself. UNC-86 (UNCoordinated 86) is a POU-type homeodomain transcription factor required for determination of mechanosensory neurons among other functions in different neuronal lineages (Finney and Ruvkun, 1990; Finney et al., 1988). At the beginning of this project MEC-17's function was unknown as explained above. CEH-14 (*C.elegans* homebox - 14) is a LIM homeodomain transcription factor required for development of AFD thermosensory neurons and for normal thermotactic behavior (Cassata et al., 2000).

First, we performed bioinformatic analysis to identify mammalian orthologues (Table 1). We found six LIM homebox genes to be orthologues of *mec-3* and *ceh-14* and 3 POU domain genes to be orthologues of *unc-86*. Interestingly, *mec-17* had only one orthologue in the mouse genome annotated as *2610110G12Rik*, a gene of unknown function. Since the *C.elegans* genome is much more condensed than mammalian the redundancy is very common when searching for *C.elegans* orthologues in mammals and indeed most *mec* genes have several mammalian orthologues, but *mec-17* was a unique case where a single gene was present in the mammalian genome.

Table 1. List of mammalian orthologues of C.elegans transcription factors involved in somatosensation:

Mouse	C.elegans	Full name
LHX1	MEC-3, CEH-14	LIM homebox 1
LHX2	MEC-3	LIM homebox 2
LHX3	CEH-14	LIM homebox 3
LHX4	CEH-14	LIM homebox 4
LHX5	MEC-3, CEH-14	LIM homebox 5
LHX9	MEC-3	LIM homebox 9
POU4F1	UNC-86	POU domain class 4, TF 1
POU4F2	UNC-86	POU domain class 4, TF 2
POU4F3	UNC-86	POU domain class 4, TF 3
2610110G12RIK	MEC-17	Unknown

Having identified the genes of interest we decided to confirm their expression in mouse dorsal root ganglia (DRGs) and to see if they were more expressed there than in other representative tissues (we isolated mouse liver, kidney, lungs, heart, brain and spinal cord in addition to DRGs). Our RT-qPCR (Figure 7) analysis revealed that none of the tested genes is expressed exclusively in DRGs, although some genes (LHX5) are more expressed in neuronal tissues than elsewhere. These results made us focus our attention only on *2610110G12Rik* that hereafter I will refer to as ATAT1.

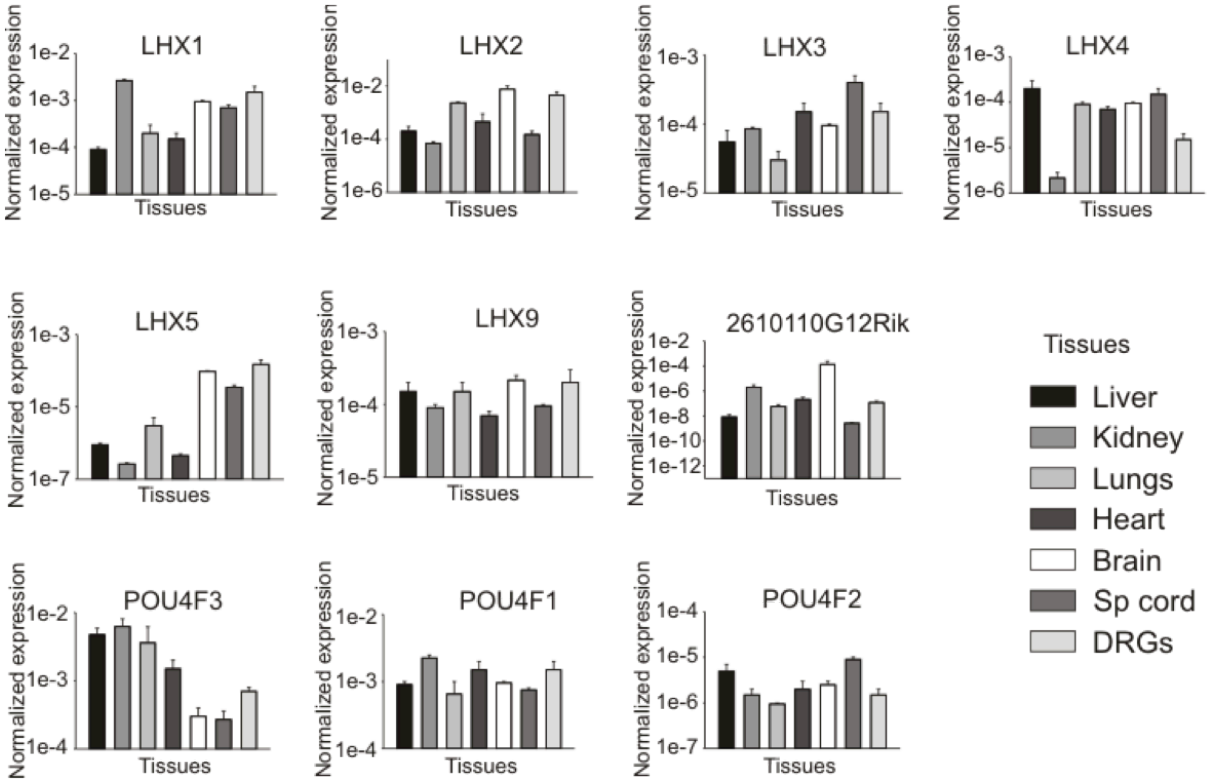

Figure 7. RT-qPCR results of mammalian transcription factors possibly involved in somatosensation. Expression is normalized to ubiquitin. All experiments were performed in triplicates. Four non-neuronal and three different neuronal tissues were tested.

2.1.2 ATAT1 is a highly conserved gene with many splice variants in mammalian transcriptome

Initial screening of the *mec-17/atat1* family of genes revealed that this gene is present in all animals whose genomes are available. It is not present in prokaryotes, yeast or higher plants, but algae genes of unknown function display sequence similarities with the *mec-17/atat1* family (Figure 8). Interestingly, most of the higher animals still have only one copy of this gene which suggests that over expression is possibly lethal. The organisms with double copies of this gene are *C.elegans* and *Drosophila*. In *C.elegans* in addition to *mec-17* there is another gene recently named *atat-2* (Shida et al., 2010).

Comparing protein sequences of the MEC-17/ATAT1 family enabled us to find the most conserved region of the protein that overlaps with the domain found by Steczkiewicz et al. (2006). Striking conservation is found within the domain region with protozoan ATAT1 being almost 80% similar to the mouse one (Figure 9).

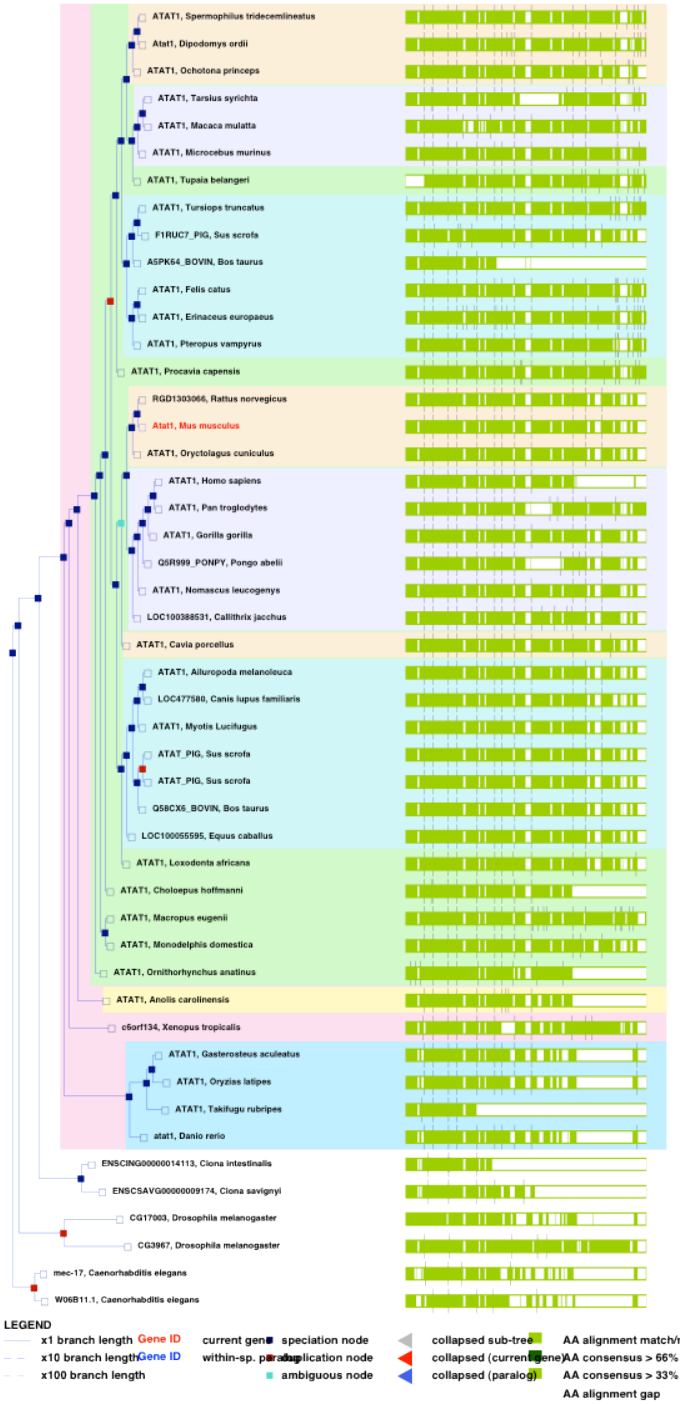

Figure 8. Tree of ATAT1 family genes. ATAT1 genes are found in all animals whose genomes are stored in Ensembl database. The figure is taken from Ensembl website.

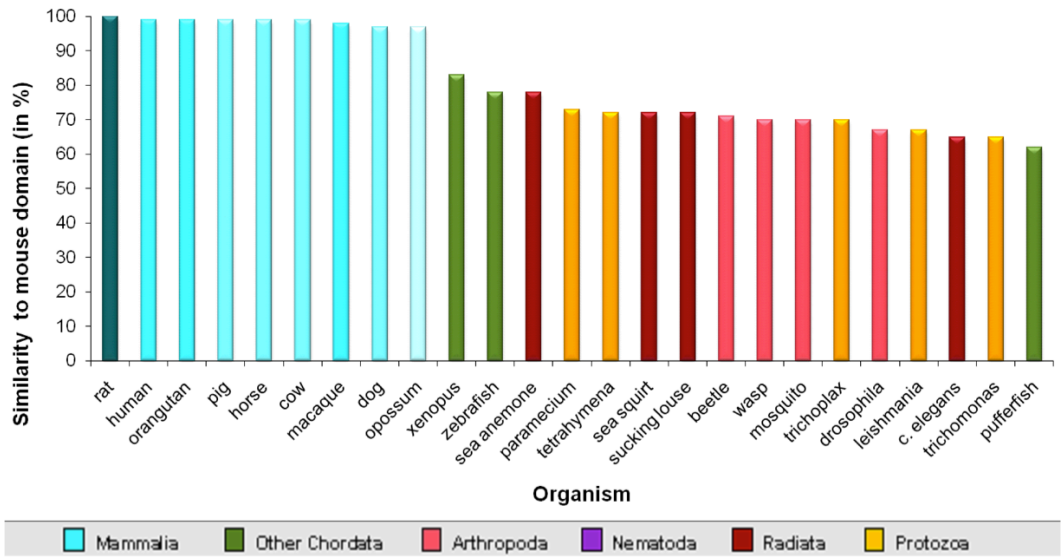

Figure 9. Domain conservation of ATAT1 protein family. Domain was identified using bioinformatical databases and tools (Ensembl, Panther) and sequences were aligned using ClustalW. Domain is almost identical within mammals and around 70% similar between mouse and all other tested animals, including protozoa.

In the mouse genome, the *atat-1* gene (ENSMUSG00000024426) is located on chromosome 17 and consists of 16 exons. Ensembl database predicts 17 transcripts of this gene, out of which seven have a functional protein coding product. Three others are degraded by nonsense mediated decay, five are expressed introns and the rest are translated but lead to nonfunctional protein product. Seven functional transcripts are schematically represented in Figure 10. For five of these transcripts we designed specific primers to test their expression in various mouse tissues hypothesizing that splice variants are tissue specific (Figure 11). We performed RT-qPCR and noticed that all tested transcripts are expressed in all tested tissues, but with different levels of expression. Generally, all transcripts were expressed at much lower levels than the housekeeping ubiquitin gene. These data suggest that alternative splicing does not regulate ATAT1 expression at the gross tissue level so we decided to continue our research using splice variant *Atat1-005* for all further experiments. This splice variant is the one annotated as the reference one in NCBI database and it is also the highest expressed one in most of the tissues.

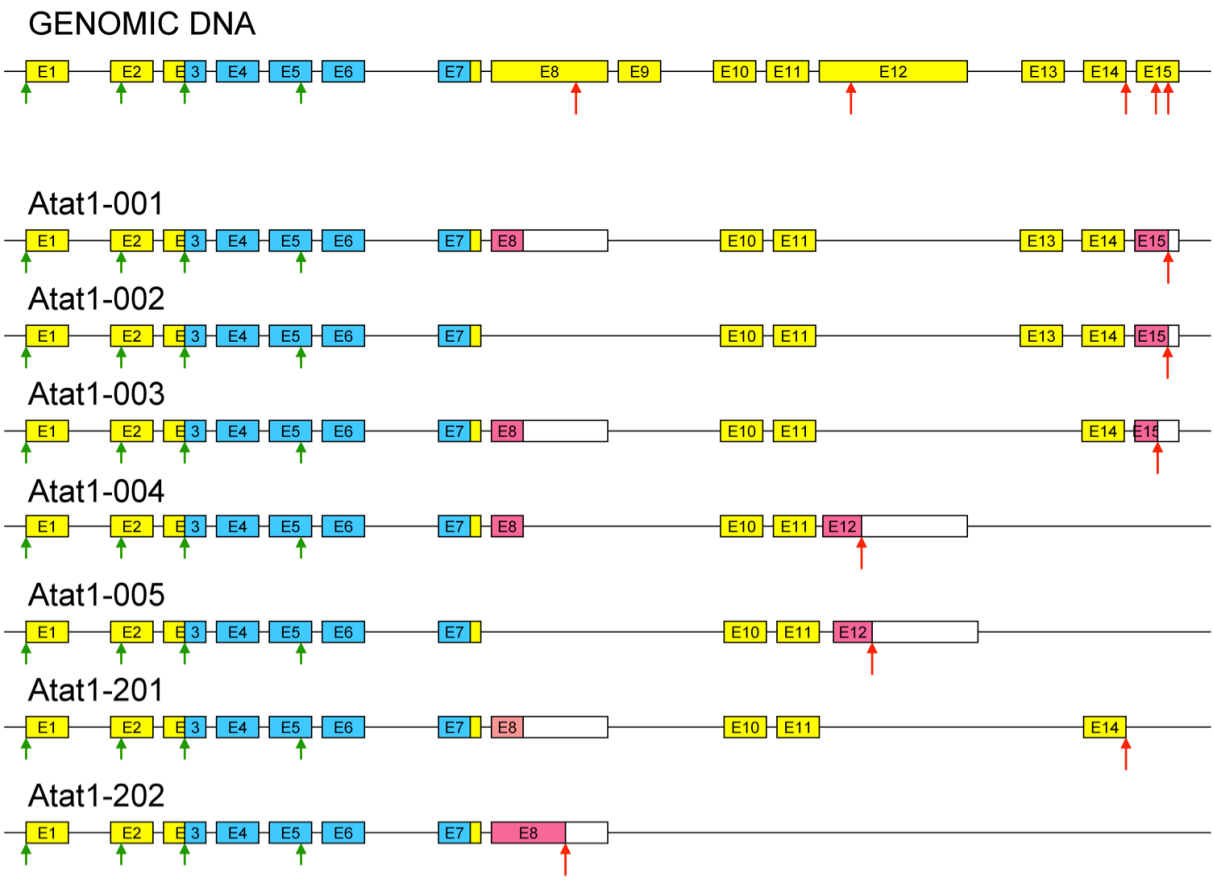

Figure 10. ATAT1 splice variants. Seven transcripts with a functional protein-coding product are presented. Atat1-005 is the reference sequence used in all further experiments. Green and red arrows indicate Start and Stop codons respectively. Exons are labeled in yellow and marked with a letter "E" and a number. Exons forming the acetyltransferase domain are indicated in blue. Truncated exons are marked in pink. All data are taken from Ensembl database.

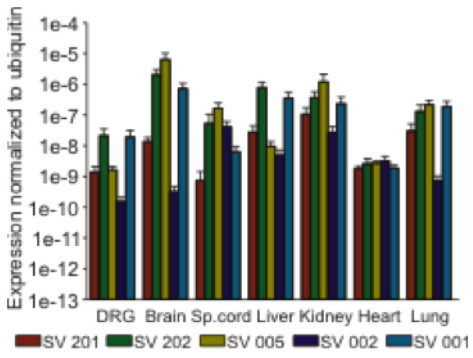

Figure 11. Expression of ATAT1 splice variants in different tissues. Five different transcripts were analyzed by RT-qPCR (n=3). All transcripts are expressed in low levels in all tested tissues.

2.1.3 Expression pattern of ATAT1 on the whole animal level

We examined the expression pattern of ATAT1 in more detail by performing *in situ* hybridization using a probe directed against the domain region that is common to all functional transcripts (exons 3 - 7, see Figure 10). We first tested if ATAT1 is expressed during embryonic development and we found strong signal in the central nervous system of E16.5 mice (Figure 12). Next we performed detailed analysis of adult tissues and found that ATAT1 has strong expression in the nervous tissues. We found particularly high signal in hippocampus (Figure 13A), cortex (Figure 13B), cerebellum (Figure 13C) and DRG (Figure 13E). Interestingly, the highest signal in non-neuronal tissues was observed in testis (Figure 13D).

These data mirror the levels of α-tubulin acetylation on the whole body level. Tubulin acetylation is present in most cell types but it is especially enriched in neurons (Fukushima et al., 2009) where it is considered to be involved in neuronal polarization (Witte and Bradke, 2008). Generally, brain is considered to be the organ with the highest levels of tubulin acetylation. Testis, on the hand, is the location for maturation of male germ cells with their characteristic heavily-acetylated flagellum.

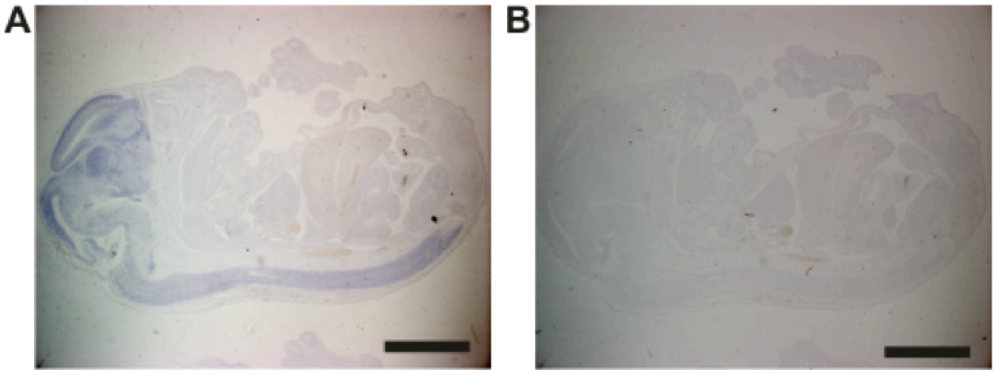

Figure 12. Expression pattern of ATAT1 in mouse embryos. *In situ* hybridization for ATAT1 domain shows strong ATAT1 mRNA expression in the central nervous system of E16.5 mice (A). (B) is a control - hybridization with a sense probe. Scale bars indicate 100μm.

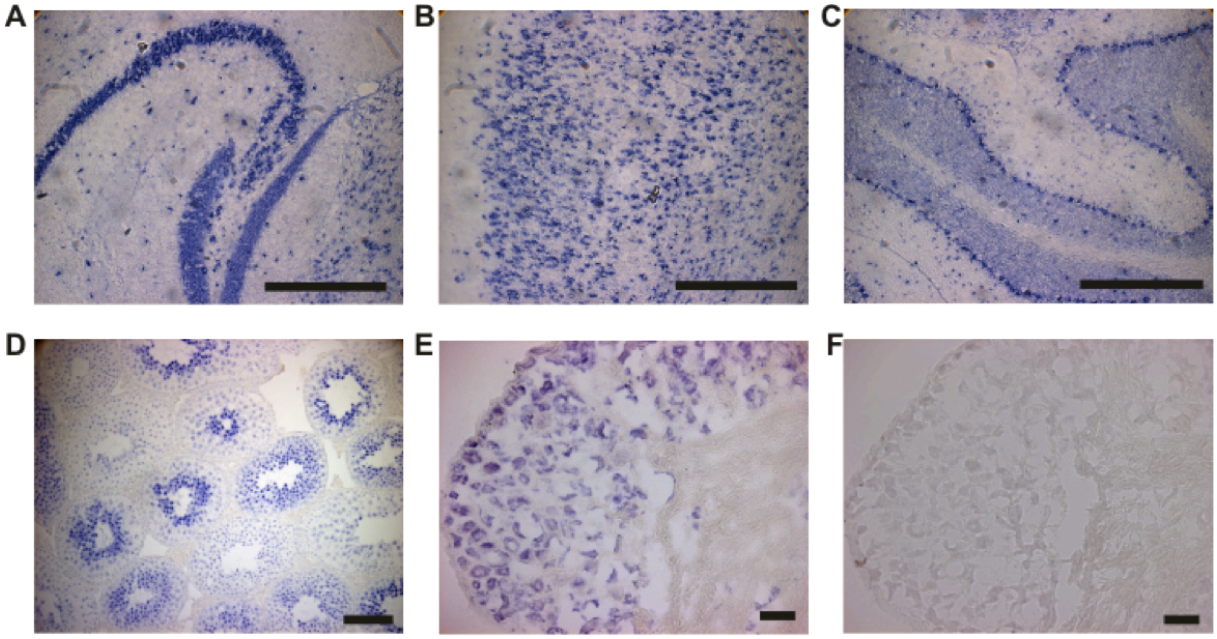

Figure 13. *In situ* hybridization for ATAT1 in 2 months old adults. Mice display expression in the nervous system, especially hippocampus (A), cortex (B), cerebellum (C) and DRG (E) and also testis (D). (F) is control hybridization with a sense probe. Scale bars indicate 500µm (A, B, C), 50µm (D) or 40µm (E, F).

2.1.4 Subcellular expression pattern of ATAT1

To examine a subcellular distribution of ATAT1 we used an antibody against the human version of the protein and immunostained mouse primary sensory neurons (Figure 14A). ATAT1 protein is especially enriched in axons, but also present in soma. In the nucleus we found very weak signal that might also be background. Co-staining with anti-acetylated tubulin antibody showed complete co-localization between ATAT1 and microtubules in axons where we were able to detect individual microtubule bundles (Figure 14B).

To confirm co-localization with microtubules we ectopically expressed ATAT1 in several immortalized cell lines and primary mouse neurons that we stained with tubulin or acetylated tubulin antibody. We also over expressed ATAT1 with some of the most known microtubule associated proteins like Tau and a plus-end binding protein EB3 (End binding protein 3) and found that they too co-localize. In transfected NIH3T3 cells we observed pronounced co-localization of YFP-ATAT1 with Tau-CFP (Figure 14E). Over expression of YFP-ATAT1

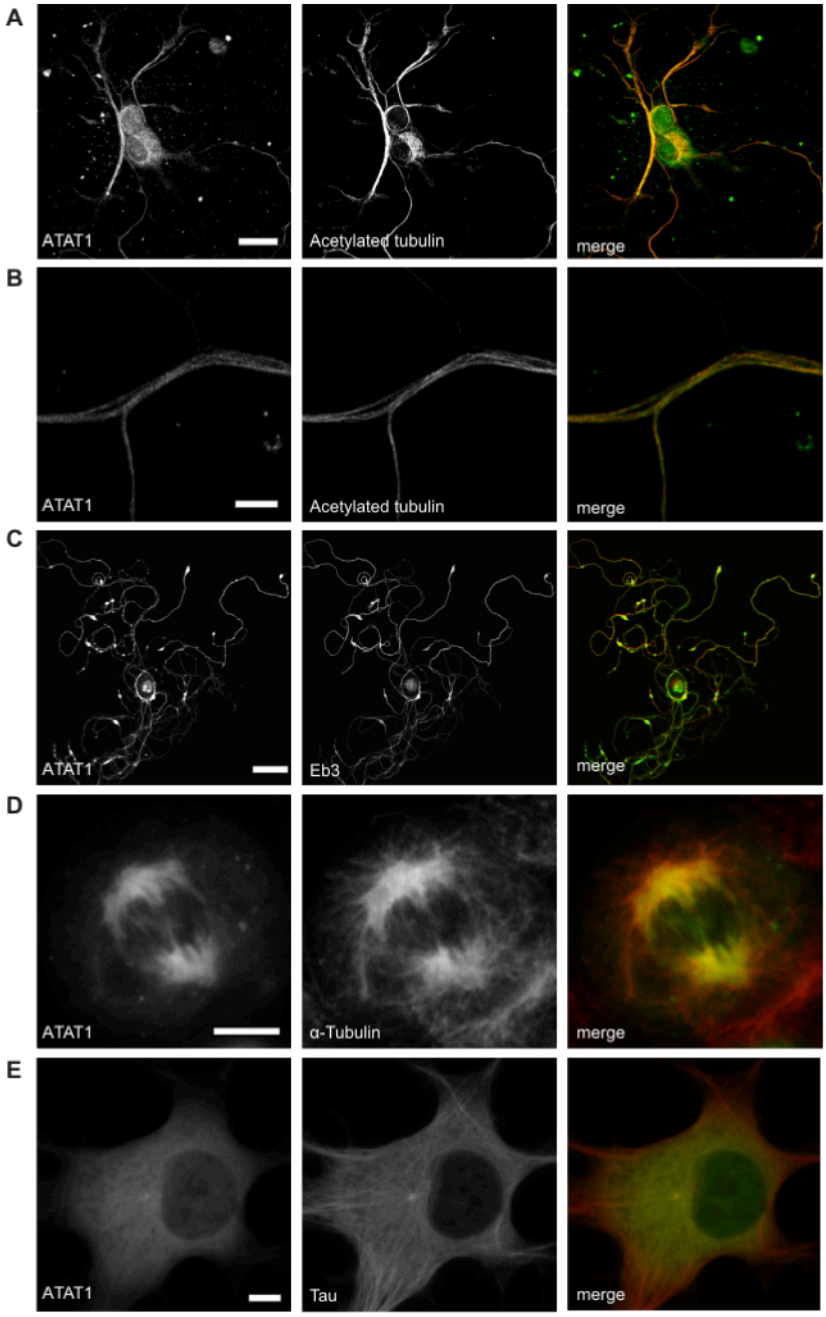

Figure 14. Subcellular localization of ATAT1. Endogenously expressed ATAT1 in DRG neruons co-localized with acetylated tubulin, especially in axons (A and B). (C) DRG neurons were transfected with YFP-ATAT1 and EB3-RFP and grown in culture for 2 days. The expression of both proteins in particularly obvious on axonal ends and branching points. (D) CHO cells transfected with YFP-ATAT1 and stained with anti-α-tubulin antibody show that during cell division ATAT1 is fully recruited to the mitotic spindle. (E) In NIH3T3 cells transfected YFP-ATAT1 co-localizes with Tau-CFP. Scale bars indicate 20µm (A), 5µm (B, D, E) or 40µm (C).

and RFP-EB3 in sensory neurons (Figure 14C) shows that ATAT1 is enriched in axonal ends and branching points, and it is generally more present in axons than in soma. Interestingly, of

all the tested MAPs, EB3 showed highest co-localization with ATAT1 in neurons and also in CHO cells (data not shown). We noticed that during cell division ATAT1 is completely localized on the mitotic spindle (Figure 14D) suggesting a possible role in the cell cycle.

2.1.5 ATAT1 is an α-tubulin acetyltransferase

Since ATAT1 protein family belongs to acetyltrasferase enzymes and our initial observations on whole animal and intracellular level showed expression of ATAT1 in tissues with high tubulin acetylation and co-localization with microtubules and MAPs we reasoned that ATAT1 is a microtubule acetyltransferase.

To test this we first, over expressed YFP-ATAT1 in CHO cells and assayed the changes in tubulin acetylation by immunofluorescence and immunoblotting with a well-known 6-11b-1 monoclonal antibody (Piperno and Fuller, 1985) against acetylated K40 of α-tubulin. Using confocal microscopy (Figure 15 A and B) we observed a four fold increase in the signal of 6-11b-1 antibody in cells over expressiong YFP-ATAT1 compared to the mock YFP transfected cells. Similar result was obtained by immunoblotting cell extracts with the same antibody (Figure 16C and 17C-D).

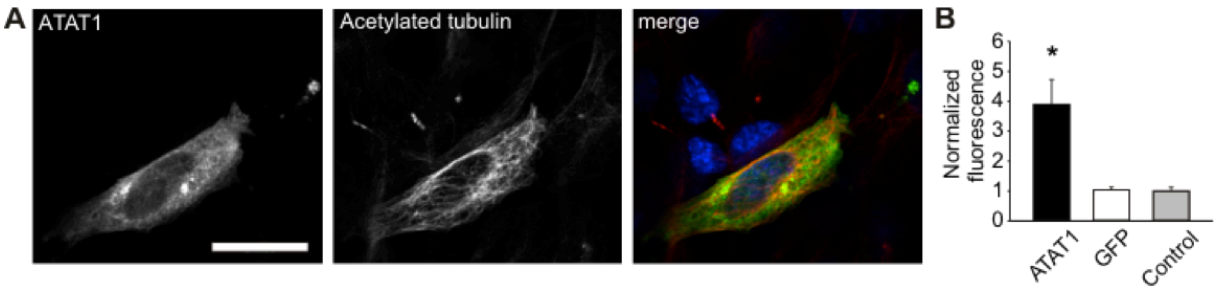

Figure 15. Over expression of ATAT1 increases tubulin acetylation. (A and B) CHO cells were transiently transfected with YFP-ATAT1 or mock GFP and stained with 6-11b-1 acetylated tubulin antibody (A). Quantification (B) shows average fluorescent intensity ($p<0.015$, $n=20$).

Next, we used shRNA against mouse ATAT1 mRNA to test for decrease in tubulin acetylation. We obtained 4 shRNAs and tested them in mouse NIH3T3 cells. The best one showed 60% decrease in expression of ATAT1 (Figure 16A) and a similar decrease in tubulin acetylation (Figure 16B and C).

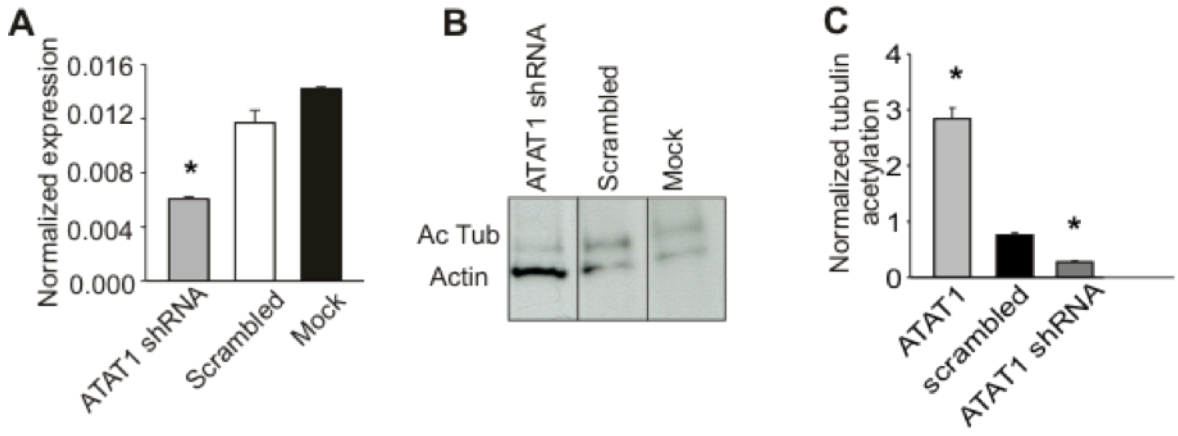

Figure 16. Knock down of ATAT1 decreases tubulin acetylation. shRNA targeted against ATAT1 reduced expression levels of ATAT1 in NIH3T3 cells (A) measured by qRT-PCR ($p<0.01$, $n=3$) and endogenous tubulin acetylation (B). (C) Tubulin acetylation is decreased by 70% in shRNA transfected cells ($p<0.01$, $n>3$).

Finally, we generated a cataytically inactive mutant of ATAT1 by mutating three amino acids in the putative AcCoA binding domain (Steczkiewicz et al., 2006). ATAT1 has the highest similarity with histone acetyl-transferases in Motif A that probably binds AcCoA before transfering the acetyl group to a substrate. The central part of this motif is an α-helix that is highly conserved in all animals (Figure 17A). We disrupted this helix by mutating three residues (G134W-G136W-L139P) and named it ATAT1-GGL (Figure 17B). CHO cells over expressing ATAT1-GGL showed no increase in tubulin acetylation by western blot (Figure 17 C and D) suggesting that the mutated protein is indeed catalytically inactive.

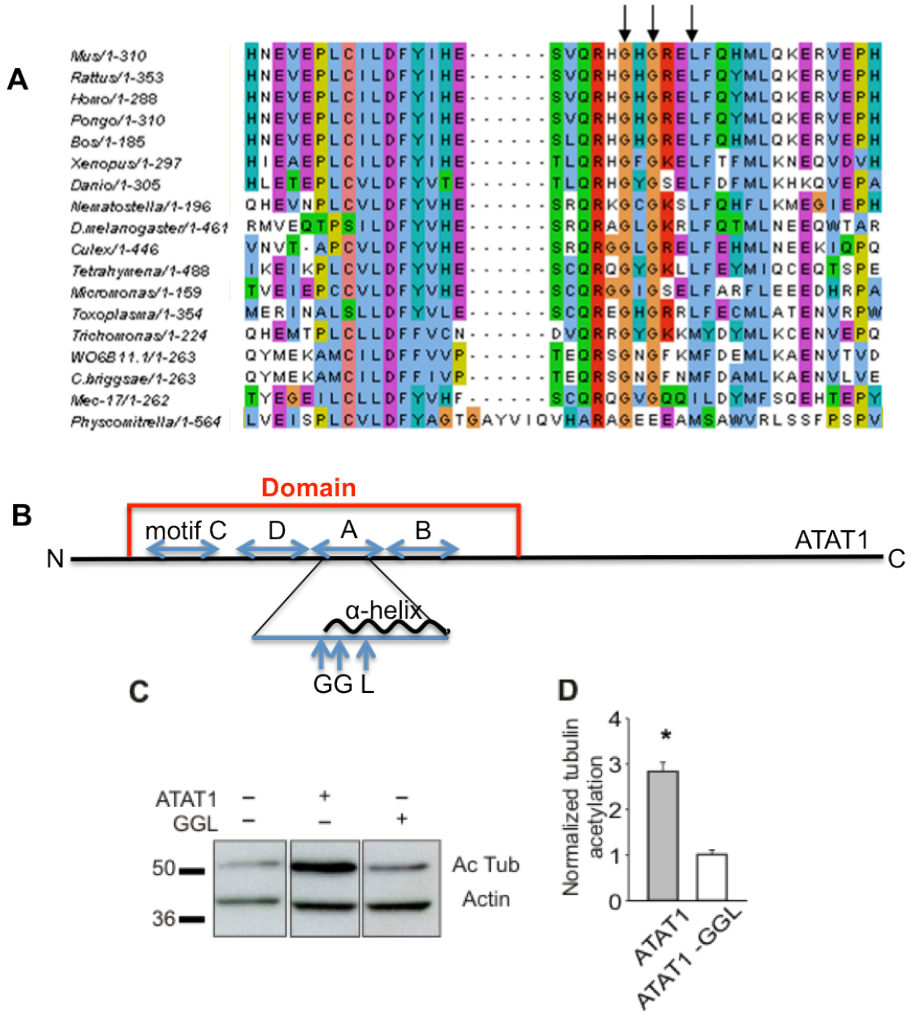

Figure 17. Catalytically inactive mutant does not acetylate microtubules. (A) Evolutionary conservation of the residues in α-helix that is part of Motif A that is responsible for binding AcCoA. (B) Schematic representation of the Motif A and three mutated residues. (C) Representative western blot showing increase in α-tubulin acetylation by 6-11b-1 antibody upon ATAT1 transfection and no increase upon ATAT1-GGL transfection. (D) Quantification of (C) ($p<0.01$, $n>3$).

2.1.6 α-Tubulin and ATAT1 itself are the only targets of ATAT1

In the past several years lysine acetylation has emerged as one of the major posttranslational modifications of cytoplasmic proteins (Choudhary et al., 2009). Having identified a novel acetyl transferase we ought to determine if there were other potential targets, except tubulin, in mammalian cells. We approached this question with two methods - immunofluorescence and immunoblotting.

First, we used a pan acetyl K antibody that recognizes many different acetylated lysines in the cell (more than 3000 sites). CHO cells that were over expressing YFP-ATAT1 showed dramatic increase in cytoplasmic acetylation (Figure 18) compared to mock YFP transfected cells. Interestingly, levels of acetylation in the nucleus remained the same.

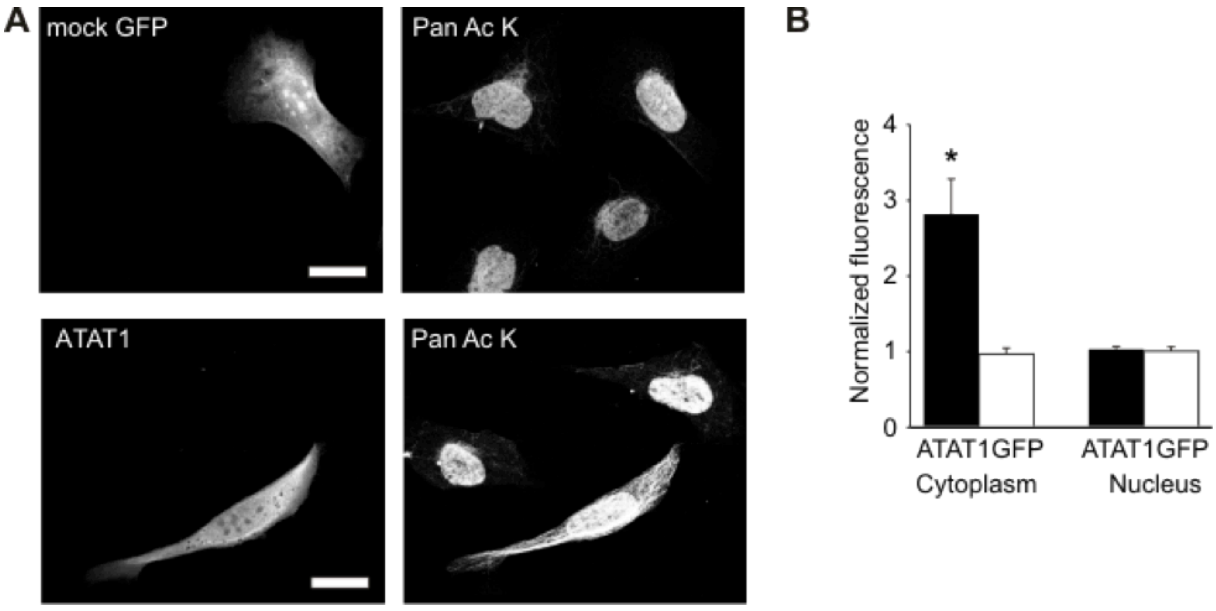

Figure 18. ATAT1 increases acetylation in the cytoplasm. (A) CHO cells were transfected with YFP-ATAT1 or mock YFP and subsequently stained with pan acetyl lysine antibody. (B) Quantification of (A) showing increase in cytoplasmic acetylation with no change in the nucleus.

Still using immunofluorescence we decided to understand if all the cytoplasmic acetylation can be colocalized with microtubules. To do that we performed a triple staining of transfected CHO cells and noticed that all ATAT1-mediated acetylation is associated with microtubules (Figure 19). These data suggest that only α-tubulin and proteins that colocalize with it can be targets of ATAT1.

In order to discriminate between microtubules and microtubule associated proteins we lysed transfected HEK cells and immunoblotted them against pan acetyl lysine antibody (Figure 20A). The results show that only the tubulin band (at 50kDa) displayed an increase after ATAT1 over expression.

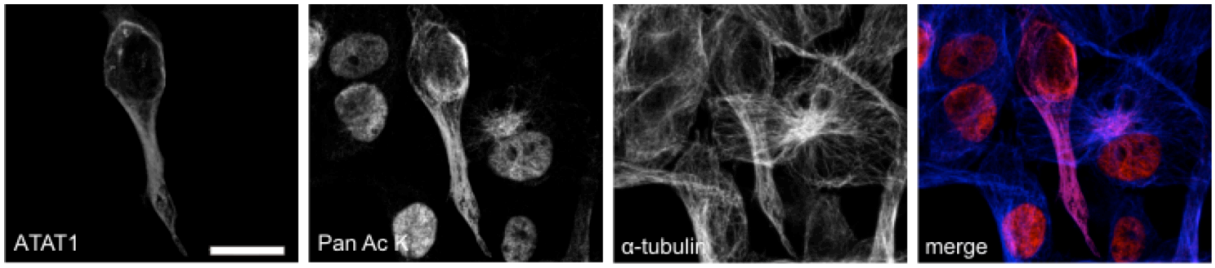

Figure 19. All ATAT1 mediated acetylation in the cytoplasm is colocalized to microtubules. CHO cells were transfected with YFP-ATAT1 and subsequently stained with pan acetyl lysine and α-tubulin antibodies. The merge images show that all cytoplasmic acetylation comes from microtubules.

We next sought to challenge the system by applying an inhibitor of deacetylases called trichostatin A (TSA). We over expressed ATAT1 (non-tagged) and YFP as a control in NIH3T3 cell and treated them with TSA before harvesting. In ATAT1 transfected cells, immunoblotting against pan acetyl lysine antibody (Figure20B) showed a dramatic increase of two bands - tubulin at 50kDa and another band at 37kDa which we believe is ATAT1 itself. As a control of the TSA treatment we see that tubulin acetylation is increased also in the mock transfected cells compared to non-treated cells.

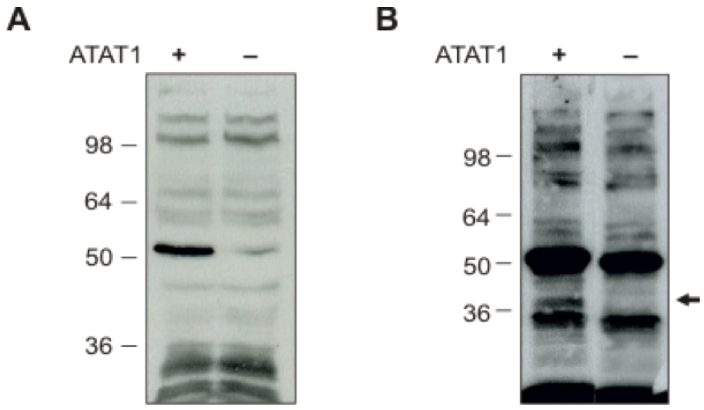

Figure 20. Tubulin and ATAT1 itself are the only targets of ATAT1. (A) HEK cells were transfected with YFP-ATAT1 and mock YFP and subsequently immunoblotted against pan acetyl lysine antibody. (B) NIH3T3 cells were transfected with ATAT1 and mock YFP and treated with TSA before harvesting. Immunoblot against pan acetyl lysine antibody shows increase in acetylation of two proteins - tubulin and ATAT1.

Taken together, these data show that in three different mammalian cell lines ATAT1 over expression causes increases in tubulin acetylation, and the only other target that can be seen when the system is challenged is ATAT1 itself, suggesting that ATAT1 is a tubulin-specific acetyl transferase.

2.1.7 ATAT1 directly acetylates microtubules

We next determined whether ATAT1 interacts directly with microtubules. Interaction was first tested by co-immunoprecipitation of tubulin with flag-tagged ATAT1 on whole cell extracts. CHO cells were transfected with flag-tagged ATAT1 and mock flag tag, after which Co-IP was performed with anti-flag antibody. The results (Figure 21A) show weak tubulin band in the ATAT1 elution. To further confirm this we isolated a microtubule fraction from transfected cells and after two rounds of ultracentrifugation we were able to detect ATAT1 in the microtubule fraction while all the contaminants (such as actin) were removed (Figure 21B). These results show that ATAT1 and tubulin do interact directly but in a rather transient way.

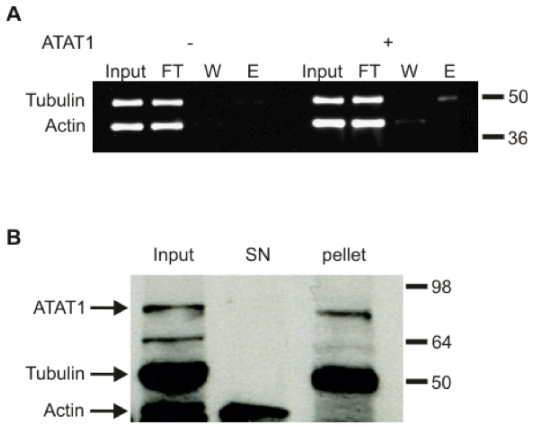

Figure 21. ATAT1 interacts directly with tubulin. (A) CHO cells were transfected with flag-tagged ATAT1 and mock flag tag and harvested. Protein extracts were immunoprecipitated with flag antibody. Weak tubulin band is present in the ATAT1 elution but absent in the control elution. (B) CHO cells were transfected with YFP-ATAT1 and subsequently cytoplasmic extracts were ultracentrifuged two times. After the second centrifugation ATAT1 is still present in the microtubule fraction while contaminants like actin are in the supernatant.

To show that ATAT1 can directly acetylate microtubules we designed a radioactive assay with purified bovine brain tubulin, 13C AcCoA and recombinant ATAT1. ATAT1 was cloned in a his-tag plasmid, expressed in bacteria, purified using the His tag column and finally digested to remove the tag. Recombinant ATAT1 readily acetylated microtubules in the radioactive *in vitro* assay (Figure 22A and B). We established that the mass ratio 4:1 between ATAT1 preparation and tubulin is optimal for our assay. This ratio cannot be considered as physiological since ATAT1 is an enzyme and in the cell it should be present in several fold less concentration than tubulin. Rather, we believe that this ratio is a consequence of the low purity of ATAT1 preparation, where presumably certain percentages of the degradation products lose their activity. The time needed for the acetylation reaction to saturate was 30min (Figure 23B). This is in disagreement with Shida et al. (2010) (Shida et al., 2010) who later reported that 12 hours are needed for the saturation. Although our assay is done on 37°C and theirs on 25°C, such temperature dependence is unlikely and the difference might be explained by differences in purity of the preparation or reaction conditions that affect enzymatic kinetics.

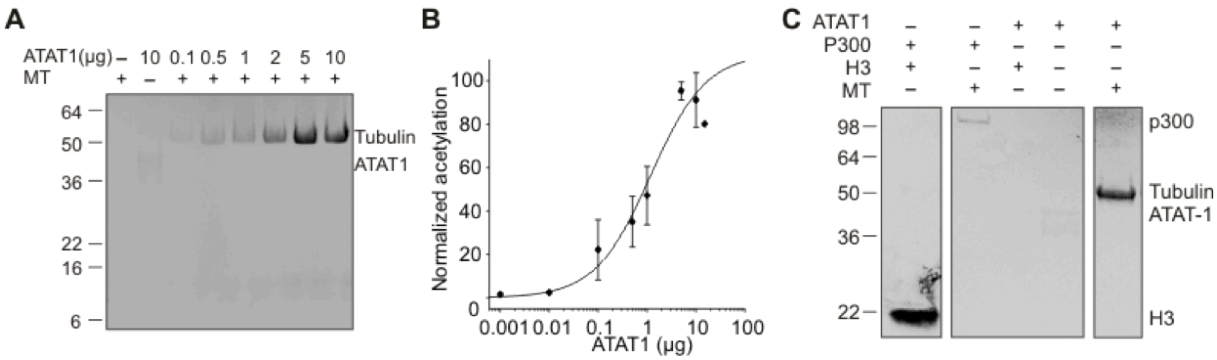

Figure 22. ATAT1 directly acetylates microtubules. (A) Autoradiography of ATAT1 mediated [^{14}C]acetyl incorporation into polymerized microtubules. In the absence of tubulin, autoacetylation is more evident. (B) Concentration-dependence of ATAT1 mediated acetylation (n=3). (C) ATAT1 specifically acetylates microtubules *in vitro*. Autoradiography of [^{14}C]acetyl incorporation. ATAT1 readily acetylates microtubules (MT), but does not acetylate histones (H3). In the reaction with histones and without tubulin a band at 37kDa is visible that corresponds to ATAT1 itself. The histone acetyl-transferase P300/CBP strongly acetylates histones, but does not influence microtubule acetylation.

Furthermore, we demonstrated the specificity of the assay by replacing histone H3 and histone acetyltransferase p300/CBP as alternative substrate or enzyme (Figure 22C). While p300 readily acetylated H3, there was neither acetylation of microtubules by p300/CBP, nor H3 by ATAT1. These data show that ATAT1 is the first and only acetyltransferase described so far that does not acetylate histones. ATAT1 autoacetylation was detected also in this *in vitro* assay which confirmed our initial observation in cells. The ATAT1 band is the most obvious in the absence of tubulin (Figure 22A and C).

Microtubules have been shown to be acetylated in their polymerized form (L'Hernault SW, 1983; Webster DR, 1989) and we investigated whether ATAT1 shows preference towards polymerized microtubules. Interestingly, we noticed that ATAT1 acetylates soluble tubulin very poorly (Figure 23). To differentiate between polymerized microtubules and the ones being polymerized we added GTP and glycerol at different time points. These two compounds are routinely used for polymerization of microtubules and the amount of time needed for the reaction to saturate was around 20min in our hands. Hence, for the "polymerized" microtubules we added GTP and glycerol 30min before ATAT1 and AcCoA were added, while for the "polymerizing" microtubules we added all the components at the same time. Our results show that ATAT1 acetylated "polymerized" microtubules faster than the "polymerizing" ones (Figure 23). However the fastest of all was incorporation of acetyl group into stable microtubules. These microtubules were polymerized by a treatment with a microtubule stabilizer taxol. This implies that acetylation happens mainly on polymerized microtubules with preference towards stable over dynamically instable microtubules.

To explore the specificity of ATAT1 mediated acetylation further, we subjected *in vitro* reaction samples to mass spectrometry (MS) analysis. For this purpose we used [^{13}C]acetylCoA that is very suitable for MS since it is not radioactive and it has a mass difference of 2Da compared to the 12C acetyl. This mass difference enabled us to discriminate between the sites acetylated before the reaction started and the sites acetylated

during the reaction. As expected, we detected incorporation of [^{13}C]acetyl onto K40 of α-tubulin (Table 2). Intriguingly, we also identified four separate acetylated lysine residues on ATAT1 itself, spanning the acetyl transferase domain (K56 in motif C and K146 in motif A, (Steczkiewicz et al., 2006) and the unstructured C-terminus (K210 and K221, Table 2).

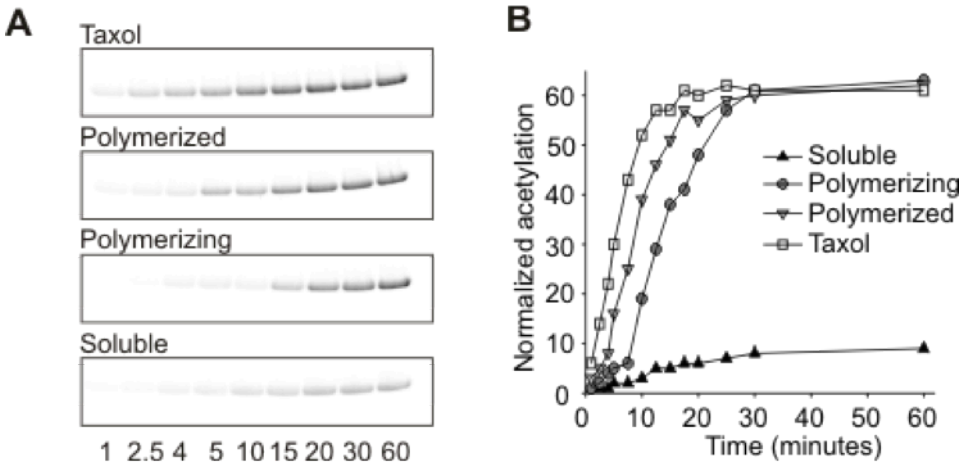

Figure 23. ATAT1 preferentially acetylates polymerized tubulin. "Taxol" and "Polymerized" microtubules were treated with 3μM taxol or 1mM GTP + 15% glycerol respectively for 30 minutes before the acetylation reaction. "Polymerizing" microtubules were polymerized with 1mM GTP and 15% glycerol during the acetylation reaction, and "Soluble" microtubules were incubated with 1mM GDP and without glycerol during acetylation. (A) Example of autoradiography. Reactions were stopped by adding SDS loading buffer at times indicated below (in minutes). (B) Quantification of (A).

Table 2. Identification of acetylated lysine residues on α-tubulin and ATAT1.

Protein	Acetylation sites	Region
α-tubulin	K40	Lumen
ATAT1	K56	Ac domain – motif C
ATAT1	K146	Ac domain – motif A
ATAT1	K210	C-terminus
ATAT1	K221	C-terminus

2.1.8 Autoacetylation of ATAT1 increases its catalytic activity at microtubules

We investigated ATAT1 autoacetylation in more detail to determine whether it might function as a regulatory mechanism for acetylation of microtubules. We first examined the kinetics of the *in vitro* reaction and observed that autoacetylation took 24 hours to saturate (Figure 24A and B). This was approximately 50 times slower than tubulin acetylation and [^{14}C]acetyl incorporation never attained levels equivalent to that of tubulin. We next investigated the effects of ATAT1 autoacetylation on its catalytic activity at tubulin. We preincubated ATAT1 with or without [^{14}C]acetyl-CoA for 24 hours and then added tubulin and measured [^{14}C]acetyl incorporation (Figure 24C). Autoacetylation of ATAT1 strongly increased tubulin acetylation indicating that this may be an important regulatory loop for enzymatic activity (Figure 24D). Importantly, incubation of ATAT1 without AcCoA for 24 hours did not make the enzyme less efficient since it showed similar level of tubulin acetylation as control (a standard 30-min reaction with fresh components).

To explore the importance of autoacetylation further at the cellular level, we first mutated three of the lysine acetylation targets identified in mass spectrometry experiments to arginine to eliminate acetylation at these sites (K56, K210 and K221: ATAT1-3R). Transfection of this mutant strongly diminished ATAT1 autoacetylation upon TSA treatment indicating that these residues are the major targets for ATAT1 mediated self-acetylation (Figure 24G). Importantly, we also observed a dramatic reduction in tubulin acetylation in the presence of ATAT1-3R compared to wild type ATAT1 (Figure 24E and F). The reduction was approximately 50%. Later, we identified a fourth site on ATAT1 (K146) and we made a quadruple mutant that showed further reduction in acetylation (Figure 24H, approximately 65% reduction). Taken together, these data demonstrate that self-acetylation of ATAT1 is functionally significant and that it could underlie an important regulatory mechanism for tubulin acetylation.

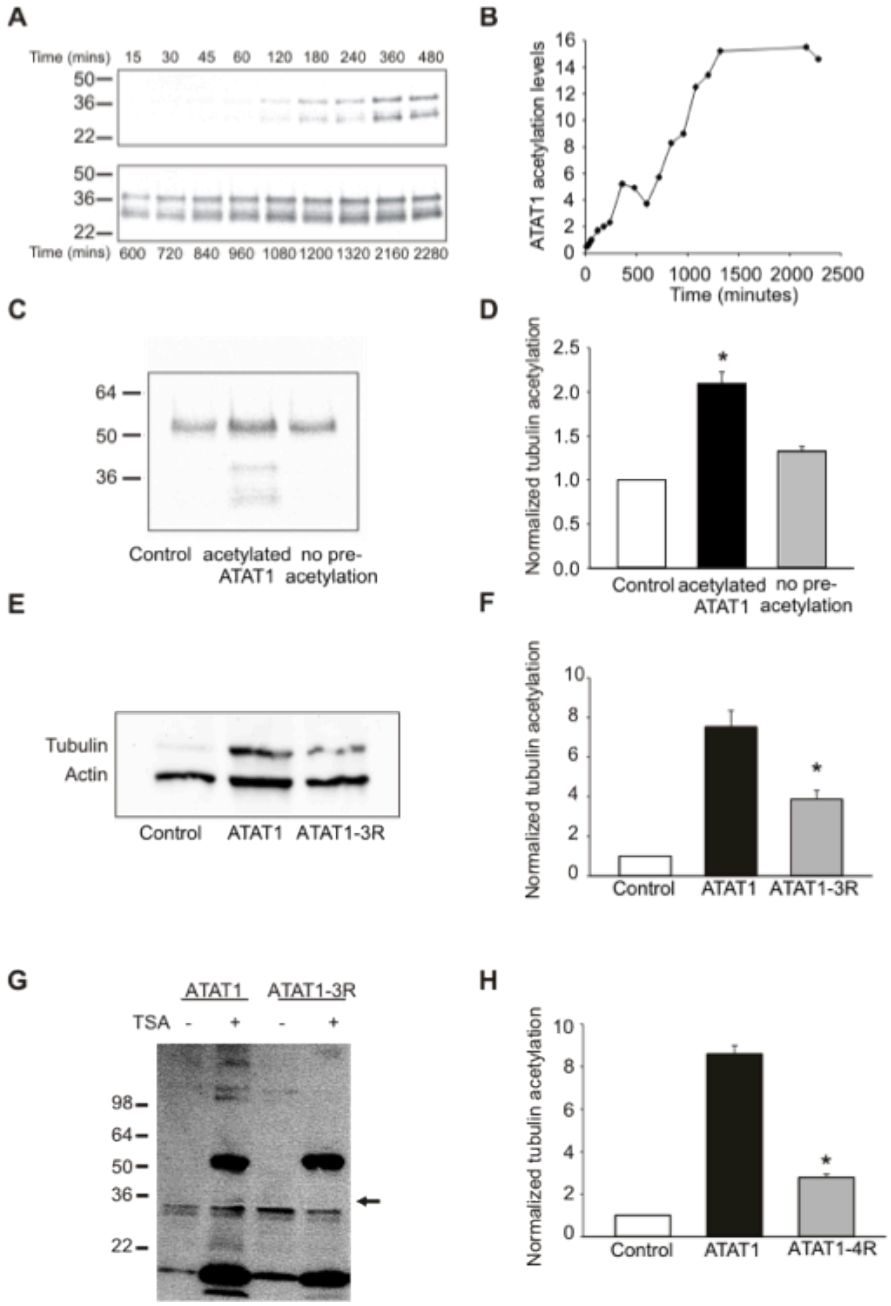

Figure 24. Autoacetylation increases catalytic activity of ATAT1. (A and B) Autoradiography of [^{14}C]acetyl incorporation into ATAT1. Recombinant ATAT1 is present as two bands (37kDa and 30kDa). For both bands the saturation of autoacetylation reaction is achieved after 24 hours (n=3). (C and D) Pre-incubation of ATAT1 with [^{14}C]acetyl-CoA for 24 hours increases its subsequent catalytic activity at tubulin (n=3, $p<0.02$). (E and F) ATAT1 autoacetylation regulates its catalytic activity *in vivo*. Immunoblot (E) of mock, ATAT1 and ATAT1-3R transfected NIH3T3 cell extracts against acetylated tubulin and actin (n=3, $p<0.02$). (G) ATAT1-3R acetylation is undetectable. Acetyl-lysine immunoblot of NIH3T3 cells treated or not treated with TSA (5μM) for 4 hours. Additional band (arrow) that corresponds to ATAT1 itself is absent in ATAT1-3R over expression. (H) Same as (F) just with ATAT1-4R. Tubulin acetylation is reduced by 65%.

2.2 ATAT1 influences microtubule stability and dynamics

2.2.1 ATAT1 reduces microtubule stability

The relationship between acetylation and microtubule stability has been one of the most important questions in this field. Stable microtubules accumulate many posttranslational modifications including acetylation (Hammond et al., 2008), but it is still not known whether acetylation actively stabilizes microtubules since there is evidence on both sides (Haggarty et al., 2003b; Matsuyama et al., 2002b; Palazzo et al., 2003; Tran et al., 2007a; Zhang et al., 2008a). Since most of the previous experiments have been done by modifying the activity of HDAC-6 and using inhibitors of both deacetylation and acetylation we decided to approach this problem using our novel tools and findings on the function of ATAT1.

Detyrosination of α-tubulin is a well-described posttranslational modification that takes place at the C-terminus of α-tubulin where the last residue, a tyrosine can be removed. It has been shown that detyrosination happens on stable microtubules and using a monoclonal antibody that specifically recognizes detyrosinated tubulin, one is able to distinguish stable from short-lived microtubules.

Surprisingly, over expression of either ATAT1 or the catalytically inactive mutant ATAT1-GGL led to a dramatic reduction in the intensity of staining for detyrosinated tubulin, and significantly decreased the number of cells containing stable microtubules (Figure 25). These unexpected observations indicate that increased acetylation *per se* is not sufficient to stabilize microtubules. Levels of tubulin acetylation were approximately four-fold higher in cells transfected with ATAT1 (Figure 15), yet these cells displayed fewer stable microtubules. Furthermore, since decreased microtubule stability persisted in cells expressing the acetyl-transferase inactive mutant, our data suggest that ATAT1 might exert its influence by interacting directly with microtubule associated proteins.

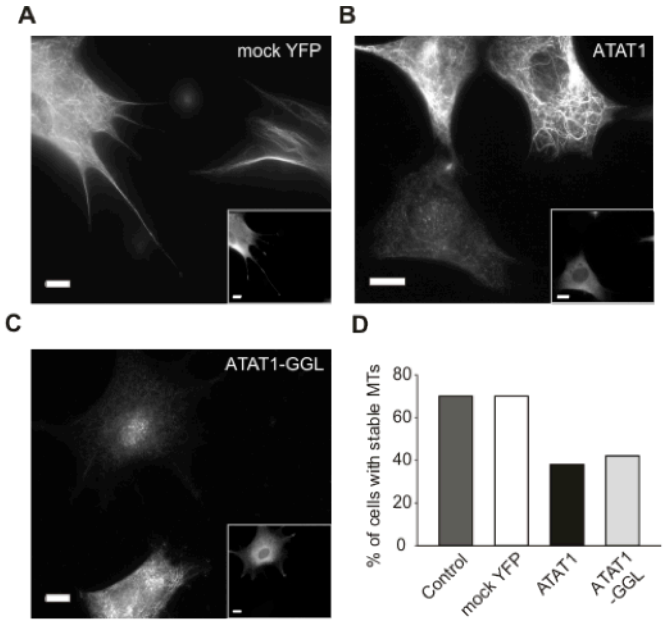

Figure 25. ATAT1 reduces microtubule stability. NIH3T3 cells, transfected with mock YFP (A), ATAT1 (B) and ATAT1-GGL (C) were stained with anti-detyrosinated tubulin antibody. ATAT1 and ATAT1-GGL transfected cells (insets) show reduced detyrosination. Scale bars indicate 20µm. (D) The proportion of cells with stable microtubules is reduced upon transfection with ATAT1 and the catalytically inactive mutant ATAT1-GGL (n=100).

2.2.2 Interactions of ATAT1 with MAPs

To explore interactions between ATAT1 and other microtubule associated proteins we followed a dual approach; earlier observations of complete colocalization between ATAT1 and EB3 prompted us to examine this interaction in more detail and in parallel we performed a pull down of ATAT1-binding proteins from mouse brain.

We isolated cytoplasmic protein extracts from wild-type C57BL/6 mice and passed them through a column where recombinant ATAT1 was conjugated to the beads. The control was just passed through an empty column and ATAT1 was added in the control tube before loading on the gel. This way ATAT1 itself (present in multiple bands) could not interfere with results. Loading the elutions on a 2D gel showed 4 major bands present in the ATAT1 side (Figure 26). The gel was stained with silver and the bands were cut and sequenced using Mass Spectrometry. The best-fit candidates are listed in Table 3. It is worth noticing that all of them

are microtubule associated proteins. Kinesin transport has earlier been shown to be influenced by acetylation (Reed et al., 2006) so Kinesin-2 would be an interesting candidate to test the influence of microtubule-dependent transport by ATAT1-mediated acetylation.

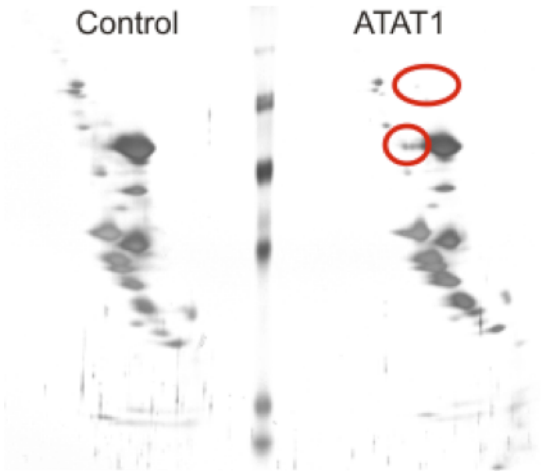

Figure 26. Interaction partners of ATAT1. 2D gel stained with silver showing bands of interaction partners of ATAT1. Control pull down was done by passing the brain extracts through an empty column and ATAT1 has been added afterwards as a gel control.

Table 3. List of proteins sequenced by MS from the bands cut in Figure 20.

Mol.weight	Most probable candidate
200 kDa	MAP-2
98 kDa	Dynamin 1, 2, 3
80 kDa	MAP-6
70 kDa	Kinesin-2

At the same time we performed an in-depth analysis of the ATAT1-EB3 interaction guided by previous observations on their colocalization. We first fused N- and C-terminal halves of YFP protein to EB3 and ATAT1 respectively and used Bimolecular Fluorescence Complementation (BiFC) to monitor protein-protein interactions (Hu and Kerppola, 2003). Strikingly, we observed a rapidly developing signal on microtubules as fragments of the fluorescent fusion proteins came together (Figure 27A). The control reactions were done with

either EB3 or ATAT1 fused with YFP halves co-transfected with the other half of YFP protein and they both yielded no signal at all (data not shown).

Next, we investigated this interaction more quantitatively by measuring Förster resonance energy transfer (FRET) between EB3 and ATAT1. Strong FRET signal was observed in cells expressing EB3-CFP and ATAT1-YFP that was particularly prominent on microtubule-like structures (Figure 27B). We quantified FRET by calculating apparent FRET efficiency (EFRET) across cells and observed significant increases in signal that concentrated on microtubules (Figure 27C). This correlated with high levels of EB3 expression and probably reflects EB3 decoration of the microtubule lattice as occurs during over expression (Stepanova et al., 2003). We further validated our FRET measurements by applying nocodazole to cells to dissociate EB3 from microtubules (Stepanova et al., 2003). Nocodazole treatment resulted in a dramatic reduction in FRET at the cell periphery and a reorganization of the microtubule network. Taken together these results indicate that EB3 and ATAT1 interact physically on microtubules. Since EB3 is used as a marker of microtubule dynamics we continued our research using this protein.

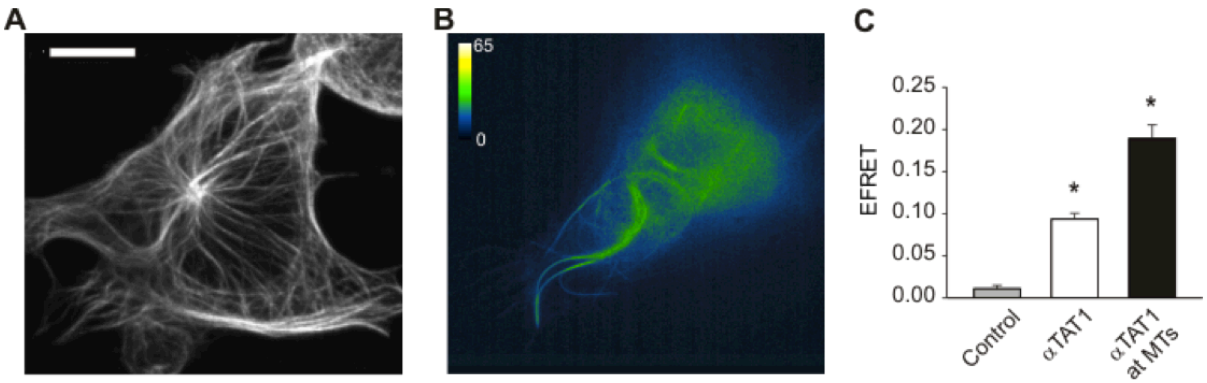

Figure 27. ATAT1 interacts with EB3. Representative BiFC (A) and FRETC (B) images of NIH3T3 cells transfected with ATAT1 and EB3. (C) EFRET signal is highest on microtubules (n>20).

2.2.3 ATAT1 influences microtubule plus-end dynamics

In vivo, microtubules are not constantly polymerized, they rather continually go through cycles of polymerization and depolymerization known as dynamic instability (Mitchison and Kirschner, 1984). End-binding proteins travel on microtubule tracks from the MTOC (Microtubule organizing center) towards the periphery. Imaging of these proteins can be used to quantify the parameters of microtubule growth (polymerization), shrinkage (depolymerization) and intermittent pause.

We used a recently developed computational tracking package (*plusTipTracker* (Matov et al., 2010; Myers et al., 2011; Thoma et al., 2010) to infer microtubule growth, pause and shrinkage events from live-cell images of EB3-RFP. We quantified the speed, displacement and lifetime of EB3 particles for each of these events and evaluated the effects of ATAT1 depletion and over expression on dynamic instability. shRNA targeted against ATAT1 reduced the speed and displacement of microtubules undergoing growth, pause and shrinkage ($p=0.04$, two-way ANOVA for all parameters versus control); a mild effect that might reflect the low basal levels of ATAT1 in NIH3T3 cells and 65% efficiency of the knock-down. However, over expression of ATAT1 induced substantial increases in speed (Figure 28A-E) and displacement of EB3 particles (Figure 28F-J), and also significantly increased the length of time particles spent at pause (Figure 28K). To elucidate the role of tubulin acetylation in this process we examined the effects of the catalytically inactive mutant ATAT1-GGL. This mutant closely copied the behavior of wild type ATAT1 and displayed similar effects on the speed, displacement and pause duration of EB3 particles.

These results show that acetylation is not required for ATAT1-mediated acceleration of microtubule plus-end dynamics, but that ATAT1 protein itself is necessary for this process.

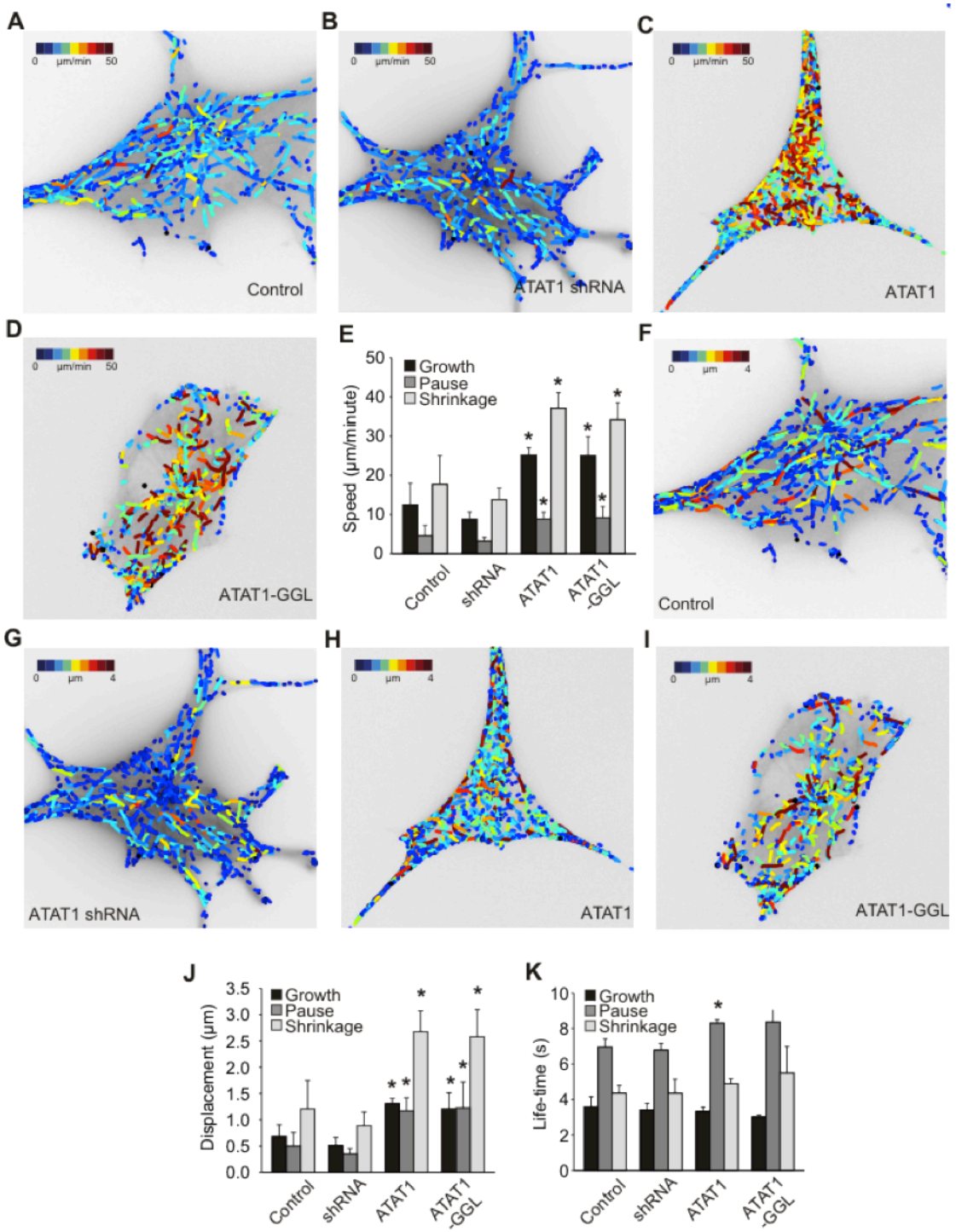

Figure 28. ATAT1 regulates microtubule dynamics. (A-D) Live cell images with a color-coded overlay representing EB3 particle growth speed. NIH3T3 cells were transfected with RFP-EB3 and mock YFP (A), ATAT1 shRNA (B), YFP-ATAT1 (C) or YFP-ATAT1-GGL (D) respectively. Video microscopy data were analyzed using the *plusTipTracker* software package. Data for plus-tip growth, pause and shrinkage are represented in (E) (n=20). (F - J) ATAT1 increases the displacement of EB3 particles. Live cell images with a color-coded overlay representing EB3 particle displacement. NIH3T3 cells were transfected with RFP-EB3 and mock YFP (F), ATAT1 shRNA (G), YFP-ATAT1 (H) or YFP-ATAT1-GGL (I) respectively. (J) Quantification of (F - I). (n=20). (K) Life-time of EB3 pauses is increased upon ATAT1 and ATAT1-GGL over expression (n=20).

2.3 Both enzymatic and structural roles of *mec-17* are important for touch sensation and neuronal morphology

2.3.1 *mec-17* but not *atat-2* mutants show morphological defects

To investigate the effect of ATAT1-class proteins *in vivo* I went to Martin Chalfie's laboratory in New York to analyze *C.elegans* mutants of this gene. As mentioned previously, *C.elegans* is one of the few organisms that has two members of the ATAT1 family. In addition to *mec-17*, there is also the recently named *atat-2* (standing for α-tubulin acetyltransferase 2). Apart from the previously mentioned original *mec*-17 allele, *u265,* which contains two missense mutations (Chalfie and Au, 1989; Zhang et al., 2002), the *C. elegans* Knockout Consortium (Moerman, 2008) produced deletion alleles for both *mec-17(ok2109)* and *atat-2(ok2415)*.

We touch tested all the above strains and confirmed that *mec-17(u265)* animals show touch-insensitivity only in the adult age (Figure 29A). We also observed a dramatic touch insensitivity of *mec-17(ok2109)* animals from the early larval stages (Figure 29A). *atat-2* animals, on the other hand, showed very mild reduction in touch sensitivity that was not enhanced even in the *mec-4(u45ts)* sensitized background (Figure 29B). Interestingly, the double mutant (*mec-17;atat-2*) showed the most dramatic loss of touch sensitivity, that was significantly lower than in *mec-17* animals (Figure 29A).

The effect on touch sensitivity correlates with the expression of these genes. While *mec-17* has been known as one of the most expressed genes in touch receptor neurons (Zhang et al., 2002), atat-2 is expressed in much lower amounts. We measured the expression of both of these genes in wild type L4 animals using single molecule fluorescence *in situ* hybridization (SM-FISH) and noticed highly significant difference in the expression in PLM neurons

(Figure 29C). While *atat-2* had 1-12 mRNA molecules per cell, we found 23-68 *mec-17* mRNA molecules in the same cells. This high level of expression suggests a unique role of *mec-17* in touch receptor neurons. To test if the *atat-2* expressed at the levels of *mec-17* could rescue touch insensitivity we over expressed *atat-2* under the *mec-17* promotor. This resulted in touch insensitive animals with morphologically impaired touch receptor neurons (Figure 29D). These defects, which demonstrate a gain-of-function phenotype for *atat-2* overexpression, are never seen with the *mec-17* genomic transformants.

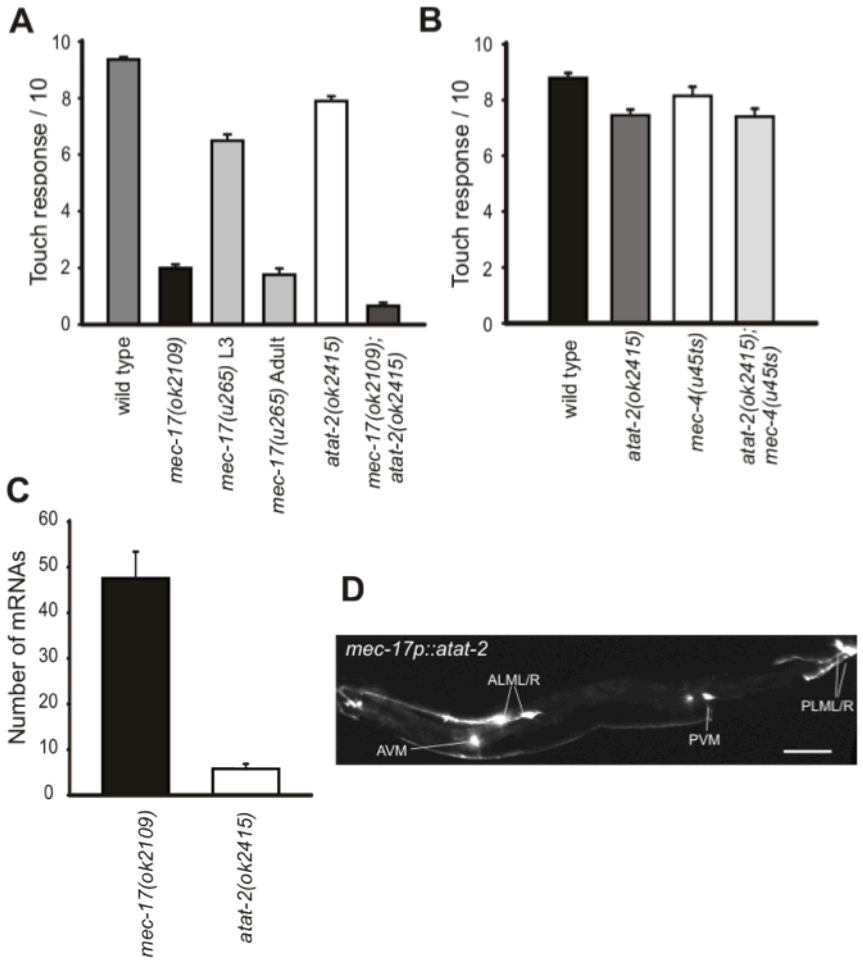

Figure 29. Mutant phenotype and expression of *mec-17* and *atat-2*. (A) Touch sensitivity is largely reduced in *mec-17* mutant animals and slightly decreased in *atat-2* mutants. Adult animals from each strain were touched alternately in the head and tail a total of ten times and the number of responses (mean ± S.E.M.) was recorded (n=30). (B) The slight touch insensitive phenotype of *atat-2* mutant is not enhanced in animals with the sensitizing *mec-4(u45ts)* mutation. (C) PLM neurons in wild type larvae have more *mec-17* mRNA (mean number of molecules ± S.E.M.; n = 10) than *atat-2* mRNA. (D) *atat-2* over expressed under the promotor of *mec-17* results in animals with morphologically impaired TRNs. Scale bar indicates 40µm, TRNs are indicated with lines.

MEC-17 and ATAT-2 differ also in the expression pattern. While *mec-17* is a gene specific for sensory neurons (apart from touch receptor neurons it is found to be expressed at lower levels also in PVD neurons that respond to harsh touch), *atat-2* is expressed in many different types of neurons and its expression pattern is quite similar to the expression pattern of *mec-12*, the only acetylatable α-tubulin in *C.elegans*.

Although only *mec-17* seems to be seriously affecting touch sensitivity, both *mec-17* and *atat-2* are sufficient for microtubule acetylation. As in mammalian cells, we measured acetylation using the antibody 6-11B-1 (Piperno and Fuller, 1985) against acetylated K40 of α-tubulin (Figure 30 and Figure 31). The staining showed no significant reduction in either *mec-17* or *atat-2* animals but showed complete lack of signal in *mec-17(ok2109);atat-2(ok2415)* animals.

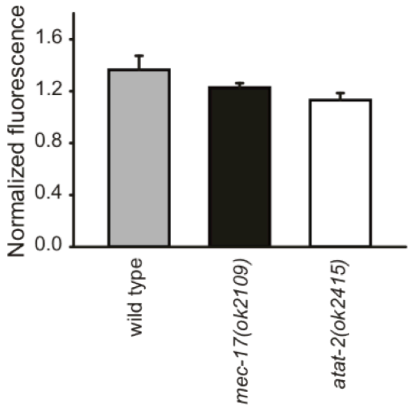

Figure 30. Loss of both *mec-17* and *atat-2* are needed for 6-11B-1-detected acetylation of TRN microtubules (n > 10). p>0.05 in both cases.

Observing *mec-17* animals with a *mec-17*Δ*::gfp* reporter or antibodies against acetylated tubulin (6-11B-1) or MEC-18 (touch receptor neuron-specific protein), we noticed several severe morphological defects (Figure 31). In both *mec-17* alleles (*u265* and *ok2109*) we noticed a multitude of axonal loops on both ALM and PLM processes in the late larvae and young adults (Figure 31A). Additionally, in the animals of the same age we also detected infrequent branches on these axons (Figure 32A). Since later in development the frequency of loops and branches remained roughly unchanged, we do not believe that loops are the

initial state of branch development. However, the most obvious phenotype was the extension of a normally short or non-existent ALM posterior process observed in the *mec-17* animals of the same age (Figure 31B and C). This process appeared very early in development, approximately 24h post hatching, and continued growing throughout the lifetime (Figure 32C). In one-day old adults it was 10+/-0.9 (mean +/- SEM; n=40) cell body diameters long. All of these features were absent in wild type animals and, interestingly, also in *atat-2* mutants, whose neurons morphologically quite resemble the wild type neurons.

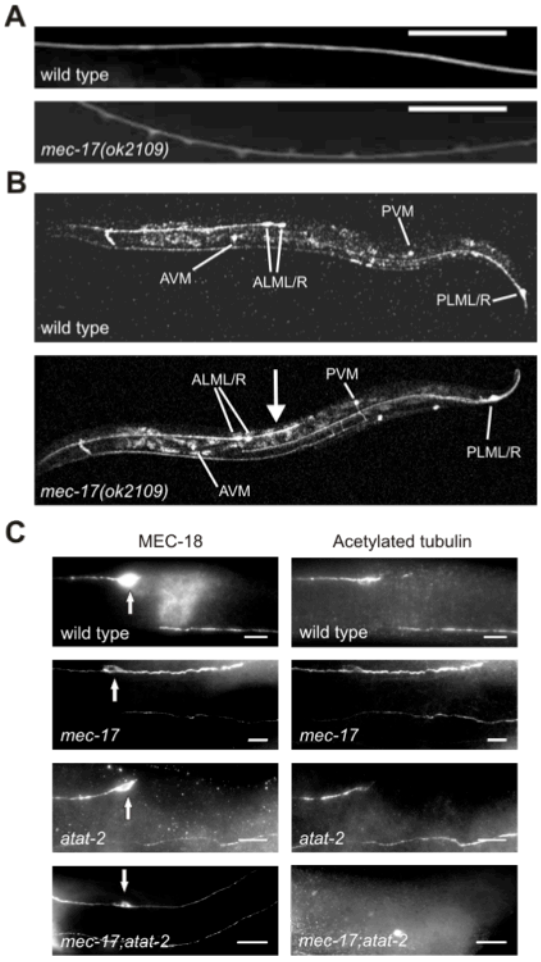

Figure 31. Loss of *mec-17*, but not *atat-2*, alters TRN structure. (A) The ALM anterior process of a young *mec-17(ok2109)* adult has many loops (using *mec-17Δ::gfp*); a similar process in a wild type neuron does not. Scale bar indicates 20µm. (B) ALM and PLM processes are longer (dots) in a young *mec-17(ok2109)* adult than in a similarly aged wild type (both express *mec-17Δ::gfp*). The positions and names of the cell bodies are indicated by lines. The most striking difference is the appearance of a long ALM posterior process (indicated by an arrow). (C) Both MEC-17 and ATAT-2 acetylate K40 in MEC-12 α-tubulin in the TRNs. Left panels show staining of ALM neurons with an antibody to MEC-18, a TRN-specific protein. Right panels show the same cells stained with 6-11B-1. The latter staining is only eliminated in the double mutant. Note that the unusual

posterior ALM process of *mec-17* contains acetylated tubulin and that mutation of *atat-2* does not alter the structure of the ALM neuron. ALM cell bodies are indicated by an arrow. Scale bars indicate 20µm.

The extraordinary posterior process usually ran directly posterior from the ALM cell body and extended until after the vulva. We believe this process was physiologically functional because it showed normal staining with 6-11B-1 antibody as the anterior process (Figure 31B) and it also exhibits the characteristic punctuated pattern when stained with the antibody against MEC-2, a protein associated to a mechanotransduction channel (Figure 32B).

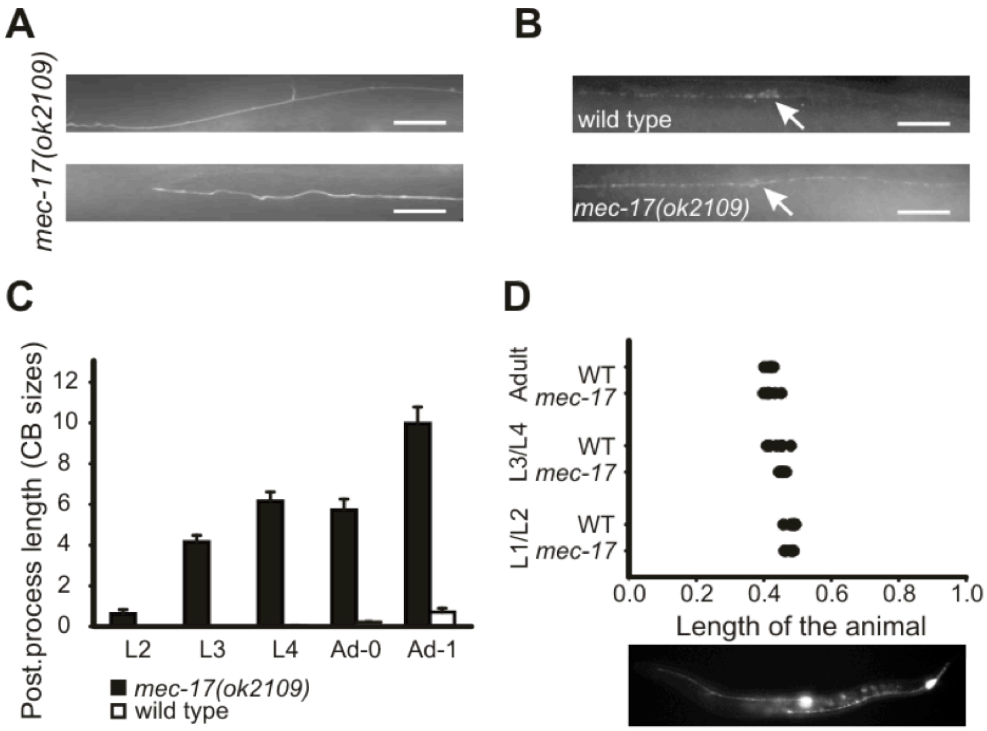

Figure 32. TRN morphological defects of *mec-17* mutants. (A) *mec-17Δ::gfp*-expressing ALMs in *mec-17(ok2109)* adults show infrequent branches (Upper panel) and curves (Lower panel). Scale bars indicate 20µm. (B) Normal MEC-2 puncta occur in the ALM posterior process (to the right of the cell body) of *mec-17* mutants (visualized with an antibody against MEC-2). Arrows indicate ALM cell body. Scale bars indicate 20µm. (C) Elongation of the ALM posterior processes of *mec-17* mutants during development. Process length is measured in 'ALM cell body size' equivalents. (D) The position of the ALM cell body does not change in *mec-17* mutants.

Other groups who have examined *mec-17* animals have not reported this phenotype, but Shida et al. (2010) noted a minor change (size of a about 1 cell body diameter) of the position of the ALM cell body. Although we see a 10 cell body diameter long process we do not see any

change in the position of the cell body at any of the three different developmental stages we tested (Figure 32D). Since the difference in size is so big we also believe that a minor change of that size would not be able to account for the production of such a dramatic posterior process.

These various morphological defects in young adult stage are not due to a general touch receptor neuron dysfunction, present in all mec animals, since none of these defects was observed in *mec-4, mec-5, mec-7* or *mec-12* animals of the same age (Figure 33). It is a *mec-17* dependent feature since *atat-2* mutants do not show any of these defects and the double mutants (*mec-17;atat-2)* show no increase in the observed phenotype.

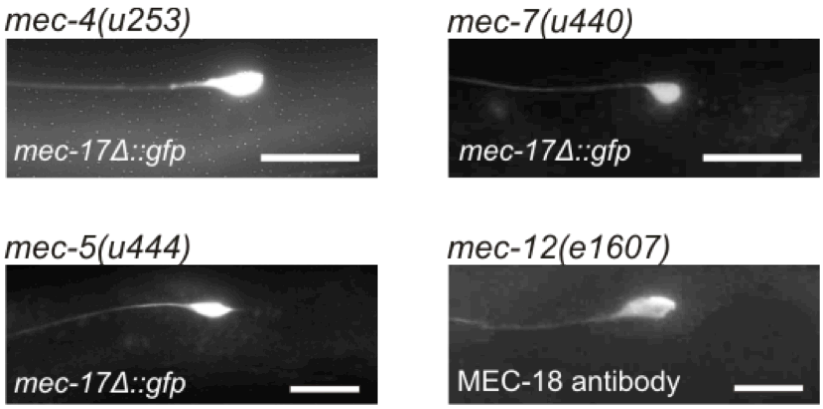

Figure 33. The morphological defects seen in young *mec-17* adults are not produced by mutations affecting TRN function (*mec-4*, *mec-5*, *mec-7* and *mec-12*). Scale bars indicate 20µm.

Most importantly, to confirm that all the phenotypes mentioned above indeed are mec-17-mediated, we generated a transformation construct with wild-type genomic DNA for *mec-17* under the *mec-17* promotor and injected it to *mec-17(ok2109)* animals. Indeed, transgenic animals displayed morphologically normal touch receptor neurons (Figure 34). Rescue of all the morphological defects suggests that *mec-17*, but not *atat-2*, is required for the proper morphology of the TRNs.

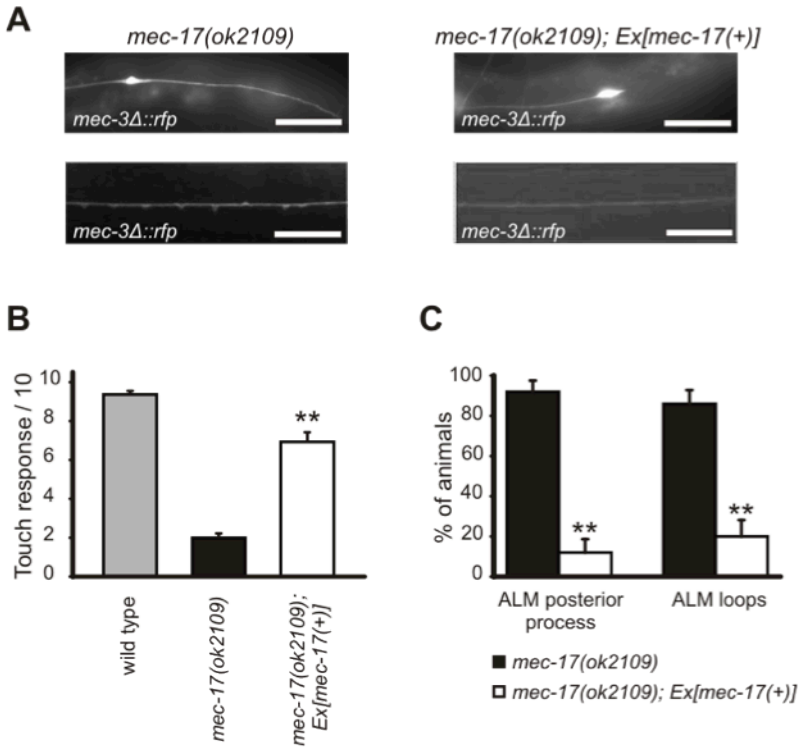

Figure 34. All the morphological defects seen in *mec-17* animals are rescued with over expression of wild type genomic DNA for *mec-17*. (A) Elongated processes and extensive looping in *mec-17* mutants are rescued by the expression of genomic *mec-17(+)*. Scale bars indicate 20µm. (B) Touch sensitivity in *mec-17* mutants is rescued by the expression of genomic *mec-17(+)* (n=20). (C) Quantification of (A) (n=20, p<<0.0001 in both cases).

2.3.2 *mec-17* and *atat-2* mutations affect the ultrastructure of microtubules

To examine the ultrastructure of microtubules in *mec-17* and *atat-2* animals we collaborated with David Hall at Albert Einstein Institute who performed electron microscopy (EM) on these animals. Although touch receptor neurons have rather long processes and microtubules are relatively short it is known that the average number of microtubules per section is constant (Chalfie and Thomson, 1979). In the images we received from David Hall we first noticed that both genes cause a reduction in the number of microtubules (Figure 35). Interestingly, the number of microtubules correlates with touch sensitivity. While wild type animals have 46.5 +/- 0.5 (n=6) microtubules per section, *mec-17(ok2109*) have 5 times less microtubules per section (8.8 +/- 0.7, n=5). *mec-17(u265)* have a less pronounced effect with 14.7 +/- 0.8

microtubules per section (n=6). *atat-2* mutation showed a small but consistent reduction in the number of touch receptor neuron microtubules (31 +/- 3.6, n=7) and the effect was the greatest in the double *mec-17(ok2109);atat-2(ok2415*) mutant (7 +/- 0.3, n=5).

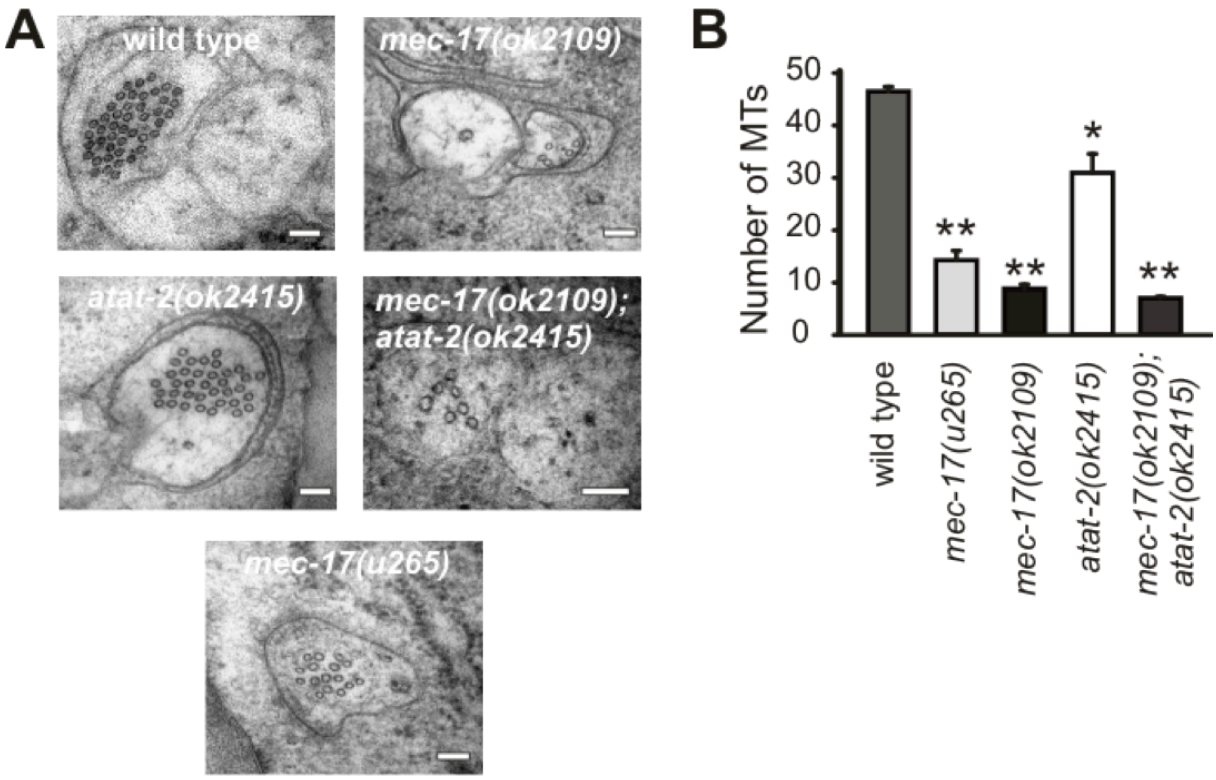

Figure 35. *mec-17* and *atat-2* mutations affect the ultrastructure of microtubules. (A) Electron microscopy image of wild type, *mec-17(ok2109*), *atat-2(ok2415*), *mec-17(ok2109);atat-2(ok2415*) and *mec-17(u265)* ALMs. All images represent the ALM neurons with the adjacent ALN cell. Bar, 100nm. (B) Quantification of the number of microtubules in these animals.

Apart from being composed of 15 protofilaments, wild type microtubules in touch receptor neurons have two additional characteristics that discriminate them from microtubules in other cell types. More than 70% of microtubules in touch receptor neurons (Figure 36) harbor electron dense material inside the lumen. Since K40 is known to be situated in the lumen of microtubules it is possible that the material seen on the EM can be either MEC-17 and ATAT-2 themselves, or some other molecules recruited to that location by either these enzymes or by K40 acetyltion. Indeed, our EM images clearly show that this luminal material is completely missing in animals carrying either the *mec-17* or *atat-2* mutation .

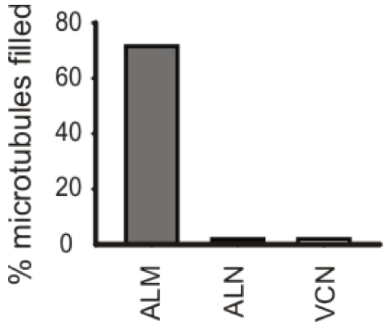

Figure 36. Graph showing percentage of microtubules filled with electron dense material in touch receptor neurons and other cells (ALN and VCN). Microtubules from 6 different animals were analyzed.

Finally, when microtubules are polymerized in the presence of high concentrations of tubulin dimers, sheets of protofilaments can be seen. These sheets, that appear as hooks in cross section, are used to determine microtubule orientation (McIntosh and Euteneuer, 1984). In our EM images we noticed several of these hooks and we believe that mec-17 and atat-2 mutations affect the orientation of the hook. Although the numbers were low, all four hooks on microtubules in wild-type cells were clockwise, whereas the three hooks on *mec-17(ok2109)* microtubules were counterclockwise. The *mec-17(u265)* mutation gave a mixed collection with two of eleven hooks clockwise. The *atat-2* deletion and the double *mec-17(ok2109); atat-2(ok2415)* mutant also gave a mix of hooks with five of seven and three of five hooks clockwise respectively.

These data indicate that both *mec-17* and *atat-2* affect microtubule ultrastructure. The number of microtubules is reduced in both mutants with *mec-17* animals showing a more pronounced phenotype. Finally, some of the microtubule characteristics like luminal material and orientation of hooks are impaired in both mutants suggesting that acetylation or the enzymes themselves are necessary for the proper structure of 15 protofilament microtubules.

2.3.3 *mec-17*-phenotypes become more severe with aging

Since the *mec-17(u265)* allele showed touch insensitivity only in adult stages, we decided to test whether *mec-17(ok2109)* animals increase their touch insensitivity during the aging process. Since these animals already as young adults show very pronounced touch-insensitivity (2/10 responses) it made it difficult to assess any increase in insensitivity. Although, we could not find any difference in touch sensitivity, the neuronal morphological phenotype was easier to quantify. And indeed we observed pronounced increase in the length of the ALM posterior process and an increased number of loops along the axon in 11-days old *mec-17(ok2109)* animals (Figure 37A and B). Growth of the posterior axon and the presence of occasional loops were also seen in aged wild type animals, as reported recently (Pan et al., 2011; Tank et al., 2011), but the effect in *mec-17* animals was much more obvious (Figure 37D). Additionally, we also observed a new phenotype, branching of the PLM neuron (Figure 37C), that was neither present in younger *mec-17* animals, nor in controls of any age.

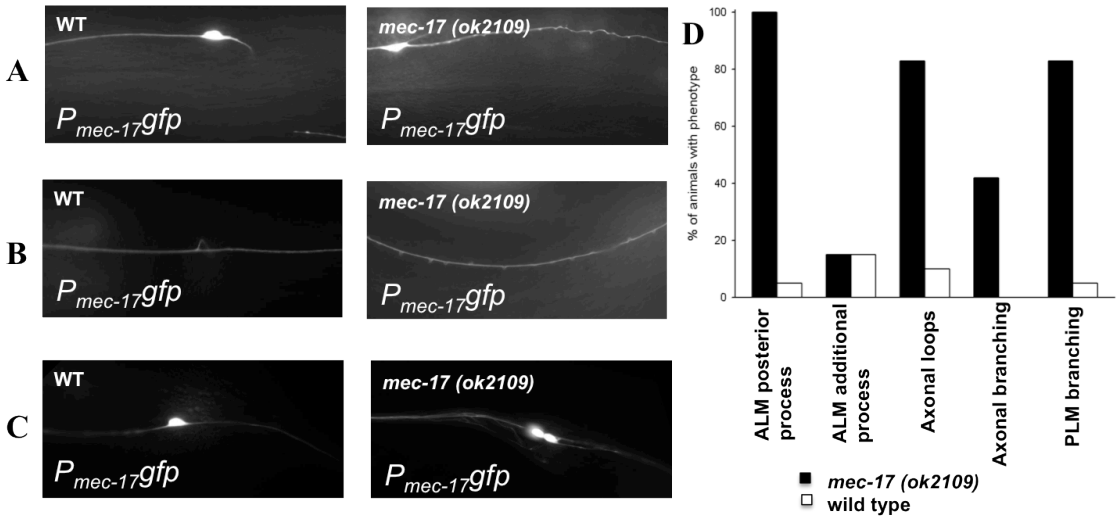

Figure 37. *mec-17*-mediated effects are more severe as the animals age. (A) wild type and *mec-17* animals with a posterior ALM process. (B) aged wild type animals have occasional loops, while *mec-17* animals have axons completely packed with them. (C) *mec-17* animals have also extraordinary branching around the PLM cell body, not observed in the wild type animals of the same age. (D) quantification of all the phenotypes (n=20, 11-days old animals).

To check if *mec-17* mutant have accelerated aging we crossed these animals with *daf-2* and *daf-16* mutants. DAF-2 is an insulin receptor and DAF-16 is a transcription factor in the insulin signalling pathway. This pathway is the best studied aging pathway in C.elegans, although others exist (Tank et al., 2011). Progeny of these crosses did not show any rescue or increase of touch-insensitivity (Figure 38A) nor any effect on the morphology of touch receptor neurons (Figure 38B). These data suggest that either *mec-17*-dependant aging is not related to the insulin pathway, or that it is downstream of both DAF-2 and DAF-16 so no effect is possible.

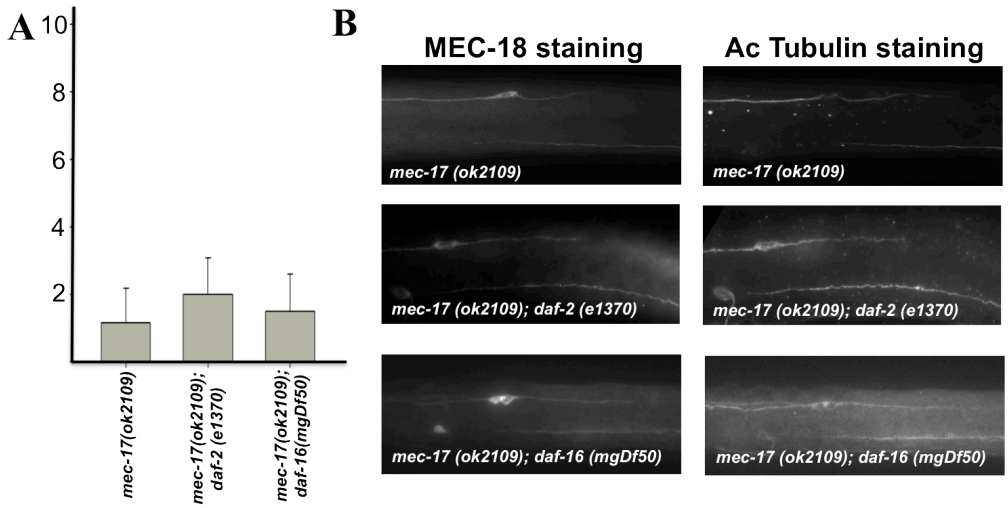

Figure 38. DAF-2 and DAF-16 do not influence mec-17 phenotypes. (A) daf-2 and daf-16 do not affect mec-17-mediated touch-insensitivity. (B) daf-2 and daf-16 do not affect the length of the ALM posterior process.

2.3.4 Ectopically expressed MEC-17 does not acetylate MEC-12

While *mec-17* is expressed only in touch receptor neurons, both *atat-2* and *mec-12* are expressed in other sensory neurons in the nose, at the tail, along the ventral cord as well as in the various motor neurons (Wormbase). To investigate if *mec-17* can acetylate *mec-12* in cells other than touch receptor neurons we generated a construct where the expression of *mec-17* was controlled by the pan-neuronal *sng-1* promotor. We injected this construct into double *mec-17;atat-2* mutants that do not show any acetylation in the body. Interestingly, although *mec-17* was indeed expressed pan-neuronally (detected by co-injection of P_{sng-1}gfp and by single-molecule FISH of *mec-17*) there was no detectable acetylation in any other type of cells except touch receptor neurons (Figure 39). These data suggest that MEC-17 alone is not sufficient to ectopically acetylate MEC-12 and that probably other touch neuron specific co-factors are needed.

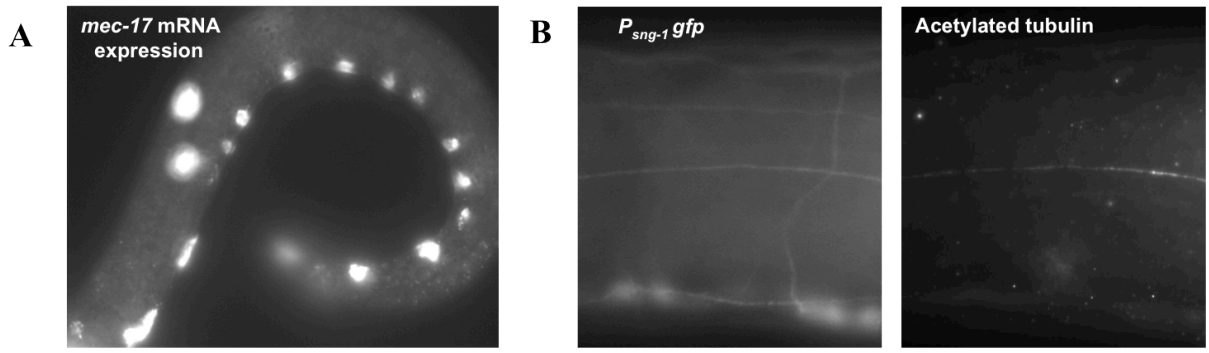

Figure 39. Ectopically expressed *mec-17* does not acetylate microtubules. (A) SM-FISH imaging showing that *mec-17* is expressed in various ventral and motoric neurons in addition to touch receptor neurons. (B) Although it is expressed, MEC-17 does not acetylate microtubules outside of the touch receptor neurons, detected by staining against the acetylated antibody.

2.3.5 Catalytically inactive *mec-17* mutants rescue most of the *mec-17* phenotypes

Having proposed that in mammalian cells ATAT1 influences microtubule dynamics through structural interactions rather than enzymatically, we sought to determine if some of the MEC-17-dependent phenotypes might be modulated by MEC-17 protein itself. To test this we prepared two different catalytically inactive mutants. First, we generated a mutant analogous to the mammalian ATAT1-GGL (we mutated only the two glycines into tryptophanes) and named it *mec-17(dW)* (double tryptophan - W). We also made a mutant with a point mutation of an acidic residue in the domain, named *mec-17(D144N)* (Shida et al., 2010). This mutant has already been used by Shida et al. (2010), who showed that mammalian ATAT1-D157N could not acetylate microtubules *in vitro*. In *C.elegans* they show that *mec-17(D144N)* cannot rescue touch sensitivity of *mec-17* mutants. Additionally, the authors show results were *mec-17(D144N)* reduces touch sensitivity of *mec-17* animals, explaining this as a dominant negative effect (Shida et al., 2010). Our results on of touch-sensitivity of *mec-17* animals differ a lot from the ones presented by Shida et al. (2010). Whereas we measured only 20% of touch sensitivity (Figure 29A), Shida et al. (2010) report the touch sensitivity of 50% compared to the wild type. In order to confirm our observations from mammalian cells we sought to test the touch sensitivity of both *mec-17(dW)* catalytically inactive mutants and *mec-17D144N* mutants created by Shida et al. (2010).

We made transgenic *mec-17* and double *mec-17;atat-2* mutants expressing MEC-17(+), MEC-17dW or MEC-17D144N from the *mec-17* promotor. We also made mutants with *mec-17dW* integrated into the genome. Since mec-17 animals still showed signal after staining with the acetylated tubulin antibody, we used transgenic lines made in the double *mec-17;atat-2* background to assess the acetylation status of the microtubules. Our results show that, although MEC-17(+) rescues acetylation in touch receptor neurons, both catalytically inactive mutants show no acetylation whatsoever (Figure 40).

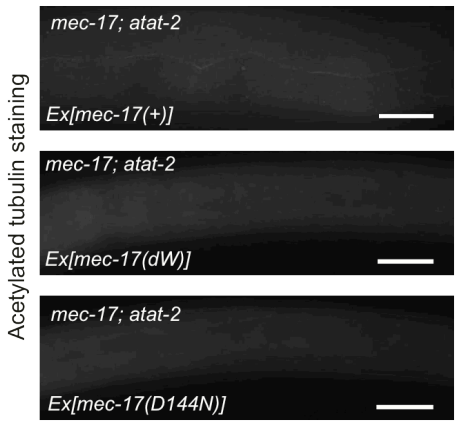

Figure 40. Catalytically inactive mutants do not acetylate microtubules. Double *mec-17;atat-2* mutants were injected with *mec-17(+), mec-17(dW)* and *mec-17(D144N)* respectively. Double mutants show no acetylation whatsoever, but with *mec-17(+)* over expression acetylation in touch receptor neurons is restored. This effect is missing with the over expression of the catalytically inactive mutants.

Having confirmed that the mutants were indeed catalytically inactive we tested all the animals for touch response and we observed an equivalent rescue of touch sensitivity in all the lines (Figure 41A), suggesting that acetylation is not needed for mechanosensation, contrary to what has been suggested by Shida et al. (2010).

We also tested the morphology of touch receptor neurons of these animals. As shown in Figure 41B, *mec-17dW* and *mec-17D144N* both rescue the posterior process of the ALM neurons. They do not, however, rescue all the phenotypes observed. As previously mentioned, *mec-17* animals show a large number of loops all along the axon and *mec-17(+)* rescues this phenotype. Interestingly, *mec-17dW* and *mec-17D144N* do not rescue this phenotype suggesting that although some effects of *mec-17* depend on the protein itself (like the touch sensitivity and the ALM posterior process), some other effects (like axonal loops) depend on its enzymatic activity.

Finally, we also sent these animals for electron microscopy analysis of microtubule ultrastructure. The EM images (Figure 41C) reveal a partial rescue in the number of microtubules with the over expression of the catalytically inactive *mec-17(dW)* in the *mec-17* genetic background (30 +/- 4 compared to 8.8 +/- 0.7). However, over expression of the same

construct did not affect the number of microtubules in the *mec-17;atat-2* mutant background (8 +/- 1 compared to 7 +/- 0.3).

Taken together these data suggest that at both the *in vitro* and *in vivo* level ATAT1/MEC-17 has other roles beyond its enzymatic activity. Interestingly, our data show that some of the phenotypes caused by *mec-17* can be rescued by the catalytically inactive mutants, but some cannot, suggesting that *in vivo* there are specific roles of MEC-17-mediated acetylation and interactions between MEC-17 and other proteins including tubulin.

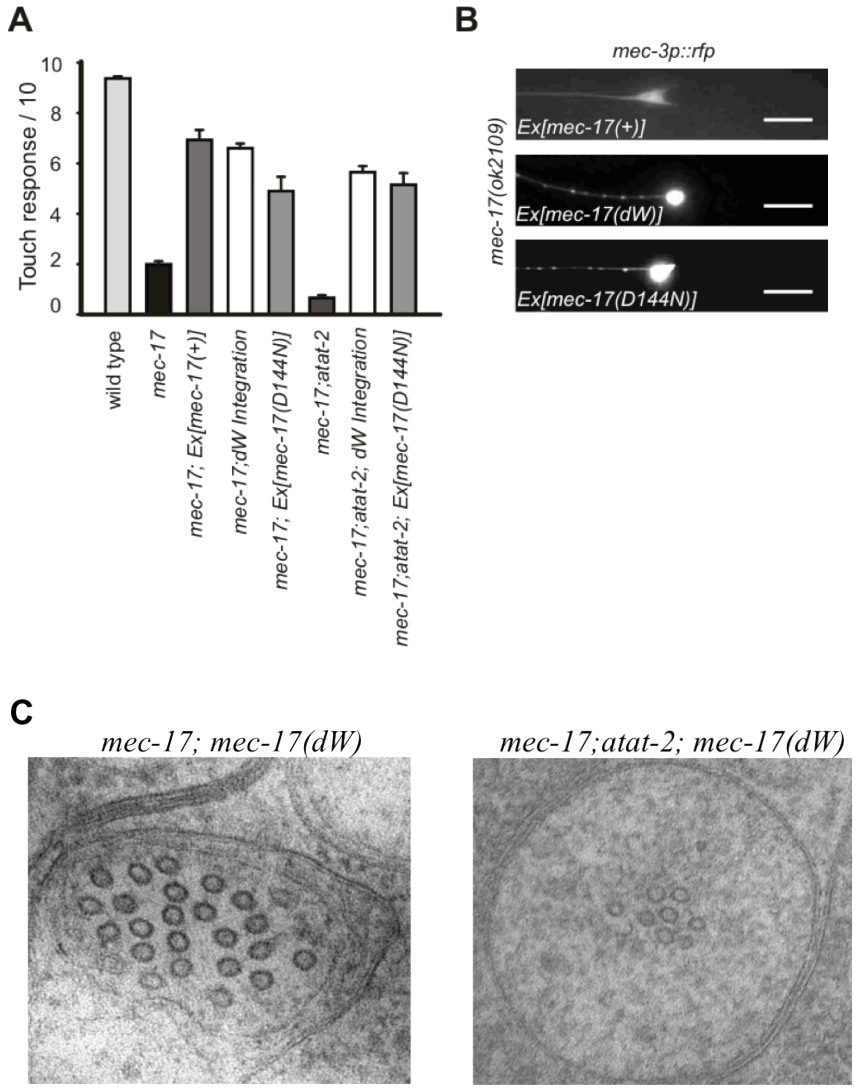

Figure 41. Catalytically inactive mutants rescue some of the *mec-17* phenotypes. (A) Touch sensitivity is equivalent in rescues of *mec-17* and *mec-17;atat-2* with both *mec-17(+)* and *mec-17(dW)*. (B) Posterior process of the ALM is absent in *mec-17* animals over expressing *mec-17 (+), mec-17(dW)* or *mec-17(D144N).* The loops, however, are not rescued with the catalytically inactive mutants. (C) *mec-17(dW)* partially rescues the number of microtubules per section.

3 Discussion

The major finding of this investigation is the characterization of a novel enzyme family that acetylates microtubules. I demonstrated that ATAT1, mammalian homologue of MEC-17, is a major microtubule acetyltransferase in mammalian cells. Furthermore, I show that ATAT1 expression mimics the expression of acetylated tubulin on the whole-animal level. I also show that ATAT1 undergoes self-acetylation that might be important for its main action on tubulin. Additionally, ATAT1 influences stability and dynamics of microtubules, probably through direct interaction with other molecules, rather than via its enzymatic activity. Finally, I demonstrate that in *C.elegans mec-17* is necessary for proper morphology of the touch receptor neurons and microtubule ultrastructure in these cells. Interestingly, also *in vivo,* the MEC-17 protein, rather than acetylation, might underlie some of these phenotypes.

3.1.1 ATAT1 is a microtubule acetyltransferase

Using a combination of *in vitro* biochemistry, imaging studies and *in vivo* assays I demonstrate that ATAT1 is a major microtubule acetyltransferase. Over expression of ATAT1 increases K40 acetylation four fold, while knock-down substantially reduces it in mouse NIH3T3 cells (Figures 15-17). Our results also show that ATAT1 is a major microtubule acetyltransferase in two other cell types from different mammalian organisms (namely CHO and HEK cells) suggesting that generally in mammalian systems the majority of microtubule acetylation is mediated by ATAT1. Additionally, I demonstrate that by disturbing an α-helix in the AcCoA binding site the enzyme displays no acetylation activity anymore. Moreover, mouse ATAT1 efficiently acetylates bovine and porcine microtubules *in*

vitro (Figure 22). Our data, together with two recently published reports (Akella et al., 2010; Shida et al., 2010) establish that ATAT1 is a major tubulin acetyltransferase.

Our experiments on the expression and acetyltransferase activity of ATAT1 argue for a constrained role of ATAT1 at microtubules. Previous data on tubulin deacetylases HDAC6 and Sirt2 show that both of these enzymes have additional substrates, aside from microtubules. To investigate if ATAT1 also displays acetylation activity towards other targets I examined its expression pattern and assessed its activity towards other proteins *in vitro* and in cells. The endogenous localization of ATAT1 mRNA and protein overlaps with the distribution of acetylated tubulin (Figures 11-13), where ATAT1 is most expressed in nervous tissues and testis, exactly the organs with the highest microtubule acetyation. Flagella of male germ cells harbour a large amount of acetylation and neurons accumulate many different microtubule PTMs, with acetylation being the most prominent and probably implicated in neuronal polarization and directed transport (Fukushima et al., 2009). Also intracellulary, we found endogenous ATAT1 co-localized with microtubules and often completely absent from the nucleus (Figure 14). Similarly, over expression of ATAT1 induces detectable acetylation only on microtubules, and α-tubulin is the principal acetylated protein in whole cell extracts (Figure 14 and 17-20). Intriguingly, we also observed that ATAT1 itself becomes acetylated upon pharmacological inhibition of the endogenous α-tubulin deacetylase HDAC6. Self-acetylation was detected also in *in vitro* assay where incubation of ATAT1 with AcCoA resulted in incorporation of the acetyl group on ATAT1 itself. This assay also showed that ATAT1 is unable to acetylate histone H3 (Figure 22) making it to date the first acetyltransferase discovered without activity towards histones. Combined, these data show that ATAT1 acetylates only microtubules and itself, suggesting that all the ATAT1-mediated effects might be connected to its activity only on microtubules.

While our data suggest that ATAT1 is the major tubulin acetyltransferase, whether it is the only one is still a matter of discussion. ATAT1 homologue is not present in the genome of

Chlamydomonas reinhardtii and this organism is known to possess tubulin acetylation (LeDizet and Piperno, 1987; Maruta et al., 1986). Of interest, ELP3 might play a role in the development, but its function in adults is not clear. Additionally, ELP3 fails to detectably acetylate microtubules in PtK2 cells, its *in vitro* acetylation activity is very weak and, in *C.elegans, elp-3* mutants still show strong microtubule acetylation in touch receptor neurons (Akella et al., 2010; Creppe et al., 2009; Shida et al., 2010; Solinger et al., 2010). Also, our data show that in double *mec-17;atat-2* mutant there is no tubulin acetylation left in touch receptor neurons, suggesting that *elp-3* has no contribution there (Figure 31). Thus, current data suggest that ATAT1-family proteins are the major tubulin acetyltransferases. Moreover, in mammals and *C.elegans* they might be the only proteins with strong tubulin acetyltransferase activity.

3.1.2 ATAT1 autoacetylation

Our initial observation of ATAT1 autoacetylation led us to hypothesize that autoacetylation might regulate ATAT1's activity towards tubulin. We explored this idea further *in vitro* and demonstrated that autoacetylation of ATAT1 is functionally significant though at acetylation levels that are substantially lower than those of tubulin (Figure 24). From our *in vitro* analysis it is difficult to gauge whether this process is an essential requirement for catalytic activity at tubulin, since presumably, ATAT1 is undergoing acetylation continually. However, cellular experiments using non-acetylatable mutants, suggest that self-acetylation is critical for activity at tubulin and that levels of ATAT1 acetylation may serve as a means to regulate enzymatic activity (Figure 24). In support of this hypothesis, autoacetylation of acetyltransferases has been described previously and shown to be essential for several different classes of histone acetyltransferase (Berndsen et al., 2007; Collins et al., 2007; Santos-Rosa et al., 2003; Thompson et al., 2004). Mechanistically, autoacetylation could

regulate enzymatic activity either by acting as an intermediate for transfer of the acetyl group to its substrate (Yan et al., 2002), or via conformational effects on the enzyme and subsequent alterations in complex formation (Wang et al., 2008). Structural information on ATAT1 is needed to uncover which of these mechanisms applies to ATAT1. However the observation that multiple lysine residues are acetylated and that these are distributed across different regions of the proteins, suggests that principal effects may be exerted through conformational changes of the protein.

3.1.3 ATAT1 and microtubule dynamics

The role of α-tubulin acetylation in microtubule stability has been the subject of extensive debate. Several studies have reported that acetylation of α-tubulin increases the stability of microtubules, while others have observed no change (Haggarty et al., 2003a; Matsuyama et al., 2002a; Palazzo et al., 2003; Tran et al., 2007b; Zhang et al., 2008b). We reasoned that the identification of ATAT1 as the primary α-tubulin acetyltransferase should allow us to approach this issue and determine whether acetylation influences microtubule dynamics. Using two independent methodologies (accumulation of detyrosinated tubulin in cells and EB3-RFP particle tracking), we find that over expression of ATAT1 actually decreases microtubule stability (Figure 25). Moreover, this occurs in the presence of increased α-tubulin acetylation indicating that acetylation status *per se* does not influence microtubule dynamics.

Our data (Figure 28) from EB3 particle tracking experiments revealed several intriguing mechanistic insights into ATAT1 function. Firstly, they indicate that since ATAT1 accelerated dynamics of growth, shrinkage and pause events, it is likely that the protein influences the rate of assembly and disassembly of tubulin subunits from the microtubule tip or lattice, rather than recruitment of soluble tubulin dimers to microtubules. This supports our *in vitro* data in which we show that polymerized microtubules are a more effective substrate

than soluble tubulin. Secondly, the observation that the duration of EB3 pauses increases in the presence of ATAT1, suggests that ATAT1 may also interfere with EB3 particle formation; a finding supported by the physical interaction between EB3 and ATAT1 (Figure 27). Finally, and most surprisingly, the demonstration that an acetyltransferase-inactive ATAT1 mutant phenocopies the behavior of the wild type protein, indicates that ATAT1's action at microtubule tips occurs in the absence of α-tubulin acetylation. We propose that the physical presence of ATAT1 and its interactions with tubulin or other as yet unidentified regulatory proteins are the key factors in regulating microtubule stability. In support of this hypothesis, catalytically inactive mutants of the tubulin deacetylase HDAC6 have also been demonstrated to modulate microtubule dynamics without altering acetylation (Zilberman et al., 2009b). Taken together it is likely that these proteins have additional roles at microtubules that extend beyond their classical enzymatic activites.

3.1.4 Acetylation inside the microtubule lumen

The location of the acetylation site K40 inside the lumen of microtubules has triggered much debate in the past decades. The identification of ATAT1 and characterization of some of its functions enables me to explore an alternative view on this topic. ATAT1 is a 36kDa molecule with a proposed Stokes radius of 3.5nm so by its size it fits the entrance into microtubule lumen that, in 11-protofilament microtubules, is around 14nm wide. However, studies on the diffusion of the 6-11b-1 antibody predict that several years would be needed to reach equilibrium (Odde, 1998). More recently, it has been suggested that the antibody enters the lumen during the procedure of fixation when holes could be created on the microtubule lattice (Draberova et al., 2000). This model obviously cannot work for ATAT1, because it readily enters the lumen and causes K40 acetylation in live cells. Since the diffusion from the ends seems impossible in the case of ATAT1, the other option would be incorporation of the

enzyme in the lumen during the polymerization process. Our studies *in vitro* suggest that this is not the case either since ATAT1-mediated acetylation occurs earlier in polymerized than in polymerizing microtubules (Figure 23). Another explanation would be that ATAT1 enters laterally into already polymerized microtubules. This process has not yet been described for any protein, but it has been proposed for the small compound taxol. Taxol is roughly four times smaller in size than ATAT1 and it has been proposed to enter either via 17-Å pores between the protofilaments or via occasional large openings (Diaz et al., 2003; Diaz et al., 1998). Again, ATAT1 is too big for the 17-Å pores, but the idea of lateral diffusion in my opinion is plausible. Since the description of dynamics instability (Mitchison and Kirschner, 1984), other models of microtubule dynamics have attracted less attention. One of these models, microtubule breathing model (Inoue, 1981), might gain new interest in the light of recent discoveries. In this model there is a continuous exchange of subunits between microtubules and free soluble tubulin which causes lateral openings that can enable bigger molecules to enter the lumen. I believe that this might be a route for ATAT1 to enter the lumen. An interesting question is whether ATAT1 itself takes part in the formaton of openings on the lattice, since presumably this process does not happen randomly, but on specific sites. Probably other PTMs that are present on the cytosolic side of a microtubule might take part in this specificity as well. Our interesting *in vitro* observation showing that taxol-stabilized microtubules accumulate acetylation faster than dynamic ones (Figure 23), suggest that taxol enters the lumen through these hotspots and then subsequent addition of ATAT1 causes acetylation to happen faster since the stable pores are already present. In any case ATAT1 and taxol should be sufficient to create these openings for two reasons. Firstly, our *in vitro* reaction contains only AcCoA and microtubules. Secondly, the saturation of the acetylation reaction happens after around 30min, which leaves no time for diffusion from the microtubule ends.

Further structural information is needed to elucidate completely this process. Thus far, the K40 loop has been resolved in the crystal structure of the tubulin dimer (Gigant et al., 2000), but not in the structure of microtubules (Nogales et al., 1999). Consequently, we do not know the exact position of the loop inside the microtubule lumen, but presumably its K40 is positioned in a way to be easily-accessible. Autoacetylation of ATAT1 might play an important role here. As discussed above, I believe that autoacetylation changes the conformation of the enzymes making it more prone to acetylate tubulin. I propose that this could happen in two ways. Firstly, conformation change upon self-acetylation could occur in the cytosol rendering ATAT1 more prone to enter the lumen of a microtubule through a pore. Alternatively, ATAT1 that is already inside the lumen might get acetylated locally in order to adopt a conformation in which it would be able to acetylate K40. Further information on the structure of ATAT1, together with the information of the AcCoA local availability is needed.

Finally, the effect ATAT1 exerts on microtubule dynamics (Figure 28) might not depend exclusively on plus-end dynamics. It is possible that ATAT1 might accelerate microtubule dynamics also by creating pores and stimulating exchange of subunits within a polymer. This way ATAT1 would reach the lumen where the acetylation site is located, but at the same time creation of pores would lead to changes in EB-3 dynamics that we measured as increased speed and length of the tracks (Figure 28). The most surprising result of this study was the observation that catalytically inactive ATAT-GGL causes the same effect on microtubule dynamics as the wild type form. Hypothetically, ATAT1's ability to acetylate microtubules is not needed for the entry into the lumen. It would be interesting to elucidate whether AcCoA is available locally in the lumen of microtubules or it is recruited there on ATAT1. Presumably, it is present locally since ATAT1-GGL mutant that cannot bind AcCoA still affects microtubule dynamics. Hence, the explanation could be that ATAT-GGL enters the lumen, creating pores that affect microtubule dynamics and stability, but once in the lumen it cannot bind AcCoA nor acetylate microtubules.

Some other MAPs, such as tau, are thought to be in the lumen as well (Kar et al., 2003). We found a strong co-localization between tau and ATAT1 in NIH3T3 cells (Figure 14), suggesting that acetylation or interaction with ATAT1 might recruit tau to specific sites along the lumen. Recently, Tau has been found to be acetylated (Cohen et al., 2011; Min et al., 2010), but the enzyme responsible for this is P300, which leads me to exclude the possibility of acetylation of tau by ATAT1. However, tau has been found to bind to HDAC6 and inhibit its activity (Perez et al., 2009). Further studies are needed to investigate whether tau might also exert an effect on ATAT1 and vice versa.

3.1.5 Functions of ATAT1 *in vivo*

ATAT1/MEC-17 does not influence viability in invertebrates. MEC-17-KO *Tetrahymena thermophila* cells are viable and show normal growth rate (Akella et al., 2010). We and the others (Akella et al., 2010; Shida et al., 2010) show that in *C.elegans mec-17* and *atat-2* animals are also viable and fertile. Interestingly, double *mec-17;atat-2* mutants are also viable, suggesting that tubulin acetylation is not essential for *C.elegans* survival. However, there are currently no *in vivo* studies on ATAT1 in mammals. Therefore, we have started generating an $ATAT1^{-/-}$ mouse line (Appendix 1) that will be checked for viability, fertility and development. Since *Tetrahymena* is evolutionary very distant from mammals and *C.elegans* has a very fast evolution it is possible that in mammals global effects of ATAT1 are going to be more severe.

In *C.elegans*, specific neuronal phenotypes have been detected. Firstly, *mec-17* has been associated with the loss of touch sensitivity (Chalfie and Au, 1989). We and the others confirmed these results with a novel knock-out line *ok2109*. However, our data on touch sensitivity of *mec-17(ok2109)* differ from the ones published by the others (Akella et al., 2010; Shida et al., 2010). While they find touch sensitivity reduction of roughly 60%, we see

a stronger effect with 80% reduction. Additionally, our data on touch sensitivity of *mec-17;atat-2* animals largely agree with those of Akella et al. (2010), but diverge from those of Shida et al. (2010). While we and Akella et al. (2010) show that the double mutant responds to 1 out of 10 touches, Shida et al. (2010) do not find any enhancement of the *mec-17* phenotype. All these difference probably come from different ways of preforming the touch test, rather than from background mutations since all groups presumably use the *mec-17(ok2109)* allele from the *C.elegans* consortium. While Shida et al. (2010) show that touch-insensitivity phenotype is caused by the lack of acetylation, we demonstrate that even acetylation-inactive mutants display rescue of touch sensitivity (Figure 41A). To confirm our findings we used the mutant generated by Shida et al. (2010) and we found rescue of touch sensitivity which is different from what Shida et al. (2010) reported with the same mutant. Additionally, MEC-12 mutants with Lys40$^-$ mutation are still touch sensitive (Fukushige et al., 1999), which strongly agrees with our findings suggesting that acetylation *per se* is not needed for touch sensitivity.

In addition to touch sensitivity we investiagated further effects of MEC-17 and ATAT-2 in *C.elegans*. We found that the number of microtubules is impaired in these animals and that the electron dense material from the lumen is absent. This suggests that these enzymes regulate the structure of microtubules and the recruitment of the luminal material. We believe that in specific 15-protofilament microtubules MEC-17 and ATAT-2 have more specialized roles in organizing these large microtubules. In agreement with our model of lateral diffusion of MEC-17/ATAT1 and ATAT-2 we believe that the luminal material is constituted of either the enzymes themselves or, more probably, of other molecules that are recruited there by either acetylation or by these enzymes.

Furthermore, we also report a defect in neuronal morphology of *mec-17* animals. These defects were absent from *atat-2* animals, suggesting that specific roles of MEC-17 underlie this process. Since the catalytically inactive *mec-17-dW* rescued the posterior process and

ectopic branching, but not the loops, we propose that both direct role of the enzyme and acetylation are needed for proper neuronal development. Further studies are needed to elucidate the specific roles of each of them.

In zebra fish a knock down of MEC-17 resulted in impaired neuronal development, hydrocephalus and various other body defects (Akella et al., 2010). Without further experiments it is not clear if these results are attributed to acetylation, the enzyme itself or they are just a general consequence of morpholino injection .

As previously mentioned, in order to investigate further the effect of ATAT1 in mammals we are in the process of making $ATAT^{-/-}$ mice together with a sensory specific ATAT1 knock down (Appendix 1). The latter will enable us to test if touch sensitivity is normal in these animals and if the roles of ATAT1 in mechanosensation are conserved throughout the evolution. For this reason we established a novel test for testing touch sensitivity in mice (Appendix 2). An in-depth analysis of these animals will be performed including the electrophysiological studies on primary sensory neurons.

3.1.6 Outlook

After the identification and initial characterization of ATAT1 described in this study and partially confirmed by two other groups (Akella et al., 2010; Shida et al., 2010), we believe that further work is needed to fully elucidate the biology of ATAT1. Firstly, structural data are needed to understand the mechanism of acetylation and autoacetylation of ATAT1 as well as the mechanism of entering the microtubule lumen and interacting with the K40 loop. On the whole animal level we believe that the $ATAT1^{-/-}$ mice, that we are generating (Appendix 1), will answer some of the important questions such as if ATAT1 is necessary for survival in mammals and if its role in mechanosensation is conserved. Further genetic studies will be needed to assess if the future phenotypes of the mice lacking ATAT1 are dependent on

acetylation or on the enzyme itself. Additionally, specific roles of ATAT1 in testis should be investigated and the possible effect on male fertility measured.

Our results of interaction between ATAT1 and kinesins (Table 3) might open a new avenue of research that can be particularly important in the studies of neurodegenerative diseases, such as Alzheimer disease and Huntington disease, where the role of the microtubule-mediated transport is essential and where HDAC-6 and Sirt2 have already been shown to take part. A hypothetical interaction with tau protein might be investigated further in the light of these findings.

4 Conclusions

Over the past three and a half years I have identified a novel acetyltransferase and elucidated its function *in vitro* and *in vivo*. The main conclusions from the work are summarized below:

- ATAT1 is a microtubule acetyltransferase
- The only targets of ATAT1 are K40 on α-tubulin and several lysine residues on ATAT1 itself
- Self-acetylation regulates the acetyltransferase activity of ATAT1 on tubulin
- EB3 recruits ATAT1 to microtubule plus-ends to regulate microtubule dynamics
- ATAT1 protein rather than acetylation is affecting microtubule stability
- In *C.elegans atat1/mec-17* mutants show impaired development of touch receptor neurons, touch insensitivity and abnormal microtubule ultrastructure
- Catalytically inactive *atat1/mec-17* rescues most of the phenotypes in *C.elegans*, suggesting that also *in vivo* structure of ATAT1/MEC1-17 is essential

I believe that this work made a significant contribution to the field and I hope that it will establish new avenues of research. The function of microtubule acetylation and ATAT1 remain to be elucidated in mammalian organism for which reason I started generating mice lacking ATAT1 (Appendix 1).

5 Materials and methods

5.1 General procedures

5.1.1 Cell culture

CHO-K1, HEK-293 and NIH3T3 cells were used. All cell lines were kept in DMEM medium supplemented with 10% heat-inactivated FBS (Invitrogen), 1% Penicilin-Streptomicin mix, 1% non-essential amino acids (only for NIH3T3 cells) and 1%L-Glutamine (only for NIH3T3 and HEK-293 cells).

CHO and HEK cells were transfected using FuGENE HD Transfection reagent (Roche) according to the manufacturer's instructions. NIH3T3 cells were transfected using the Nucleofector system (Amaxa Biosystems) following the manufacturer's instructions. For imaging purposes around 1 million cells were transfected and seeded on 35-mm dishes. For biochemical experiments 5 million cells were used and seeded on 10-cm dishes. Unless indicated, experiments were conducted on cells 24-30 hours after transfection.

Primary DRG neurons for all purposes were collected from adult mice of both sexes. DRGs were isolated and cleaned of axons and then transfered to an eppendorf tube where they were incubated for 30min with collagenase IV (Sigma) in collagenase medium (DMEM Gibco 41965). After washing with PBS, DRGs were incubated for additional 30min with trypsin/EDTA (Invitrogen) after which they were triturated with 25g, 22g and 18g needles for 5 times each and passed through a 40µm cell strainer. Individual cells were centrifuged and transfected using the Nucleofector system SCN program 6 (Amaxa) according to the manufacturer's instructions. Afterwards neurons were recovered in the DRG medium (DMEM Gibco 41965, 10% heat-inactivated horse serum Gibco 26050-088 and 1% P/S) and left in the incubator for 24-30 hours.

5.1.2 *C.elegans* general procedures

Unless otherwise indicated strains were maintained and studied at 20° according to (Brenner, 1974) on the OP50 strain of *E. coli*. The wild-type strain N2 (Brenner, 1974) and the *mec-17(u265)* strain (Zhang et al., 2002) have been previously described. *mec-17(ok2109)* and *atat-2(ok2415*) strains were obtained from the *C. elegans* Genetic Center. Strains *mec-17(ok2109); atat-2(ok2415)* and *mec-17(ok2109); mec-17Δ::gfp* were created by standard genetics and verified either phenotypically or by PCR where necessary. Stable lines expressing *sng-1p::mec-17, mec-17(+)*, *mec-17dW and mec-17D144N* were generated by microinjection as described below. Strain expressing *mec-17Δ::gfp* was described by (O'Hagan et al., 2005).

5.1.3 Microinjections

All microinjections were performed by Irini Topalidou. Transgenic animals were generated by microinjecting *mec-17(ok2109)* or *mec-17(ok2109)*; *atat-2(ok2415*) strains with 5 ng of *mec-17(+)*, *mec-17dW*, or *mec-17D144N* together with 5 ng of *mec-3p::HsRed1*. Stable lines with at least 60% inheritability were used for our further analysis. For the ectopic expression N2 and *mec-17(ok2109)*; *atat-2(ok2415*) animals were microinjected with 5 ng of *sng-1p::mec-17* and 5 ng of *sng-1p::gfp*. The extrachromosomal array of a rescuing *mec-17dW* stable line was integrated into the genome by irradiation using the protocol and conditions described by (Chelur and Chalfie, 2007)

5.1.4 Antibodies

All the antibodies used in this study are listed in Tables 4 and 5.

Table 4. List of primary antibodies used in this study. By type antibodies can be monoclonal (M) or polyclonal (P). Host animals used for production of these antibodies are mouse (MS), rabbit (RB) and chicken (CH). Techniques for which the antibody has been used in this study are: immunofluorescence (IF), immunoblotting (WB) and immunoprecipitation (IP). IF-CE indicates that the antibody has been used for the immunofluorescence in *C.elegans*.

Antibody to	Type	Host	Techniques	Details
α-Tubulin	M	MS	IF, WB, IP	T5168, Sigma
α-Tubulin	M	RB	IF	2125, Cell Signaling
Acetylated α-tubulin	M	MS	IF, WB	T7451, Sigma
Acetylated α-tubulin	M	MS	IF-CE	6-11B-1, Santa Cruz
Detyrosinated α-tubulin	P	RB	IF	AB3201, Millipore
C6orf134/ATAT1	P	RB	IF	ab58742, Abcam
Actin	M	MS	IF, WB	MAB1501, Chemicon
Pan acetyl-lysine	P	RB	IF, WB	AB3879, Chemicon
pan acetyl-lysine	P	RB	IP	ICP0380, Immunechem
Anti-flag M2	M	MS	WB	200472 Stratagene
Anti-flag M2-HRP	M	MS	WB	A8592 Sigma
anti-GFP	P	CH	IF, WB	ab13970, Abcam
MEC-18	M	MS	IF-CE	Chalfie lab
MEC-2	M	MS	IF-CE	Chalfie lab

Table 5. List of secondary antibodies used in this study. The legend is the same as in the Table 4. In addition, new hosts were used: sheep (SH), donkey (DO) and goat (GT).

Name	Type	Host	Technique	Details
Anti-mouse	IgG-Alexa 488	GT	IF	Invitrogen
Anti-rabbit	IgG-Alexa 488	GT	IF, IF-CE	Invitrogen
Anti-chicken	IgG-Alexa 488	GT	IF	Invitrogen
Anti-mouse	IgG-Alexa 555	GT	IF	Invitrogen
Anti-rabbit	IgG-Alexa 555	GT	IF	Invitrogen
Anti-mouse	IgG-Alexa 546	GT	IF	Invitrogen
Anti-rabbit	IgG-Alexa 546	GT	IF	Invitrogen

Anti-mouse	Cy^{TM}3-conjugated	GT	IF-CE	Jackson Laboratories
Anti-mouse	IgG-Alexa 633	GT	IF	Invitrogen
Anti-rabbit	IgG-Alexa 633	GT	IF	Invitrogen
Anti-mouse	IgG-Alexa 647	GT	IF	Invitrogen
Anti-rabbit	IgG-Alexa 647	GT	IF	Invitrogen
Anti-mouse	HRP-conjugated	SH	WB	NA934V,GE Healthcare
Anti-rabbit	HRP-conjugated	DO	WB	NA931V,GE Healthcare

5.2 Molecular biology

5.2.1 Mammalian plasmids and molecular cloning

Mouse ATAT1 cDNA (ENSMUST00000056034) was used for all subcloning purposes. All ATAT1 splice variants were first cloned into pGEM-T vector using pGEM-T Easy Vector System (Promega) and then subcloned into the pEYFP-C1 vector and verified by sequencing. Reference sequence, splice variant 203, that we used in all further experiments, was amplified before cloning into pGEM-T vector using the following primers:

Forw ATGGAGTTCCCGTTCG
Rev TCAGTATCGACTCTCATC

From pGEM-T ATAT1 was subloned into pEYFP-C1 and pFLAG-CMV2 vectors using SalI and BamHI restriction enzymes and the following primers:

Forw TATAGGATCCGGAATTCGATTAGGAG
Rev TACAGTCGACGAGTTCCCGTTCG

ATAT1-C terminal fusion with a strep tag was obtained by subloning ATAT1 from the pEYFP-C1 vector in pEXPR-IBA103 vector, where strep tag is located downstream of the multiple cloning site. pEXPR-IBA103 vector was linearized using the PCR and the following primers:

5’ primer GCTTGCGGCCGCAGATCTAGCTTAAG
3’ primer TTTTTCGAACTGCGGGTGGCTCC

Subsequently, infusion reaction (Clontech) was performed using the following primers:

Forw CCGCAGTTCGAAAAAGCTATGGAGTTCCCGTTCGATG
Rev TCTGCGGCCGCAAGCTTTTCAGTATCGACTCTCATC

ATAT-1 N terminal fusion was carried in the same way, just using pEXPR-IBA105 vector, where strep tag is located upstream of the multiple cloning site.

For the co-localization studies and imaging of microtubule dynamics pTagRFP-EB3 plasmid (Evrogen, FP365) was used. For the co-localization studies with ATAT1, Tau was subcloned from the Tau/pET29b (Addgene, 69872-3) plasmid into superCFP-C1 vector using BamHI and XhoI restriction enzymes and the following primers:

Forw ATATCTCGAGTGGCTGAGCCCCGCCAGGAGTT
Rev ATATGGATCCCAAACCCTGCTTGGCCAGG

For the BIFC experiment pEYFP-C1 vector was used to produce YFP-C and YFP-N fragments. Following primers were used for the infusion reaction:

YFP-C_forw CGCCCGGCGTGCAAAATTCCGAACGATCTGAAACAGAAAGTGATGAACCATGCCGA CAAGCAGAGAAC
YFP-C_rev GGTGGCGACCGGTAGCGC
YFP-N_forw TCCGGACTCAGATCTCGAG
YFP-N_rev ATGGTTCATCACTTTCTGTTTCAGATCGTTCGGAATTTTGCACGCCGGGCGCATGATA TAGACGTTGTGGC

ATAT1 was fused with the YFP-C fragment and EB-3 with the YFP-N fragment using the following primers:

ATAT1_1 GCTACCGGTCGCCACCATGGAGTTCCCGTTCGATG
ATAT1_2 TTTGCACGCCGGGCGGTATCGACTCTCATCAGATC
EB3_1 AAAGTGATGAACCATGCCGTCAATGTGTAGTCCAC
EB3_2 AGATCTGAGTCCGGACTAGTACTCGTCCTGGTCTTC

Six different construct were made for FRET: 3 CFP-constructs and 3 different versions of ATAT1 with a YFP tag. CFP constructs were generated using the infusion reaction with 150ng of the SuperCFP-C1 vector vector and 50ng of inserts. Inserts where the following: YFP (for the generation of pSuperCFP-YFP Tandem), EB-3 and Traf2Traf (for the generation of the negative control construct pSuperCFP-Traf2Traf-YFP). SuperCFP-C1 vector (a gift from C.Gross) was digested with the restriction enzyme XhoI before the infusion reaction.

PCRs were performed with the annealing temperature of 62°C except for Traf2Traf where annealing was performed at 57°C. YFP_1 and YFP_2 primers were used for the generation of the pSuperCFP-YFP Tandem construct. EB3_1 and EB3_2 were used for subloning EB_3 from the pRFP-EB3 vector into pSuperCFP. SuperCFP-Traf2Traf-YFP construct was obtained using TRAF_1 and YFP_2 primers.

YFP_1	GGACTCAGATCTCGAGTGAGCAAGGGCGAGGAG
YFP_2	GGACTCAGATCTCGAGTGAGCAAGGGCGAGGAG
EB3_1	GGACTCAGATCTCGAGCCGTCAATGTGTACTCCACAT
EB3_2	GAAGCTTGAGCTCGACTAGTACTCGTCCTGGTCTTCTTGTT
TRAF_1	GGACTCAGATCTCGAGAGAGCCTGGAGAAGAAG

For the purpose of FRET experiments, 2 new ATAT1 constructs were generated. pYFP(N1)-ATAT1 was generated from pEXPR-IBA103-ATAT1 vector, using the infusion reaction. The reaction was performed with 200ng of vector (linearized with BamHI enzyme) and 45ng of insert obtained with the following primers:

Forw	GAGTCGATACGGATCCGTGAGCAAGGGCGAGGAG
Rev	CGACCTCGAGGGATCCTCACTTGTACAGCTCGTCC

Finally, ATAT1-longlink-YFP was also prepared for the FRET experiment. ATAT1 was amplyfied from the pYFP-C_fragment-ATAT1 vector for the BIFC using the following primers:

ATAT1long_1	ACATTTGTAGAGGTTTTACTTGC
ATAT1long_2	ATGGTTCATCACTTTCTGTTTC

Using the following primers YFP was amplyfied from the pEYFP vector:

YFPlong_1	AAAGTGATGAACCATGTGAGCAAGGGCGAGGAGCTG
YFPlong_2	AAACCTCTACAAATGCTACTTGTACAGCTCGTCCATGC

Final construct was prepared by infusing 150ng of vector and 50ng of insert.

For the recombinant protein production, ATAT1 was subloned into the His-C tag pETM-14 vector (EMBL, Protein purification core facility) using NcoI and XhoI restriction enzyme.

All PCRs were performed using Phusion high-fidelity PCR master mix (Finnzymes) according to manufacturer's instructions. For the dephosphorylation of all the vectors shrimp alkaline phosphatase (Roche) was used. The clonings done by infusion were peformed using

the In-Fusion Advantage PCR Cloning kit (639620, Clontech) according to manufacturer's instructions. Chemically competent DH5α bacteria (Invitrogen) were used for all the purposes.

5.2.2 *C.elegans* plasmids

The *sng-1p::gfp* plasmid was a gift from J. Kratz. The *mec-3p::HsRed1* plasmid was made earlier in Chalfie lab by inserting the *PstI/BamHI* 1.9 kb *mec-3p* fragment derived from TU#723 strain from Chalfie lab into pPD95.77_HcRed1.

The *mec-17(+)* rescuing clone was made by inserting a 5.7 kb *mec-17* genomic fragment into pBSII_KS (Stratagene) using PstI and NotI restriction enzymes. *mec-17* genomic fragment beginnins with 1.6 kb upstream of the ATG and contains approximately 500 bp downstream of the STOP codon. The primers used were:

mec-17_1	GGTGACCATTCTTCAGGTAGGGTAAAC
mec-17_2	CGAATAAAAGATTGTCCACTCACGGAAT

The *sng-1p::mec-17* plasmid was made in two steps; first a 1.9 kb *sng-1p* fragment derived from *sng-1p::gfp* using the restriction enzymes PstI and BamHI was inserted into pBSII_KS (Stratagene). Then a 3,8 kb *mec-17* genomic fragment was inserted at the *NotI* site of the first construct. *mec-17* genomic fragment starts at ATG and finishes approximately 500 bp downstream, The primers used to obtain it were:

mec-17_3	ATGCAAGTCGACGCCGACCTCCGAC
mec-17_4	CGAATAAAAGATTGTCCACTCACGGAAT

The *mec-17p::atat-2* fusion was made using the PCR-based method of (Hobert, 2002). Genomic DNA was used as a template in two PCR reactions using the combination of the following primers:

PCR-1_F: TAGACAAACTCATTACCCTTCATTTTCTGAAATTAC

PCR-1_R: CCGTAAAAATTGTTGACAAATCGAATGCGATCTCCATGATCGAA
TCGTCTCACAACTGATCCATCGGTG

PCR-2_F: CACCGATGGATCAGTTGTGAGACGATTCGATCATGGAGATCGCATTCGA
TTTGTCAACAATTTTTACGG

PCR-2_R: GACGTACTCCGGTTAGTAATACCATAACTG

The products of PCR-1 and -2 were used as a template together with primers PCR-1_F and PCR-2_R for the gene fusion.

5.2.3 Point mutagenesis

All point mutageneses were carried out with the QuikChange II XL site-directed mutagenesis kit (200521, Stratagene).

ATAT1-GGL catalytically inactive mutant was created by following substitutions: G1403T, C1405G, G1409T and T1419C which resulted in amino acid mutations: G134W, G136W, L139P.

ATAT1-4R autoacetyl-inactive mutant was created by the following substitutions:

K56R	A164G; G165A
K146R	A434G
K210R	A626G; G627A
K221R	A659G; G660A

The *mec-17dW* and *mec-17D144N* plasmids were made using *mec-17(+)* construct as a template and the following primers:

mec-17(dW) TTATGTTCACTTCTCATGTCAACGCCAATGGGTTTGGCAACAAATTCTAGATTACAT GTTCTCTC

mec-17(D144N) GAACCTTATCAATTGGCTCTTAATAATCCATCAGTCACTCTTC

For all the point mutageneses, XL 10-Gold ultracompetent cells (Stratagene) were used for transformation.

5.2.4 shRNA

Four separate shRNA plasmids were tested in knock-down experiments and their effectiveness quantified by qRT-PCR. sh32 corresponding to the sequence GCTCAAGTTCCTGAATAAGCACTACAACC (Origene) was the most successful.

5.2.5 Quantitative real-time PCR

RNA from mouse tissues and NIH3T3 cells was isolated using an RNeasy Micro Kit (Qiagen) according to the manufacturer's instructions. mRNA was reverse transcribed by Superscript II reverse transcription (Invitrogen) using polyT primers. Quantitative PCR was performed on a LightCycler 480 PCR instrument (Roche) using 2xSYBR green I master (Roche) with 50ng of cDNA and 5μM primers mix. The expression data were normalized to ubiquitin as a reference gene.

PCR program:

Step	Temp.	Duration	Cycles
Denaturation	95°C	10:00	1x
Denaturation	95°C	00:10	45x
Annealing	58°C	00:15	
Elongation	72°C	00:10	
Denaturation	95°C	00:05	1x
Annealing	65°C	01:00	1x
Temp.ramp	97°C	N/A	Continous
Pause	16°C	Forever	-

5.3 Histology

5.3.1 *In situ* hybridization

Mouse tissues isolated from E16.5 and adult wild type C57BL/6 mice were fixed in 4% paraformaldehyde and embedded in paraffin. *In situ* hybridization was performed according to procedures previously described (Mirabeau et al., 2007) and using a probe that targets first seven exons that are common for all splice variants. The probe was cloned using the following primers: 5'ATGGAGTTCCCGTTCG and 5'GCTGATGGGCAAAG. Images were acquired on a microscope (DM6000B, Leica) with 10x, 0.25 numerial aperture dry lens fitted with a DFC290 camera and processed with Adobe Photoshop (Adobe Systems).

5.4 Imaging

5.4.1 Immunofluorescence

For immunocytochemistry, cells were fixed in 4% paraformaldehyde in PBS for 15 min at room temperature, washed in PBS and permeabilized with 0.05% Triton-X. Non-specific binding was blocked by incubating in 3% goat serum for 30 min. Incubations with primary antibodies were carried out overnight in 4% BSA. Subsequently, coverslips were washed three times with PBS and incubated with a fluorescent secondary antibody for two hours at room temperature. After three washes, coverslips were mounted and examined on a Leica SP5 confocal microscope at room temperature using a 63x objective. Images were processed and fluorescent signal was quantified using ImageJ.

For *C.elegans* immunofluorescence, animals were synchronized and prepared for microscopy using standard methods. All the primary antibodies were used at 1:200 dilution. GFP fluorescence and immunofluorescence were observed using a Zeiss Axiophot II microscope**.** All images were taken with a Diagnostic Instruments Spot 2 camera.

5.4.2 Live cell imaging

Three-cube FRET imaging was performed on room temperature on an Axiovert 200 microscope (Zeiss) equipped with a DUAL-View beam splitter (Optical Insights). The system was calibrated with two fluorophore tandem constructs of differing linker length (SuperCFP-YFP Tandem and pSuperCFP-Traf2Traf-YFP) as described by (Chen et al., 2006). ImageJ was used for image processing (background subtraction, thresholding), calculation of FRET efficiency and the unbiased selection of regions of interest for analysis. For BiFC analysis, mouse cDNA for ATAT1 or EB3 were fused with N- and C-fragments of pEYFP vector (Hu

and Kerppola, 2003). NIH3T3 cells were transiently transfected with plasmids and analyzed after 24 hours.

To record microtubule plus end dynamics in live cells, NIH3T3 cells were transfected with RFP-EB3 and YFP-ATAT1, YFP-ATAT1-GGL, ATAT1 shRNA or mock YFP. Cells were imaged after 48 hours on a Nikon Eclipse Ti system with a 100x objective for 1 minute at 1 frame per second, in a chamber at 37°C as previously described (Matov et al., 2010). To process and track EB3 movement the software package *plusTipTracker* was used as described (Matov et al., 2010).

5.4.3 *C.elegans* live imaging

Live animals were anesthetized using 0.3 M 2–3 butanedione monoxime in 10 mM Hepes. GFP and RFP fluorescence were observed using a Zeiss Axiophot II microscope**.** All images were taken with a Diagnostic Instruments Spot 2 camera.

5.4.4 Electron Microscopy

Electron microscopy on *C.elegans* was performed by Dr. David Hall in the Center for *C.elegans* anatomy at Albert Einstein College of Medicine, New York. Animals were cultured for several generations on standard NGM plates and prepared for transmission electron microscopy using standard methods (Hall et al., 2011). Briefly, adults were fixed with 3.5% glutaraldehyde and 1% paraformaldehyde in 0.12 M sodium cacodylate. Eighty-nanometer transverse sections were cut and poststained with uranium acetate and lead citrate. A Philips CM10 electron microscope with an attached Morada digital camera (Olympus) was used to acquire the images. Microtubules were counted in at least 8 sections per cell.

5.5 Biochemistry

5.5.1 Protein preparation and immunoblotting

For biochemistry cells were harvested and protein extracts were prepared using the lysis buffer (50mM Tris pH8, 150mM NaCl, 5mM MgCl2, 1mM DTT, 0.5% DOC, 0.5% Triton X-100, protease inhibitors Roche, 20% glycerol). Briefly, harvested cells were washed twice in PBS, resuspended in lysis buffer, incubated on ice for 15 min and then sonicated using Bioruptor Ultraconic Sonicator (UCD-2005O-Diagenode) with 3 pulses of 30 seconds each. Afterwards, extracts were incubated on ice again for 15min and proteins were collected from the supernatant after 10min centrifugation at 4°C. For the western blot extracts 4xSDS loading buffer was added and samples were loaded on a precast protein gel (MiniProtean TGX 456-1093, Biorad). Gels were usually ran at 100V for one hour in the electrophoresis buffer (25mM Tris pH 8.3, 250mM glycine, 0.1% SDS). Semi-dry transfer was performed afterwards using Trans-Blot SD (Biorad) machine, pure nitrocellulose transfer and immobilization membrane (Protran, NBA085C) and transfer buffer (24mM Tris base, 192mM gylcine, 20% methanol). Membranes were blocked in 5%milk (Roth, T145.1) and subsequently incubated with the primary antibody overnight. Next day they were washed 3 times with PBS-T and incubated with the secondary antibody for 1 hour. After 3 more washed with PBS-T the ECL reaction was performed using the ECL western blot detection agent (RPN2106, GE Healthcare) following the manufacturer's instructions. The membrane was exposed and the signal was detected using the Geliance 1000 Imaging System (Perkin Elmer). The signal was quantified using ImageJ.

His-tagged ATAT1 was purified by EMBL Protein purification facility following the protocols established there (Grimm et al., 2009).

For all purposes protein extracts were quantified using the 8-sample Spectrophotometer ND-800 (Nanodrop) or Bradford assay (Biorad).

5.5.2 Immunoprecipitation

Immunoprecipitations (IPs) with anti-flag M2 antibody were performed overnight at 4°C using a rotating wheel. Before the antibody was incubated with the beads for 3 hours in the same wheel at 4°C. IPs were carried out in the same lysis buffer as other protein exractions (see before). After IP the samples were centrifuged and the flow through was collected. Subsequently 3 washes with a washing buffer (100mM Tris-Cl pH8, 150mM NaCl, 1mM EDTA) were performed and finally proteins were eluted either using immediately SDS loading buffer if they were to be ran on the gel immediately after or if they were to be used for other experiements elution was performed with 3x FLAG peptide (F4799, Sigma) according to manufacturer's indications.

5.5.3 2D gels

2D gels were done as previously described (Hartinger et al., 1996). Briefly, first dimension gel was prepared one day in advance. After 10% separator gel (see below) was polymerized 5% stacking gel (see below) was added on the top. First electrophoresis was ran at 12mA for the first 10min and then at 80mA. Afterwards gel was stained with Coomassie for 10min and then destained and equilibrated in 100mM Tris buffer pH6.8. The lanes were cut and second dimension gel was assambled and run for 12 hours at 100V. Second dimension gel was a standard SDS gel.

Separator gel 10% (20ml)		**Stacking gel 1D 5% (10ml)**	
6.6ml	30%-0.8% Acrylamide/bisacrylamide	1.6ml	30% Acry-Bis
0.7ml	1.7% bisacrylamide	1g	urea
5ml	0.3M K phosphate buffer pH 2.1	1.3ml	1.7% bisacrylamide
3.6g	Urea	2.5ml	K-phosphate buffer pH 4.1 0.5M
1ml	Ascorbic acid 80mM	3ml	water
32ul	FeSO4 5mM	0.5ml	ascorbic acid 80mM
0.2ml	16BAC 250mM	8.5ul	FeSO4 5mM
		70ul	16BAC 250mM
		0.5ml	H2O2 (1:750)

5.5.4 Silver staining of protein gels

Silver staining of gels for mass spectrometry was performed using the protocol from the EMBL Proteomics facility. Briefly, gel was rinsed with ddH_20 and fixed for 45min on room temperature in a fixing solution (40% methanol, 10% acetic acid). Subsequently, gel was washed with ultra pure water for 1.5hours, incubated with 0.02% (w/v) sodium thiosulfate for 3min, then washed twice briefly with ultra pure water and incubated in 0.1% (w/v) silver nitrate in dark at 4°C for 30min. Afterwards, gel was washed twice with ultra pure water again and then developed in 0.04% formaldehyde in 2% (w/v) sodium carbonate. The reaction was stopped with addition of 5% acetid acid after which gel was washed again briefly with ultra pure water. All the chemical used for silver staining were obtained from Sigma. For all other purposes silver staining of gels was performed using the Pierce Silver Stain Kit (24612, Thermo Scientific).

5.5.5 Isolation of microtubule fraction

Isolation of microtubules and MAPs was performed following the protocol (Avila et al., 2008). Briefly, 8 20cm tissue culture plates with CHO cells over expressing ATAT1 or mock YFP were used. The cells were harvested, spun down and the pellet was resuspended in A buffer with proteinase inhibitors (Roche). After shearing with G18, 20, 22 and 26 needles the extracts were centrifuged at 50.000 rpm at 2°C for 90min, after which taxol was added to 20mM and GTP to 0.5mM. The extracts were then warmed up to 37°C for few minutes and subsequently chilled on ice for further 15min. Next, they were transfered to a chilled centrifuge tube and underlaid with cold PEG buffer containing 10% sucrose, 20mM taxol and 0.5mM GTP. The microtubule fraction was pelleted through the sucrose cushion by centrifugation at 29.000rpm for 30min at 2°C. The fraction was washed one with PEG buffer and then loaded on the gel. Control of fractionation was performed without taxol and GTP.

5.5.6 *In vitro* acetylation reaction

Purified tubulin was kept in General Tubulin Buffer (80mM PIPES pH6.9, 2mM $MgCl_2$, 0.5mM EDTA). Reactions were made in 10µl ADE buffer (Shida et al., 2010), with 1µg bovine brain tubulin (TL238, Cytoskeleton), 4µg recombinant ATAT1 preparation and 8µM AcCoA (A2056, Sigma) or ^{14}C AcCoA (NEC313N010UC, Perkin Elmer), unless otherwise indicated. Reactions were incubated at 37°C for the time indicated, and stopped with addition of the SDS loading buffer. Gels were fixed in the fixing solution (40% methanol, 10% acetic acid) and dried for 1 hour at 80°C using the Model 583 Gel Dryer (Biorad). Subsequently, dry gels were exposed to phosphoimager for 3 days. Phosphoscreen was scanned using the Fluorescent Image Analysis System FLA-5100 (Fujifilm). The signal was quantified using ImageJ.

5.5.7 Mass spectrometry

Mass spectrometry was performed in the San Raffaele Scientific Institute in Milan, in collaboration with the protein microsequencing facility, by Annapaola Andolfo and me. The standard *in vitro* reaction (described above) was scaled up 40 times using ^{13}C AcCoA (Sigma). Control reaction was carried out without AcCoA. After 1 hour at 37°C the reaction was reduced and alkylated with DTT and IAA. An aliquot was analyzed on the gel using anti-acetylated tubulin antibody. The reaction was resuspended in Ambic and in-solution digestion was performed. Trypsin and Glu-C were used for α-tubulin digestion and trypsin and chymotrypsin for ATAT1 digestion. Enrichment of acetylated peptides and MS analysis were performed according to procedures previously described (Choudhary et al., 2009). Briefly, 40µl of beads with anti-acetyl lysine antibody were washed and subsequently incubated with the digestion products overnight at 4°C. The following day, flow-through was collected. After 4 washes with Mops buffer and 2 washes with water, the pepties were eluted using 0.1%TFA.

Final volume of the eluate was 40µl. The eluates were cleaned through a column and loaded on MS/MS and Orbitrap machines. The data were analyzed using Mascot search.

5.6 Behavior test

5.6.1 Touch assays

We assayed gentle touch sensitivity in blind tests as described (Chalfie and Sulston, 1981). We quantified the response by counting the number of responses to 10 touches delivered alternately near the head and tail in 30 animals (or 30 characterized transformants in strains with extragenic arrays).

6 Bibliography

Akella, J.S., Wloga, D., Kim, J., Starostina, N.G., Lyons-Abbott, S., Morrissette, N.S., Dougan, S.T., Kipreos, E.T., and Gaertig, J. (2010). MEC-17 is an alpha-tubulin acetyltransferase. Nature *467*, 218-222.

Akhmanova, A., and Steinmetz, M.O. (2008). Tracking the ends: a dynamic protein network controls the fate of microtubule tips. Nat Rev Mol Cell Biol *9*, 309-322.

Allfrey, V.G., Faulkner, R., and Mirsky, A.E. (1964). Acetylation and Methylation of Histones and Their Possible Role in the Regulation of Rna Synthesis. Proc Natl Acad Sci U S A *51*, 786-794.

Allis, C.D., Berger, S.L., Cote, J., Dent, S., Jenuwien, T., Kouzarides, T., Pillus, L., Reinberg, D., Shi, Y., and Shiekhattar, R. (2007). New nomenclature for chromatin-modifying enzymes. Cell *131*, 633-636.

Avila, J., Soares, H., Fanarraga, M.L., and Zabala, J.C. (2008). Isolation of Microtubules and Microtubule Proteins. Current Protocols in Cell Biology, 3.29.21 - 23.29.28.

Bannister, A.J., Miska, E.A., Gorlich, D., and Kouzarides, T. (2000). Acetylation of importin alpha nuclear import factors by CBP/p300. Curr Biol *10*, 467-470.

Barnes, T.M., Jin, Y., Horvitz, H.R., Ruvkun, G., and Hekimi, S. (1996). The Caenorhabditis elegans behavioral gene unc-24 encodes a novel bipartite protein similar to both erythrocyte band 7.2 (stomatin) and nonspecific lipid transfer protein. J Neurochem *67*, 46-57.

Bautista, D.M., Jordt, S.E., Nikai, T., Tsuruda, P.R., Read, A.J., Poblete, J., Yamoah, E.N., Basbaum, A.I., and Julius, D. (2006). TRPA1 mediates the inflammatory actions of environmental irritants and proalgesic agents. Cell *124*, 1269-1282.

Belmadani, S., Pous, C., Fischmeister, R., and Mery, P.F. (2004). Post-translational modifications of tubulin and microtubule stability in adult rat ventricular myocytes and immortalized HL-1 cardiomyocytes. Mol Cell Biochem *258*, 35-48.

Berndsen, C.E., Albaugh, B.N., Tan, S., and Denu, J.M. (2007). Catalytic mechanism of a MYST family histone acetyltransferases. Biochemistry *46*, 623-629.

Black, M.M., and Keyser, P. (1987). Acetylation of alpha-tubulin in cultured neurons and the induction of alpha-tubulin acetylation in PC12 cells by treatment with nerve growth factor. J Neurosci *7*, 1833-1842.

Bounoutas, A., and Chalfie, M. (2007). Touch sensitivity in Caenorhabditis elegans. Pflugers Arch *454*, 691-702.

Bounoutas, A., O'Hagan, R., and Chalfie, M. (2009a). The multipurpose 15-protofilament microtubules in C. elegans have specific roles in mechanosensation. Curr Biol *19*, 1362-1367.

Bounoutas, A., Zheng, Q., Nonet, M.L., and Chalfie, M. (2009b). mec-15 encodes an F-box protein required for touch receptor neuron mechanosensation, synapse formation and development. Genetics *183*, 607-617, 601SI-604SI.

Boyes, J., Byfield, P., Nakatani, Y., and Ogryzko, V.V. (1998). Regulation of activity of the transcription factor GATA-1 by acetylation. Nature *396*, 594-598.

Brenner, S. (1974). The genetics of Caenorhabditis elegans. Genetics *77*, 71-94.

Brownell, J.E., Zhou, J., Ranalli, T., Kobayashi, R., Edmondson, D.G., Roth, S.Y., and Allis, C.D. (1996). Tetrachymena histone acetyltransferase A: a homolog to yeast Gcn5p linking histone acetylation to gene activation. Cell *84*, 843-851.

Calixto, A., Ma, C., and Chalfie, M. (2010). Conditional gene expression and RNAi using MEC-8-dependent splicing in C. elegans. Nat Methods *7*, 407-411.

Cambray-Deakin, M.A., and Burgoyne, R.D. (1987). Posttranslational modifications of alpha-tubulin: acetylated and detyrosinated forms in axons of rat cerebellum. J Cell Biol *104*, 1569-1574.

Cassata, G., Kagoshima, H., Andachi, Y., Kohara, Y., Durrenberger, M.B., Hall, D.H., and Burglin, T.R. (2000). The LIM homeobox gene ceh-14 confers thermosensory function to the AFD neurons in Caenorhabditis elegans. Neuron *25*, 587-597.

Chalfie, M. (2009). Neurosensory mechanotransduction. Nat Rev Mol Cell Biol *10*, 44-52.

Chalfie, M., and Au, M. (1989). Genetic control of differentiation of the Caenorhabditis elegans touch receptor neurons. Science *243*, 1027-1033.

Chalfie, M., and Sulston, J. (1981). Developmental genetics of the mechanosensory neurons of Caenorhabditis elegans. Dev Biol *82*, 358-370.

Chalfie, M., and Thomson, J.N. (1979). Organization of neuronal microtubules in the nematode Caenorhabditis elegans. J Cell Biol *82*, 278-289.

Chalfie, M., and Thomson, J.N. (1982). Structural and functional diversity in the neuronal microtubules of Caenorhabditis elegans. J Cell Biol *93*, 15-23.

Chalfie, M., and Wolinsky, E. (1990). The identification and suppression of inherited neurodegeneration in Caenorhabditis elegans. Nature *345*, 410-416.

Chelur, D.S., and Chalfie, M. (1996). The saga of cloning mec-17.... continues. East Coast Worm Meeting.

Chelur, D.S., and Chalfie, M. (2007). Targeted cell killing by reconstituted caspases. Proc Natl Acad Sci U S A *104*, 2283-2288.

Chelur, D.S., Ernstrom, G.G., Goodman, M.B., Yao, C.A., Chen, L., R, O.H., and Chalfie, M. (2002). The mechanosensory protein MEC-6 is a subunit of the C. elegans touch-cell degenerin channel. Nature *420*, 669-673.

Chen, H., Puhl, H.L., 3rd, Koushik, S.V., Vogel, S.S., and Ikeda, S.R. (2006). Measurement of FRET efficiency and ratio of donor to acceptor concentration in living cells. Biophys J *91*, L39-41.

Chen, S., Owens, G.C., Makarenkova, H., and Edelman, D.B. (2010). HDAC6 regulates mitochondrial transport in hippocampal neurons. PLoS One *5*, e10848.

Choudhary, C., Kumar, C., Gnad, F., Nielsen, M.L., Rehman, M., Walther, T.C., Olsen, J.V., and Mann, M. (2009). Lysine acetylation targets protein complexes and co-regulates major cellular functions. Science *325*, 834-840.

Chu, C.W., Hou, F., Zhang, J., Phu, L., Loktev, A.V., Kirkpatrick, D.S., Jackson, P.K., Zhao, Y., and Zou, H. (2011). A novel acetylation of beta-tubulin by San modulates microtubule polymerization via down-regulating tubulin incorporation. Mol Biol Cell *22*, 448-456.

Cohen, T.J., Guo, J.L., Hurtado, D.E., Kwong, L.K., Mills, I.P., Trojanowski, J.Q., and Lee, V.M. (2011). The acetylation of tau inhibits its function and promotes pathological tau aggregation. Nat Commun *2*, 252.

Collins, S.R., Miller, K.M., Maas, N.L., Roguev, A., Fillingham, J., Chu, C.S., Schuldiner, M., Gebbia, M., Recht, J., Shales, M*., et al.* (2007). Functional dissection of protein complexes involved in yeast chromosome biology using a genetic interaction map. Nature *446*, 806-810.

Conde, C., and Caceres, A. (2009). Microtubule assembly, organization and dynamics in axons and dendrites. Nat Rev Neurosci *10*, 319-332.

Consortium, T.C.e.S. (1998). Genome sequence of the nematode C. elegans: a platform for investigating biology. Science *282*, 2012-2018.

Costantini, C., Ko, M.H., Jonas, M.C., and Puglielli, L. (2007). A reversible form of lysine acetylation in the ER and Golgi lumen controls the molecular stabilization of BACE1. Biochemical Journal *407*, 383-395.

Coste, B., Mathur, J., Schmidt, M., Earley, T.J., Ranade, S., Petrus, M.J., Dubin, A.E., and Patapoutian, A. (2010). Piezo1 and Piezo2 are essential components of distinct mechanically activated cation channels. Science *330*, 55-60.

Creppe, C., Malinouskaya, L., Volvert, M.L., Gillard, M., Close, P., Malaise, O., Laguesse, S., Cornez, I., Rahmouni, S., Ormenese, S*., et al.* (2009). Elongator controls the migration and differentiation of cortical neurons through acetylation of alpha-tubulin. Cell *136*, 551-564.

Diaz, J.F., Barasoain, I., and Andreu, J.M. (2003). Fast kinetics of Taxol binding to microtubules. Effects of solution variables and microtubule-associated proteins. J Biol Chem *278*, 8407-8419.

Diaz, J.F., Valpuesta, J.M., Chacon, P., Diakun, G., and Andreu, J.M. (1998). Changes in microtubule protofilament number induced by Taxol binding to an easily accessible site. Internal microtubule dynamics. J Biol Chem *273*, 33803-33810.

Dompierre, J.P., Godin, J.D., Charrin, B.C., Cordelieres, F.P., King, S.J., Humbert, S., and Saudou, F. (2007). Histone deacetylase 6 inhibition compensates for the transport deficit in Huntington's disease by increasing tubulin acetylation. J Neurosci *27*, 3571-3583.

Draberova, E., Viklicky, V., and Draber, P. (2000). Exposure of lumenal microtubule sites after mild fixation. Eur J Cell Biol *79*, 982-985.

Drake, P.J.M., Griffiths, G.J., Shaw, L., Benson, R.P., and Corfe, B.M. (2009). Application of high-content analysis to the study of post-translational modifications of the cytoskeleton Journal of proteome research *8*, 28-34.

Drew, L.J., Wood, J.N., and Cesare, P. (2002). Distinct mechanosensitive properties of capsaicin-sensitive and -insensitive sensory neurons. J Neuroscience *22*, 228.

Driscoll, M., and Chalfie, M. (1991). The mec-4 gene is a member of a family of Caenorhabditis elegans genes that can mutate to induce neuronal degeneration. Nature *349*, 588-593.

Du, G., Liu, X., Chen, X., Song, M., Yan, Y., Jiao, R., and Wang, C.C. (2010). Drosophila histone deacetylase 6 protects dopaminergic neurons against {alpha}-synuclein toxicity by promoting inclusion formation. Mol Biol Cell *21*, 2128-2137.

Du, H., and Chalfie, M. (2001). Genes regulating touch cell development in Caenorhabditis elegans. Genetics *158*, 197-207.

Du, H., Gu, G., William, C.M., and Chalfie, M. (1996). Extracellular proteins needed for C. elegans mechanosensation. Neuron *16*, 183-194.

Eberl, D.F., Duyk, G.M., and Perrimon, N. (1997). A genetic screen for mutations that disrupt an auditory response in Drosophila melanogaster. Proc Natl Acad Sci U S A *94*, 14837-14842.

Emtage, L., Gu, G., Hartwieg, E., and Chalfie, M. (2004). Extracellular proteins organize the mechanosensory channel complex in C. elegans touch receptor neurons. Neuron *44*, 795-807.

Farley, F.W., Soriano, P., Steffen, L.S., and Dymecki, S.M. (2000). Widespread recombinase expression using FLPeR (flipper) mice. Genesis *28*, 106-110.

Finney, M., and Ruvkun, G. (1990). The unc-86 gene product couples cell lineage and cell identity in C. elegans. Cell *63*, 895-905.

Finney, M., Ruvkun, G., and Horvitz, H.R. (1988). The C. elegans cell lineage and differentiation gene unc-86 encodes a protein with a homeodomain and extended similarity to transcription factors. Cell *55*, 757-769.

Fukushige, T., Siddiqui, Z.K., Chou, M., Culotti, J.G., Gogonea, C.B., Siddiqui, S.S., and Hamelin, M. (1999). MEC-12, an alpha-tubulin required for touch sensitivity in C. elegans. J Cell Sci *112 (Pt 3)*, 395-403.

Fukushima, N., Furuta, D., Hidaka, Y., Moriyama, R., and Tsujiuchi, T. (2009). Post-translational modifications of tubulin in the nervous system. J Neurochem *109*, 683-693.

Gaertig, J., Cruz, M.A., Bowen, J., Gu, L., Pennock, D.G., and Gorovsky, M.A. (1995). Acetylation of lysine 40 in alpha-tubulin is not essential in Tetrahymena thermophila. J Cell Biol *129*, 1301-1310.

Garrison, S.R., Dietrich, A., and Stucky, C.L. (2011). TRPC1 contributes to light-touch sensation and mechanical responses in low-threshold cutaneous sensory neurons. J Neurophysiol.

Gigant, B., Curmi, P.A., Martin-Barbey, C., Charbaut, E., Lachkar, S., Lebeau, L., Siavoshian, S., Sobel, A., and Knossow, M. (2000). The 4 A X-ray structure of a tubulin:stathmin-like domain complex. Cell *102*, 809-816.

Gillespie, P.G., and Walker, R.G. (2001). Molecular basis of mechanosensory transduction. Nature *413*, 194-202.

Grimm, C., Matos, R., Ly-Hartig, N., Steuerwald, U., Lindner, D., Rybin, V., Muller, J., and Muller, C.W. (2009). Molecular recognition of histone lysine methylation by the Polycomb group repressor dSfmbt. Embo J *28*, 1965-1977.

Gu, G., Caldwell, G.A., and Chalfie, M. (1996). Genetic interactions affecting touch sensitivity in Caenorhabditis elegans. Proc Natl Acad Sci U S A *93*, 6577-6582.

Gu, W., and Roeder, R.G. (1997). Activation of p53 sequence-specific DNA binding by acetylation of the p53 C-terminal domain. Cell *90*, 595-606.

Gupta, M.P., Samant, S.A., Smith, S.H., and Shroff, S.G. (2008). HDAC4 and PCAF bind to cardiac sarcomers and play a role in regulating myofilament contractile activity. J Biol Chem *283*, 10135-10146.

Haggarty, S.J., Koeller, K.M., Wong, J.C., Grozinger, C.M., and Schreiber, S.L. (2003a). Domain-selective small-molecule inhibitor of histone deacetylase 6 (HDAC6)-mediated tubulin deacetylation. Proc Natl Acad Sci U S A *100*, 4389-4394.

Haggarty, S.J., Koeller, K.M., Wong, J.C., Grozinger, C.M., and Schreiber, S.L. (2003b). Domain-selective small-molecule inhibitor of histone deacetylase 6 (HDAC6)-mediated tubulin deacetylation. Proc Natl Acad Sci U S A *100*, 4389-4394.

Hall, D.H., Hartwieg, E., and Nguyen, K.C. (2011). Modern electron microscopy methods for C.elegans. Methods Cell Biol.

Hammond, J.W., Cai, D., and Verhey, K.J. (2008). Tubulin modifications and their cellular functions. Curr Opin Cell Biol *20*, 71-76.

Hartinger, J., Stenius, K., Hogemann, D., and Jahn, R. (1996). 16-BAC/SDS-PAGE: a two-dimensional gel electrophoresis system suitable for the separation of integral membrane proteins. Anal Biochem *240*, 126-133.

Hobert, O. (2002). PCR fusion-based approach to create reporter gene constructs for expression analysis in transgenic C. elegans. Biotechniques *32*, 728-730.

Hu, C.D., and Kerppola, T.K. (2003). Simultaneous visualization of multiple protein interactions in living cells using multicolor fluorescence complementation analysis. Nat Biotechnol *21*, 539-545.

Huang, M., and Chalfie, M. (1994). Gene interactions affecting mechanosensory transduction in Caenorhabditis elegans. Nature *367*, 467-470.

Huang, M., Gu, G., Ferguson, E.L., and Chalfie, M. (1995). A stomatin-like protein necessary for mechanosensation in C. elegans. Nature *378*, 292-295.

Hubbert, C., Guardiola, A., Shao, R., Kawaguchi, Y., Ito, A., Nixon, A., Yoshida, M., Wang, X.F., and Yao, T.P. (2002). HDAC6 is a microtubule-associated deacetylase. Nature *417*, 455-458.

Imhof, A., Yang, X.J., Ogryzko, V.V., Nakatani, Y., Wolffe, A.P., and Ge, H. (1997). Acetylation of general transcription factors by histone acetyltransferases. Curr Biol *7*, 689-692.

Inoue, S. (1981). Cell division and the mitotic spindle. J Cell Biol *91*, 131s-147s.

Janke, C., and Chloe Bulinski, J. (2011). Post-translational regulation of the microtubule cytoskeleton: mechanisms and functions. Nat Rev Mol Cell Biol *12*, 773-786.

Janke, C., and Kneussel, M. (2010). Tubulin post-translational modifications: encoding functions on the neuronal microtubule cytoskeleton. Trends Neurosci *33*, 362-372.

Jaworski, J., Hoogenraad, C.C., and Akhmanova, A. (2008). Microtubule plus-end tracking proteins in differentiated mammalian cells. Int J Biochem Cell Biol *40*, 619-637.

Jonas, M.C., Costantini, C., and Puglielli, L. (2008). PCSK9 is required for the disposal of non-acetylated intermediates of the nascent membrane protein BACE1. EMBO reports *9*, 916-922.

Joshi, H.C., and Cleveland, D.W. (1989). Differential utilization of beta-tubulin isotypes in differentiating neurites. J Cell Biol *109*, 663-673.

Kahn-Kirby, A.H., and Bergmann, C.I. (2006). TRP channels in C.elegans. Annual review of physiology *68*, 719-736.

Kar, S., Fan, J., Smith, M.J., Goedert, M., and Amos, L.A. (2003). Repeat motifs of tau bind to the insides of microtubules in the absence of taxol. Embo J *22*, 70-77.

Kawaguchi, Y., Kovacs, J.J., McLaurin, A., Vance, J.M., Ito, A., and Yao, T.P. (2003). The deacetylase HDAC6 regulates aggresome formation and cell viability in response to misfolded protein stress. Cell *115*, 727-738.

Kernan, M., Cowan, D., and Zuker, C. (1994). Genetic dissection of mechanosensory transduction: mechanoreception-defective mutations of Drosophila. Neuron *12*, 1195-1206.

Kim, J., Chung, Y.D., Park, D.Y., Choi, S., Shin, D.W., Soh, H., Lee, H.W., Son, W., Yim, J., Park, C.S.*, et al.* (2003). A TRPV family ion channel required for hearing in Drosophila. Nature *424*, 81-84.

Kim, S.C., Sprung, R., Chen, Y., Xu, Y., Ball, H., Pei, J., Cheng, T., Kho, Y., Xiao, H., Xiao, L.*, et al.* (2006). Substrate and functional diversity of lysine acetylation revealed by a proteomics survey. Mol Cell *23*, 607-618.

Kovacs, J.J., Murphy, P.J., Gaillard, S., Zhao, X., Wu, J.T., Nicchitta, C.V., Yoshida, M., Toft, D.O., Pratt, W.B., and Yao, T.P. (2005). HDAC6 regulates Hsp90 acetylation and chaperone-dependent activation of glucocorticoid receptor. Mol Cell *18*, 601-607.

Kung, C. (2005). A possible unifying principle for mechanosensation. Nature *436*, 647-654.

Kwan, K.Y., Allchorne, A.J., Vollrath, M.A., Christensen, A.P., Zhang, D.S., Woolf, C.J., and Corey, D.P. (2006). TRPA1 contributes to cold, mechanical, and chemical nociception but is not essential for hair-cell transduction. Neuron *50*, 277-289.

Kwon, S., Zhang, Y., and Matthias, P. (2007). The deacetylase HDAC6 is a novel critical component of stress granules involved in the stress response. Genes Dev *21*, 3381-3394.

L'Hernault SW, R.J. (1983). Chlamydomonas alpha-tubulin is post- translationally modified in the flagella during flagellar assembly. J Cell Biol *97*, 258-263.

L'Hernault, S.W., and Rosenbaum, J.L. (1985). Chlamydomonas alpha-tubulin is posttranslationally modified by acetylation on the epsilon-amino group of a lysine. Biochemistry *24*, 473-478.

LeDizet, M., and Piperno, G. (1987). Identification of an acetylation site of Chlamydomonas alpha-tubulin. Proc Natl Acad Sci U S A *84*, 5720-5724.

LeDizet, M., and Piperno, G. (1991). Detection of acetylated alpha-tubulin by specific antibodies. Methods Enzymol *196*, 264-274.

Loken, L.S., Wessberg, J., Morrison, I., McGlone, F., and Olausson, H. (2009). Coding of pleasant touch by unmyelinated afferents in humans Nat Neurosci *12*, 547-548.

Lumpkin, E.A., and Bautista, D.M. (2005). Feeling a pressure in mammalian somatosensation. Opin Neurobiol *15*, 382-388.

Lumpkin, E.A., Marshall, K.L., and Nelson, A.M. (2010). The cell biology of touch. Journal of Cell Biology *191*, 237-248.

Mann, M. (2006). Functional and quantitative proteomics using SILAC. Nat Rev Mol Cell Biol *7*, 952-958.

Maruta, H., Greer, K., and Rosenbaum, J.L. (1986). The acetylation of alpha-tubulin and its relationship to the assembly and disassembly of microtubules. J Cell Biol *103*, 571-579.

Matov, A., Applegate, K., Kumar, P., Thoma, C., Krek, W., Danuser, G., and Wittmann, T. (2010). Analysis of microtubule dynamic instability using a plus-end growth marker. Nat Methods *7*, 761-768.

Matsuyama, A., Shimazu, T., Sumida, Y., Saito, A., Yoshimatsu, Y., Seigneurin-Berny, D., Osada, H., Komatsu, Y., Nishino, N., Khochbin, S.*, et al.* (2002a). In vivo destabilization of dynamic microtubules by HDAC6-mediated deacetylation. Embo J *21*, 6820-6831.

Matsuyama, A., Shimazu, T., Sumida, Y., Saito, A., Yoshimatsu, Y., Seigneurin-Berny, D., Osada, H., Komatsu, Y., Nishino, N., Khochbin, S.*, et al.* (2002b). In vivo destabilization of dynamic microtubules by HDAC6-mediated deacetylation. Embo J *21*, 6820-6831.

McIntosh, J.R., and Euteneuer, U. (1984). Tubulin hooks as probes for microtubule polarity: an analysis of the method and an evaluation of data on microtubule polarity in the mitotic spindle. J Cell Biol *98*, 525-533.

Meyerson, B.A., Ren, B., Herregodts, P., and Linderoth, B. (1995). Spinal cord stimulation in animal models of mononeuropathy: effects on the withdrawal response and the flexor reflex. Pain *61*, 229-243.

Min, S.W., Cho, S.H., Zhou, Y., Schroeder, S., Haroutunian, V., Seeley, W.W., Huang, E.J., Shen, Y., Masliah, E., Mukherjee, C.*, et al.* (2010). Acetylation of tau inhibits its degradation and contributes to tauopathy. Neuron *67*, 953-966.

Mirabeau, O., Perlas, E., Severini, C., Audero, E., Gascuel, O., Possenti, R., Birney, E., Rosenthal, N., and Gross, C. (2007). Identification of novel peptide hormones in the human proteome by hidden Markov model screening. Genome Res *17*, 320-327.

Mitchison, T., and Kirschner, M. (1984). Dynamic instability of microtubule growth. Nature *312*, 237-242.

Moerman, D.G., and Barstead, R. J. (2008). Towards a mutation in every gene in Caenorhabditis elegans. Brief Funct Genomic Proteomic *7*, 195-204.

Myers, K.A., Applegate, K.T., Danuser, G., Fischer, R.S., and Waterman, C.M. (2011). Distinct ECM mechanosensing pathways regulate microtubule dynamics to control endothelial cell branching morphogenesis. J Cell Biol *192*, 321-334.

Nogales, E., Whittaker, M., Milligan, R.A., and Downing, K.H. (1999). High-resolution model of the microtubule. Cell *96*, 79-88.

Norris, K.L., Lee, J.Y., and Yao, T.P. (2009). Acetylation goes global: the emergence of acetylation biology. Sci Signal *2*, pe76.

North, B.J., Marshall, B.L., Borra, M.T., Denu, J.M., and Verdin, E. (2003). The human Sir2 ortholog, SIRT2, is an NAD+-dependent tubulin deacetylase. Mol Cell *11*, 437-444.

O'Hagan, R., and Chalfie, M. (2006). Mechanosensation in Caenorhabditis elegans. Int Rev Neurobiol *69*, 169-203.

O'Hagan, R., Chalfie, M., and Goodman, M.B. (2005). The MEC-4 DEG/ENaC channel of Caenorhabditis elegans touch receptor neurons transduces mechanical signals. Nat Neurosci *8*, 43-50.

Odde, D. (1998). Diffusion inside microtubules. Eur Biophys J *27*, 514-520.

Ohkawa, N., Sugisaki, S., Tokunaga, E., Fujitani, K., Hayasaka, T., Setou, M., and Inokuchi, K. (2008). N-acetyltransferase ARD1-NAT1 regulates neuronal dendritic development. Genes Cells *13*, 1171-1183.

Olsen, J.V., Blagoev, B., Gnad, F., Macek, B., Kumar, C., Mortensen, P., and Mann, M. (2006). Global, in vivo, and site-specific phosphorylation dynamics in signaling networks. Cell *127*, 635-648.

Outeiro, T.F., Kontopoulos, E., Altmann, S.M., Kufareva, I., Strathearn, K.E., Amore, A.M., Volk, C.B., Maxwell, M.M., Rochet, J.C., McLean, P.J.*, et al.* (2007). Sirtuin 2 inhibitors rescue alpha-synuclein-mediated toxicity in models of Parkinson's disease. Science *317*, 516-519.

Palazzo, A., Ackerman, B., and Gundersen, G.G. (2003). Cell biology: Tubulin acetylation and cell motility. Nature *421*, 230.

Pan, C.L., Peng, C.Y., Chen, C.H., and McIntire, S. (2011). Genetic analysis of age-dependent defects of the Caenorhabditis elegans touch receptor neurons. Proc Natl Acad Sci U S A *108*, 9274-9279.

Pearl, L.H., and Prodromou, C. (2006). Structure and mechanism of the Hsp90 molecular chaperone machinery. Annu Rev Biochem *75*, 271-294.

Perez, M., Santa-Maria, I., Gomez de Barreda, E., Zhu, X., Cuadros, R., Cabrero, J.R., Sanchez-Madrid, F., Dawson, H.N., Vitek, M.P., Perry, G.*, et al.* (2009). Tau--an inhibitor of deacetylase HDAC6 function. J Neurochem *109*, 1756-1766.

Piperno, G., and Fuller, M.T. (1985). Monoclonal antibodies specific for an acetylated form of alpha-tubulin recognize the antigen in cilia and flagella from a variety of organisms. J Cell Biol *101*, 2085-2094.

Piperno, G., LeDizet, M., and Chang, X.J. (1987). Microtubules containing acetylated alpha-tubulin in mammalian cells in culture. J Cell Biol *104*, 289-302.

Reed, N.A., Cai, D., Blasius, T.L., Jih, G.T., Meyhofer, E., Gaertig, J., and Verhey, K.J. (2006). Microtubule acetylation promotes kinesin-1 binding and transport. Curr Biol *16*, 2166-2172.

Roll-Mecak, A., and McNally, F.J. (2010). Microtubule severing enzymes. Curr Opin Cell Biol *22*, 96-103.

Sadoul, K., Boyault, C., Pabion, M., and Khochbin, S. (2008). Regulation of protein turnover by acetyltransferases and deacetylases. Biochimie *90*, 306-312.

Sadoul, K., Wang, J., Diagouraga, B., and Khochbin, S. (2011). The tale of protein lysine acetylation in the cytoplasm. J Biomed Biotechnol *2011*, 970382.

Santos-Rosa, H., Valls, E., Kouzarides, T., and Martinez-Balbas, M. (2003). Mechanism of P/CAF auto-acetylation. Nucleic Acids Res *31*, 4285-4292.

Savage, C., Hamelin, M., Culotti, J.G., Coulson, A., Albertson, D.G., and Chalfie, M. (1989). mec-7 is a beta-tubulin gene required for the production of 15-protofilament microtubules in Caenorhabditis elegans. Genes Dev *3*, 870-881.

Schatten, G., Simerly, C., Asai, D.J., Szoke, E., Cooke, P., and Schatten, H. (1988). Acetylated alpha-tubulin in microtubules during mouse fertilization and early development. Dev Biol *130*, 74-86.

Schiff, P.B., Fant, J., and Horwitz, S.B. (1979). Promotion of microtubule assembly in vitro by taxol. Nature *277*, 665-667.

Schiff, P.B., and Horwitz, S.B. (1980). Taxol stabilizes microtubules in mouse fibroblast cells. Proc Natl Acad Sci U S A *77*, 1561-1565.

Schobl (1871). Das aussere Ohr der Mause als wichtiges Tastorgan. Archiv fuer mikroskopische Anatomie, 260-268.

Schwenk, F., Baron, U., and Rajewsky, K. (1995). A cre-transgenic mouse strain for the ubiquitous deletion of loxP-flanked gene segments including deletion in germ cells. Nucleic Acids Res *23*, 5080-5081.

Seal, R.P., Wang, X., Guan, Y., Raja, S.N., Woodbury, C.J., Basbaum, A.I., and Edwards, R.H. (2009). Injury-induced mechanical hypersensitivity requires C-low threshold mechanoreceptors. Nature *462*, 651-655.

Shida, T., Cueva, J.G., Xu, Z., Goodman, M.B., and Nachury, M.V. (2010). The major alpha-tubulin K40 acetyltransferase alphaTAT1 promotes rapid ciliogenesis and efficient mechanosensation. Proc Natl Acad Sci U S A *107*, 21517-21522.

Sidi, S., Friedrich, R.W., and Nicolson, T. (2003). NompC TRP channel required for vertebrate sensory hair cell mechanotransduction. Science *301*, 96-99.

Solinger, J.A., Paolinelli, R., Kloss, H., Scorza, F.B., Marchesi, S., Sauder, U., Mitsushima, D., Capuani, F., Sturzenbaum, S.R., and Cassata, G. (2010). The Caenorhabditis elegans Elongator complex regulates neuronal alpha-tubulin acetylation. PLoS Genet *6*, e1000820.

Steczkiewicz, K., Kinch, L., Grishin, N.V., Rychlewski, L., and Ginalski, K. (2006). Eukaryotic domain of unknown function DUF738 belongs to Gcn5-related N-acetyltransferase superfamily. Cell Cycle *5*, 2927-2930.

Stepanova, T., Slemmer, J., Hoogenraad, C.C., Lansbergen, G., Dortland, B., De Zeeuw, C.I., Grosveld, F., van Cappellen, G., Akhmanova, A., and Galjart, N. (2003). Visualization of microtubule growth in cultured neurons via the use of EB3-GFP (end-binding protein 3-green fluorescent protein). J Neurosci *23*, 2655-2664.

Sudo, H., and Baas, P.W. (2010). Acetylation of microtubules influences their sensitivity to severing by katanin in neurons and fibroblasts. J Neurosci *30*, 7215-7226.

Sulston, J., Dew, M., and Brenner, S. (1975). Dopaminergic neurons in the nematode Caenorhabditis elegans. J Comp Neurol *163*, 215-226.

Sulston, J.E., and Horvitz, H.R. (1977). Post-embryonic cell lineages of the nematode, Caenorhabditis elegans. Dev Biol *56*, 110-156.

Sulston, J.E., Schierenberg, E., White, J.G., and Thomson, J.N. (1983). The embryonic cell lineage of the nematode Caenorhabditis elegans. Dev Biol *100*, 64-119.

Suzuki, K., and Koike, T. (2007). Mammalian Sir2-related protein (SIRT) 2-mediated modulation of resistance to axonal degeneration in slow Wallerian degeneration mice: a crucial role of tubulin deacetylation. Neuroscience *147*, 599-612.

Suzuki, M., Mizuno, A., Kodaira, K., and Imai, M. (2003). Impaired pressure sensation in mice lacking TRPV4. Journal of biological chemistry *278*, 22664-22668.

Syntichaki, P., and Tavernarakis, N. (2004). Genetic models of mechanotransduction: the nematode Caenorhabditis elegans. Physiol Rev *84*, 1097-1153.

Tank, E.M., Rodgers, K.E., and Kenyon, C. (2011). Spontaneous age-related neurite branching in Caenorhabditis elegans. J Neurosci *31*, 9279-9288.

Taunton, J., Hassig, C.A., and Schreiber, S.L. (1996). A mammalian histone deacetylase related to the yeast transcriptional regulator Rpd3p. Science *272*, 408-411.

Thoma, C.R., Matov, A., Gutbrodt, K.L., Hoerner, C.R., Smole, Z., Krek, W., and Danuser, G. (2010). Quantitative image analysis identifies pVHL as a key regulator of microtubule dynamic instability. J Cell Biol *190*, 991-1003.

Thompson, P.R., Wang, D., Wang, L., Fulco, M., Pediconi, N., Zhang, D., An, W., Ge, Q., Roeder, R.G., Wong, J.*, et al.* (2004). Regulation of the p300 HAT domain via a novel activation loop. Nat Struct Mol Biol *11*, 308-315.

Tran, A.D., Marmo, T.P., Salam, A.A., Che, S., Finkelstein, E., Kabarriti, R., Xenias, H.S., Mazitschek, R., Hubbert, C., Kawaguchi, Y.*, et al.* (2007a). HDAC6 deacetylation of tubulin modulates dynamics of cellular adhesions. J Cell Sci *120*, 1469-1479.

Tran, A.D., Marmo, T.P., Salam, A.A., Che, S., Finkelstein, E., Kabarriti, R., Xenias, H.S., Mazitschek, R., Hubbert, C., Kawaguchi, Y.*, et al.* (2007b). HDAC6 deacetylation of tubulin modulates dynamics of cellular adhesions. J Cell Sci *120*, 1469-1479.

Walker, R.G., Willingham, A.T., and Zucker, C.S. (2000). A Drosophila mechanosensory transduction channel. Science *287*, 2229-2234.

Wang, L., Tang, Y., Cole, P.A., and Marmorstein, R. (2008). Structure and chemistry of the p300/CBP and Rtt109 histone acetyltransferases: implications for histone acetyltransferase evolution and function. Curr Opin Struct Biol *18*, 741-747.

Wang, Q., Zhang, Y., Yang, C., Xiong, H., Lin, Y., Yao, J., Li, H., Xie, L., Zhao, W., Yao, Y.*, et al.* (2010). Acetylation of metabolic enzymes coordinates carbon source utilization and metabolic flux. Science *327*, 1004-1007.

Webster DR, B.G. (1989). Microtubules are acetylated in domains that turn over slowly. J Cell Sci *97*, 57-65.

Webster, D.R., Gundersen, G.G., Bulinski, J.C., and Borisy, G.G. (1987). Differential turnover of tyrosinated and detyrosinated microtubules. Proc Natl Acad Sci U S A *84*, 9040-9044.

Westermann, S., and Weber, K. (2003). Post-translational modifications regulate microtubule function. Nat Rev Mol Cell Biol *4*, 938-947.

Wetzel, C., Hu, J., Riethmacher, D., Benckendorff, A., Harder, L., Eilers, A., Moshourab, R., Kozlenkov, A., Labuz, D., Caspani, O.*, et al.* (2007). A stomatin-domain protein essential for touch sensation in the mouse. Nature *445*, 206-209.

Witte, H., and Bradke, F. (2008). The role of the cytoskeleton during neuronal polarization. Curr Opin Neurobiol *18*, 479-487.

Wloga, D., and Gaertig, J. (2010). Post-translational modifications of microtubules. J Cell Sci *123*, 3447-3455.

Yan, Y., Harper, S., Speicher, D.W., and Marmorstein, R. (2002). The catalytic mechanism of the ESA1 histone acetyltransferase involves a self-acetylated intermediate. Nat Struct Biol *9*, 862-869.

Zhang, S., Arnadottir, J., Keller, C., Caldwell, G.A., Yao, C.A., and Chalfie, M. (2004a). MEC-2 is recruited to the putative mechanosensory complex in C. elegans touch receptor neurons through its stomatin-like domain. Curr Biol *14*, 1888-1896.

Zhang, W., and Bieker, J.J. (1998). Acetylation and modulation of erythroid Kruppel-like factor (EKLF) activity by interaction with histone acetyltransferases. Proc Natl Acad Sci U S A *95*, 9855-9860.

Zhang, X., Yuan, Z., Zhang, Y., Yong, S., Salas-Burgos, A., Koomen, J., Olashaw, N., Parsons, J.T., Yang, X.J., Dent, S.R.*, et al.* (2007). HDAC6 modulates cell motility by altering the acetylation level of cortactin. Mol Cell *27*, 197-213.

Zhang, Y., Kwon, S., Yamaguchi, T., Cubizolles, F., Rousseaux, S., Kneissel, M., Cao, C., Li, N., Cheng, H.L., Chua, K.*, et al.* (2008a). Mice lacking histone deacetylase 6 have hyperacetylated tubulin but are viable and develop normally. Mol Cell Biol *28*, 1688-1701.

Zhang, Y., Kwon, S., Yamaguchi, T., Cubizolles, F., Rousseaux, S., Kneissel, M., Cao, C., Li, N., Cheng, H.L., Chua, K.*, et al.* (2008b). Mice lacking histone deacetylase 6 have hyperacetylated tubulin but are viable and develop normally. Mol Cell Biol *28*, 1688-1701.

Zhang, Y., Ma, C., Delohery, T., Nasipak, B., Foat, B.C., Bounoutas, A., Bussemaker, H.J., Kim, S.K., and Chalfie, M. (2002). Identification of genes expressed in C. elegans touch receptor neurons. Nature *418*, 331-335.

Zhang, Z., Yamashita, H., Toyama, T., Sugiura, H., Omoto, Y., Ando, Y., Mita, K., Hamaguchi, M., Hayashi, S., and Iwase, H. (2004b). HDAC6 expression is correlated with better survival in breast cancer. Clin Cancer Res *10*, 6962-6968.

Zhao, C., and Emmons, S.W. (1995). A transcription factor controlling development of peripheral sense organs in C. elegans. Nature *373*, 74-78.

Zhao, S., Xu, W., Jiang, W., Yu, W., Lin, Y., Zhang, T., Yao, J., Zhou, L., Zeng, Y., Li, H.*, et al.* (2010). Regulation of cellular metabolism by protein lysine acetylation. Science *327*, 1000-1004.

Zilberman, Y., Ballestrem, C., Carramusa, L., Mazitschek, R., Khochbin, S., and Bershadsky, A. (2009a). Regulation of microtubule dynamics by inhibition of the tubulin deacetylase HDAC6. J Cell Sci *122*, 3531-3541.

Zilberman, Y., Ballestrem, C., Carramusa, L., Mazitschek, R., Khochbin, S., and Bershadsky, A. (2009b). Regulation of microtubule dynamics by inhibition of the tubulin deacetylase HDAC6. J Cell Sci *122*, 3531-3541.

Zurborg, S., Piszczek, A., Martinez, C., Hublitz, P., Al Banchaabouchi, M., Moreira, P., Perlas, E., and Heppenstall, P.A. (2011). Generation and characterization of an Advillin-Cre driver mouse line. Mol Pain *7*, 66.

7 Appendices

7.1 Appendix 1: Generation of atat1$^{-/-}$ mice

In order to examine the function of ATAT1 in vivo in mammals we are in the process of generating atat1 knock-out mice. In the targeting construct the first six exons that encode the acetyl-transferase domain and that are present in all known splice variants were knocked out (Figure 1). We believe this will give rise to a completely nonfunctional protein. The sides are flanked by *loxP* sites that allow us to perform conditional mutagenesis. The embryonic stem cells have been targeted and positive clones were expanded. The first ES mice were born in May 2011. They were crossed with *Flp*$^{tg/+}$ mice and among their progeny we obtained the floxed allele. We are now in the process of making both a global knock-out by crossing with a deleter strain and a sensory neuron specific knock out by crossing with a *Cre*-line produced in our laboratory (Zurborg et al., 2011). Once we successfully obtain the desired genotype we will analyze the phenotype of these animals to clarify the functional importance of atat1 gene. In sensory neuron specific knock-out we will look for evidence of touch-insensitivity.

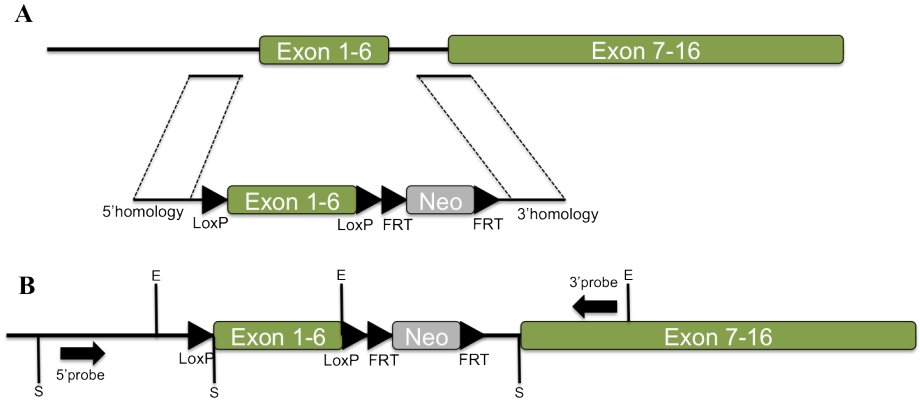

Figure 1. (A) atat1 targeted region with the targeting construct. (B) Strategy for Southern hybridization of targeted, floxed and deleted allele. E indicates site of restriction for EcoRI and S indicates site of restriction for SspI

7.1.1 atat1 targeting strategy

The atat1 targeting strategy allows *Cre*-mediated deletion of the first 6 exons from the atat1 gene. The atat1 gene-targeting vector carries a neomycine resistance (*neo*^{r}) gene flanked with two *frt* sites and a *loxP* site (*neo*^{r}*-frt2-loxP* cassette) located 3' of the exon 6 and a second *loxP* site located 5' of the exon 1. The targeting construct has been generated in the EMBL Gene Expression Service.

7.1.2 Generation of mice using homologous recombination in mouse embryonic stem cells

The targeting construct was electroporated into A9 embryonic stem (ES) cells (Passage 11) derived from a F1 hybrid of C57Bl/6 and 129 mouse genetic backgrounds (Gift of D.O'Carroll). A9 ES cells were routinely maintained in standard ES cell medium (see below) on a monolayer of Mitomycin C (Sigma, M4287) - treated primary mouse embryonic fibroblast (pMEFs). Approximately 10^7 ES cells were electroporated with the targeting construct and plated into neomycin-resistant MMC-treated pMEFs. 24h post-electroporation, selection for ES clones carrying the *neo*^{r} was started by adding G418 (250µg/ml active concentration) (GIBCO, 11811) to the ES cell medium. After seven days of selection, 300 ES cell clones were picked, expanded and frozen in ES cell freezing medium (see below). Large-scale Southern blot screening was used to identify homologous recombinants among the isolated ES cell clones. The targeting efficiency was around 5%. Four independent and correctly targeted ES cell clones were thawed, expanded and one of them was injected into 8-cell stage morulas from C57Bl/6 donors to generate ES mice heterozygous for the *atat1-targeted* allele. The injection was performed at the EMBL Transgenic facility. Upon confirmed germ-line transmission of the targeted allele, two obtained mice were crossed to

the *Flp*-expressing transgenic mice (FLPeR) (Farley et al., 2000) to remove the *frt*-flanked *neo*^{r} cassette. These resulted in generation of *atat1 loxP* allele. These mice are crossed to *Deleter-Cre* mice (Schwenk et al., 1995) and *Advilin-Cre* mice (Zurborg et al., 2011). These genetic manipulations will result in the generation of *atat1 null* allele and conditional *atat1 null* allele in the sensory system.

Standard ES cell medium

Knockout™ D-MEM (Invitrogen 10829-018)
12.5% Fetal Calf Serum (Hyclone, SH30071.03 Lot#ARJ27433)
1x Penicillin-Streptomycin, liquid (Invitrogen, 15070-063)
2mM L-Glutamine (GIBCO, 25030)
0.1mM 2-Mercapto-Ethanol (GIBCO, 31350-010)
1x Non-essential amino acids (GIBCO, 11140-035)
LIF (2µl of 1mg/ml solution per 100ml of media) (PEPCF Facility Heidelberg)

ES cell freezing medium

50% Fetal Calf Serum (Hyclone, SH30071.03, Lot#ARJ27433)
40% Standard ES cell medium
10% DMSO

7.1.3 Southern blotting of restriction-enzyme digested genomic DNA

Southern was performed using standard procedures. 5µg of digested genomic DNA per sample was resolved by agarose gel electrophoresis. The DNA fragments were transfered to Hybond^{TM}-N+ Nylon membrane (GE Healthcare, RPN203B) overnight in a classic blotting sandwich using passive capillary fransfer in alkaline solution (0.4M NaOH, 1.5M NaCl). The following primers were used to amplify a 650bp long 5'probe and 592bp long 3'probe:

atat1-5probe-F	gggaggggtaaaattttgga
atat1-5probe-R	tttggagggtaacgttttgc
atat1-3probe-F	taaagccacacatccatcca
atat1-3probe-R	agccagcctgtgagttcagt

50ng of purified probe was labeled with (32P)-GTP using the Random primers labeling kit (Invitrogen, 18187-013) accordig to manufacturer's instructions. Prior to adding the probe, the UV-crosslinked membrane (150mJ/cm^2) was prehybridized in Southern hybridization solution (0.5M Na-Phosphate buffer pH 7.2, 1mM EDTA, 3%BSA, 5%SDS) for 2h at 65°C in hybridization oven. Hybridization of labeled probe to the membrane was performed overnight. The next day, the membrane was washed in Southern washing solution (0.4M NaOH, 1.5M NaCl) three times, 20 min each wash, wrapped in Saran wrap and exposed to phosphoscreen. Phosphoscreen was scanned using the Fluorescent Image Analysis System FLA-5100 (Fujifilm).

7.2 Appendix 2: Generation of a novel behavioral test for touch perception in mice

One of the main problems in analyzing mechano-insensitive mouse phenotype is the lack of a simple behavioral test specific for the perception of touch. Although there is a wide variety of well-established tests for pain, including the paw withdrawal test, hot plate test and tail immersion test (Meyerson et al., 1995), there are no tests that could examine light touch in mice. To address this problem we examined adult wild type male animals and realized that the outer ear is a very sensitive part of the body. There is no previous published work on mechanosensation of the outer ear of the mouse and, aside from one elegant study from the 19th century (Schobl, 1871), very few data about the anatomy of the murine outer ear itself. We analyzed the response provoked by administration of von Frey filaments (Touch-test sensory evaluator, North Coast Medical Inc.) at different positions on the outer ear (Figure 1A) of mice and used the paw withdrawal method, that is used as a behavioral test for touch pain, as a control (Meyerson et al., 1995). Our results (Figure 1B) clearly show that stimulation of certain areas of the outer ear evokes easily detectable withdrawal response and the response is much lower at specific positions on the outer ear than on mouse hindpaws.

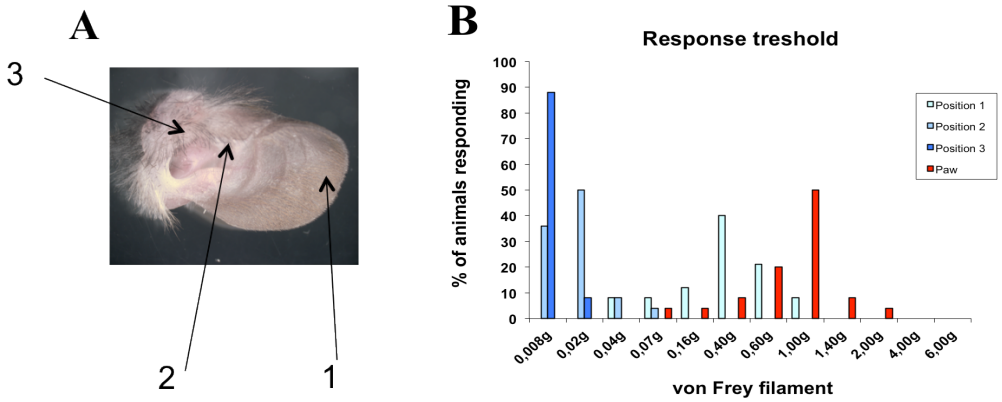

Figure 1. Novel behavioral test for light touch in mice. (A) Positions on the outer ear. (B) Response treshold at different places on the outer ear and on the hindpaw.